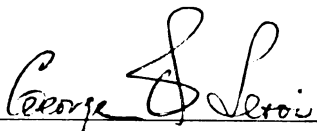This is to certify that the

thesis entitled
VIBRATIONAL SPECTRA OF
POLYCRYSTALLINE ETHANES

presented by
Massoud Hassanpour

has been accepted towards fulfillment
of the requirements for

_____Ph.D._____degree in __Chemistry__

_____
Major professor

Date September 7, 1979

O-7639

VIBRATIONAL SPECTRA OF

POLYCRYSTALLINE ETHANES

By

Massoud Hassanpour

A DISSERTATION

Submitted to

Michigan State University

in partial fulfillment of the requirements

for the degree of

DOCTOR OF PHILOSOPHY

Department of Chemistry

1979

ABSTRACT

VIBRATIONAL SPECTRA OF POLYCRYSTALLINE ETHANES

By

Massoud Hassanpour

The Raman spectra of polycrystalline C_2H_6 and C_2D_6 in the solid (II) phase are presented and shown to be consistent with the recent crystal structure reported by Van Nes and Vos. The spectra strongly support C_1 as the site symmetry, which has been under question in the literature.

The mid-infrared and/or Raman spectra of the neat, partially-deuterated ethanes: C_2H_5D, $1,1-C_2H_4D_2$, CH_3CD_3 and C_2HD_5, and of dilute mixed crystals of the partially-deuterated ethanes in one another have been obtained to learn more about the intermolecular force field of ethane and those of molecular crystals in general.

The retention of the symmetry of the parent (C_2H_6) crystal as an "effective" symmetry in the partially-deuterated crystals was concluded from the data obtained.

Various sets of atom-atom interaction potentials were used to calculate the lattice frequencies of the C_2H_6 crystal with the aid of recent single crystal x-ray data.

The "best" interaction potential was used to calculate the lattice frequencies of the partially-deuterated ethanes, assuming that the crystal structure and symmetry are unchanged by deuteration. From a comparison of the observed and calculated frequencies, it was determined that the lattice modes of the partially-deuterated crystals are amalgamated and can be described in the virtual crystal limit. Consistent with the virtual crystal theory, mutual exclusion was retained for the lattice modes of these disordered solids, illustrating the "effective" C_i site symmetry. Translational lattice frequencies of the partially-deuterated ethanes were also calculated using the potential which best predicted those of the C_2H_6 and C_2D_6 crystals.

In the dilute-mixed crystal spectra, the guest modes often exhibit multiplet structure arising from different relative orientations of the neighboring molecules. The number of energetically-inequivalent orientations is diagnostic of the "effective" site symmetry of the host lattice (i.e., symmetry in the spectroscopic rather than the mathematical sense), which was found to be C_i for each of the partially-deuterated ethanes. The magnitudes of the site (gas-to-crystal) shift, site-splitting and orientational effect show no significant isotope effect, but they are sensitive to vibrational type. This indicates that the intermolecular force constants remain unchanged in going from the C_2H_6 to the C_2D_6 crystal.

Due to the "effective " C_i site symmetry, the internal

modes of CH_3CD_3 can be treated in the pure crystal exciton formalism and are quite similar to the internal mode spectra of C_2H_6 and C_2D_6. However, the internal modes of C_2H_5D, $1,1-C_2H_4D_2$ and C_2HD_5 must be treated as mixed-crystal modes.

To

the heroic and toiling masses of Iran

ACKNOWLEDGMENTS

TABLE OF CONTENTS

LIST OF TABLES

LIST OF FIGURES

CHAPTER I

A. Introduction

It has been known for several decades that vibrational
spectra of molecules in the solid state provide valuable
information concerning crystal structure, rotational and
vibrational motions of the molecules in the unit cell and
the nature of the intermolecular forces responsible for
them.[1-3]

The first and the most significant papers on the sub-
ject published by Halford (1946),[4] Hornig (1948)[5] and by
Winston and Halford (1949,1951)[6,7] enhanced tremendously
the amount of experimental and theoretical work in this
area. The introduction of lasers as Raman sources and
the consequent availability of commercial Raman spectrometers,
as well as the availability of sophisticated far-infrared
instruments, have undoubtedly also played a significant
role in the development of the field. Much of the initial
work was devoted toward a qualitative understanding of the
vibrational spectra. The first model quantitative inter-
pretation was reported in 1962 when Dows attempted to
calculate the vibrational spectrum of the ethylene
crystal.[8] The early work in vibrational spectroscopy
of molecular crystals has been reviewed by Dows[9]

(internal modes) and Schnepp[10] (lattice modes). The more recent work in this area has been discussed by Bailly,[11] Pawley[12] and by Schnepp and Jacobi.[13]

Many researchers have focused their studies on molecular crystals of simple aliphatic hydrocarbons, such as acetylene,[14] ethylene[15-17] and ethane,[18] and on the simple aromatic hydrocarbons, such as benzene[19] and naphthalene,[20] in order to develop a more quantitative understanding of the intermolecular forces of the solids. These simple hydrocarbons are particularly attractive for study because they usually crystallize with two or four molecules per unit cell, and only three types of atom-atom interactions need be considered. This greatly simplifies the model calculations which are done to obtain a better understanding of the vibrational spectrum of a molecular crystal.

B. Background Information on Ethane in Condensed Phase

Although the IR and Raman spectra of ethane and of various deuterated ethanes in the gas and liquid phase have been studied by many workers,[21] little and incomplete work has been done on the solid phases.

The first work on the ordered crystalline (solid II) ethane was a report on the IR spectrum in the 600-3000 cm^{-1} region by Avery and Ellis (1942).[22] [See Chapter II

for the description of the solid phases of ethane.]

Schwartz, et al. (1971)[23] have studied the far-infrared
spectra of crystalline C_2H_6 and C_2D_6 at various tempera-
tures between 25°K and 90°K. Each compound showed two
absorption bands, which the isotopic frequency shifts
revealed to be translational lattice modes. Leroi (1970)[24]
studied the torsional fundamental near 300 cm^{-1} in ordered
solid (II) C_2H_6, CH_3CD_3 and C_2D_6. Preliminary Raman
spectra of neat C_2H_6, CH_3CD_3 and C_2D_6 in the crystalline
phase were obtained by Leroi and Getty (1970)[25] in this
laboratory. The observed spectra revealed that the (hex-
agonal) crystal structure proposed by Mark and Pohland
(1925)[26] on the basis of an x-ray powder pattern was in-
correct, since it predicts neither site nor correlation
field splitting correctly. By working through the pos-
sible site and factor groups which give predictions in
accord with the observations, Leroi and Getty suggested
a C_i site with C_{2h} factor group symmetry and two molecules
per unit cell for crystalline ethane. Later Eggers and
Tejada (1975)[18] published the IR spectra of ordered solid (II)
C_2H_6, C_2D_6 and their mutual solid solutions in the region
of the internal fundamentals. From their studies, Eggers
and Tejada tentatively proposed a slightly distorted
hexagonal structure with two molecules in the unit cell,
but they rejected C_i as the site symmetry. However, it
was our belief from the beginning of this research that

the most probable site symmetry would be C_i, just as for C_2H_2, C_2H_4, benzene, naphthalene and several other hydro-carbons, all non-polar compounds. The observed Raman and infrared spectra of crystalline C_2H_6 and C_2D_6 were completely consistent with inversion site symmetry. It was not until recently (and well after the work described in this thesis was initiated) that Van Nes and Vos (1978)[27] reported the single crystal x-ray analysis of two modifications of solid ethane - the plastic and the anisotropic phases - which confirmed our prediction of C_i as the site symmetry for anisotropic (ordered) crystalline ethane. In a very recent report on Raman and Infrared spectra of stable (ordered) crystal and a newly-found metastable solid phase of C_2H_6 and C_2D_6, Eggers and Wisnosky (1979)[28] came to the conclusion that the site symmetry for the stable phase of crystalline ethane is indeed C_i. Their work also includes a theoretical calculation of the fundamental frequencies of C_2H_6 and C_2D_6, as well as a calculation of the relative intensity of the external modes of crystalline C_2H_6.

The present study of the vibrational spectra of C_2H_6, C_2D_6 and partially deuterated ethane crystals: d_1, $1,1$-d_2, $1,1,1$-d_3, and d_5 has been conducted to learn more about the intermolecular force field of ethane, and of simple molecular crystals in general. We also wished to determine whether the symmetry of the parent (C_2H_6)

crystal is retained as an "effective" symmetry in the partially deuterated crystals. This provides some understanding of the effects of perturbations arising from disorder in these crystals (vide infra) on the intermolecular force fields. The retention of effective symmetry enables interpretation of the spectrum of the partially deuterated ethanes on the basis of pure crystal theories. Because of the relationship between neat crystals and isotopically mixed crystals, useful information about neat crystal intermolecular interactions can be obtained by studying the mixed crystals. This method has been shown to be very informative in the case of deuterated benzene,[29,30] and similar work on the deuterated ethylenes in this laboratory[17] has been of immense diagnostic help in the study of that system.

CHAPTER II

THEORETICAL TREATMENT OF CRYSTAL VIBRATIONS

A. The Vibrations and Selection Rules in Molecular Crystals

A distinguishing characteristic of molecular crystals
is that in such crystals the molecules preserve their
individuality in the first approximation. This is because
the interaction forces between molecules, i.e., inter-
molecular forces, are much weaker than the forces acting
between the atoms of a single molecule - the intramolecular
forces. Therefore, all possible atomic vibrations in
molecular crystals can be classified into two groups:

I. INTERNAL VIBRATIONS, which are essentially those
of the free molecule (i.e., stretching and bending, etc.
of chemical bonds in the molecule) subject to solid state
interactions.

II. EXTERNAL or LATTICE VIBRATIONS, which arise from
(approximately) rigid body motion of molecular groups as
a whole. The external modes are entirely solid state
vibrations, and are characterized by their low frequency
(usually less than 200 cm^{-1}). Lattice modes can be
further divided into two types: (a) TRANSLATIONAL modes

which arise from changes in position of the center of gravity of the molecules and (b) ROTATIONAL or LIBRATIONAL modes which involve hindered or quasi-rotation of the molecular groups about their centers of gravity.

Lattice modes are important in connection with crystal structure and make a large contribution to the specific heat of solids. Their energies vary considerably (in the 0-200 cm^{-1} range) and depend strongly on the molecular masses and moments of inertia, as well as on the nature of the bonding between the molecules. They are a property (mainly) characteristic of the solid state, and are not seen in the gas phase, although they are sometimes observed in liquids, indicating a quasi-crystalline structure in those cases. Their width, frequency and intensity are temperature- and pressure-dependent.

The coupling of internal and external vibrations, normally ignored in the analysis of the vibrational spectra of crystals, could become important as the internal and external modes approach one another in energy.

From the theory of crystal dynamics, the selection rules for a molecular vibration to be observed via infrared or Raman spectroscopy require that $\underline{K} = 0$, where $\underline{K}$ is the wave vector of a vibrational excitation travelling through the crystal with wave-like character. This arises because the interaction of a vibrational excitation with a photon must satisfy conservation of linear momentum. Therefore,

the value of the wave vector of the vibrational excitation must be of the same order as that of the probing radiation.[*] In order that K $\cong$ 0, the vibrations of (translationally) equivalent atoms in different unit cells of a molecular crystal must be identically in phase. Accordingly, the optically-active vibrations of the bulk crystal are the vibrations of a unit cell carried through the crystal, in the same phase, by the operation of translation. Consequently, a consideration of the normal modes of vibration of the unit cell suffices to enumerate the genuine modes of the crystal as a whole. The implication of the above discussion is that the number of optically-observable fundamental vibrational degrees of freedom in a molecular crystal which contains in the unit cell m molecules, each having N atoms, is simply 3 mN. Three of

---

[*]Consider, for example, the possible excitation of a given optical mode by infrared absorption, assuming this process to be allowed by symmetry. Of course, conservation of energy then requires that the photon frequency and the vibrational frequency be the same. But also, momentum must be conserved in the process. A quantized lattice vibration (phonon) acts for most practical purposes as if it possessed a momentum $\hbar K$, where K is in the range of the first Brillouin Zone ($-\pi/2a < K < \pi/2a$). It is thus required that $\hbar Q = \hbar K$, where Q is the wave vector ($= 2\pi/\lambda$) of the observed photon. Since the wavelength of infrared light is large compared to the lattice constant (a), Q is very small (10^3 cm^{-1} as compard to K = 10^8 cm^{-1}). Optical transitions will then occur essentially at K = 0. The same applies to Raman scattering processes. In this case, when a phonon is created by the inelastic scattering of a photon whose change in frequency causes its wave vector to change from Q to Q', it is required that $\hbar Q - \hbar Q' = \hbar K$. Since Q and Q' are both small, clearly their vector difference is also small.

these degrees of freedom are associated with the acoustic modes, whose frequencies are zero at K = 0; the remaining 3 mN-3 modes are optical modes. (The acoustic modes correspond to the pure translation of the entire lattice in space). Of 3mN-3 optical modes 3(m-1) are translational vibrations, 3m belong to librational modes and the remaining (3N-6)m are accounted for by internal modes, assuming a non-linear molecule. Therefore, if no degeneracies are present, the internal region would consist of 3N-6 vibrations each showing m components, usually referred to as the Davydov or factor group components. Degenerate modes of the free molecule can also be split because of the lower local symmetry in the crystal, which may no longer be consistent with the degeneracy. This latter splitting, usually called static field or site splitting, thus increases the number of components for degenerate vibrations to a maximum of 2m.

The vibrational excitations of a molecular crystal may be classified as either phonons or excitons. Phonons, which are quantized lattice vibrations, are delocalized excitations in the crystal. The internal vibrations, which are localized, are usually classified as excitons. Since the phonons are delocalized, they are quite dependent on K whereas the localized excitons are only slightly dependent on K.[1]

The number and activity of the vibrational modes of

a molecular crystal are usually derived from a symmetry consideration of the crystal. Several types of symmetry groups need be considered, including the space group, the unit cell or factor group, and the site-group symmetries of the lattice. The space group entirely describes the symmetry relations among the molecules in the lattice, including the translational symmetry. The space group symmetry minus the translational symmetry is the unit-cell symmetry, which describes the symmetry relations of the molecules in the unit cell. The site group describes the symmetry of the static field in which the molecules in the crystal interact. A correlation[31-33] of the free molecule symmetry with the site and unit cell symmetries provides information concerning the activity and number of Davydov and site group splitting components of the molecular crystal modes.

B. The Crystal Structure of Ethane

In the literature, contradictory information is available regarding the symmetry of solid ethane. Wyckoff (1966)[34] reports a hexagonal structure ($P6_3/m$ $2/m$ $2/c$, $Z = 2$) at 88 K. This structure was found from optical studies (Wahl (1914);[35] Mark and Pohland (1925)[26]) of a solid sample of ethane just below the melting point, combined with the structural information obtained by

Mark and Pohland (1925) from Debye-Scherrer diagrams taken with Zn, Cu and Cr radiation. According to Mark and Pohland, the powder lines correspond quite well to a hexagonal unit cell. No definite conclusion was made concerning the space group ($P6_3$/m 2/m 2/c was mentioned as one of the possibilities). However, this structure is inconsistent with the infrared and Raman spectra, as previously mentioned.

According to an optical and dilatometric study by Eggers (1975),[36] ethane shows the following transformations:

liquid ⟶ isotropic solid ⟶ anisotropic solid

   90.27±0.02K   89.82±0.02K
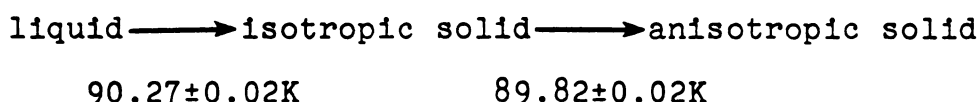
A pressure-temperature phase diagram reported at the same time by Straty and Tsumura (1976)[37] confirms the existence of the isotropic phase just below the melting point. Proton magnetic resonance measurements by Givens and McCormick (1977)[38] have given temperatures of 90.37 and 89.72 (0.05) K for the above transitions and very narrow lines for the isotropic solid. From his study, Eggers suggests that the isotropic solid is a plastic crystalline form, and that the symmetry of the anisotropic solid is lower than hexagonal. On the basis of IR spectra of the latter phase of C_2D_6, Tejada and Eggers (1975)[18] tentatively proposed a slightly distorted hexagonal structure with two molecules in the unit cell related by either a

glide plane or a screw axis.

A very recent x-ray analysis of single crystals of ethane by Van Nes and Vos[27] (1978) revealed that the (plastic) modification of crystalline C_2H_6 solid (I) at 90°K is cubic. In the cubic phase, which has symmetry Im3m, and two molecules in the unit cell, strong orientational disorder is present. The anisotropic phase of ethane, solid (II), was determined to be monoclinic with space group $P2_1/n$ and two molecules per unit cell. The two molecules in the cell lie at the inversion centers (0,0,0) and (½,½,½) and have a staggered conformation.

Recently Wisnosky and Eggers[28,39] reported a new phase for solid ethane. This new phase has been found to be metastable with a crystal structure different from the other solid phases of ethane. The pure metastable phase may be obtained at an optimum deposition temperature of 47°K, but when heated will rapidly and irreversibly transform to the stable phase, solid (II), at about 70°K. Sample deposition at temperatures above 60°K results in the formation of the stable phase. The metastable solid was sometimes formed during the course of this work. However, the current investigation is concerned with the vibrational spectra of the stable phase only.

The crystal structure of ethane in the stable monoclinic phase (solid II) is shown in Figure 1. Table 1 lists the lattice parameters and the orientational matrix
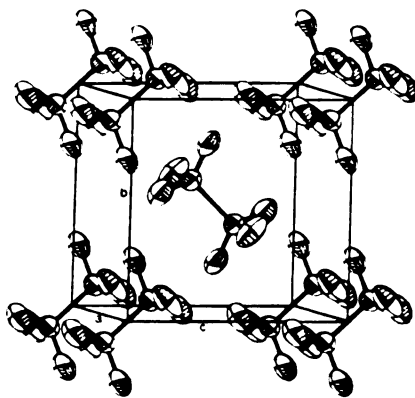
Figure 1.   Packing of the monoclinic phase of C_2H_6 (from
Reference 27).

Table 1.   Lattice parameters[a] and orientation matrix[b]
for the ethane crystal.

a = 4.226 Å   b = 5.623 Å   c = 5.845 Å

α = 90.0°   β = 90.41°   γ = 90.0°

	x	y	z
a	.2634	.4996	.8252
b	-.6859	-.5046	.5244
c	.6784	-.7041	.2098

[a]From Reference 27.

[b]See text.

for an ethane molecule centered at the origin and initially
oriented with C-C bond along the x-axis and two trans
hydrogens in the xy plane. The unit cell lengths a, b
and c correspond with Figure 1; α, β and γ are the angles
between b and c, c and a, and between a and b, respec-
tively. (Note that the unit cell is essentially ortho-
rhombic.) The orientation matrix arises from rotations
about the x, y and z axes by angles of -73.41, -42.72, and
-69.0 degrees respectively. The bond lengths, bond angles,
and the changes caused by deuteration of the free molecule,
and of the molecule in the crystal, are given in Table 2.
H(1), H(2) and H(3) denote the hydrogens belonging to the
same carbon atom in the molecule. The δ's are the changes
in bond lengths and angles caused by deuteration.

The correlation table for solid (II) ethane is given
in Table 3. Six doublets (A-modes) and six quartets
(E-modes), three of each Raman-active and three of each
IR-active, are predicted for the internal modes. Six
Raman-active librations and three IR-active translations
are expected in the lattice region (after subtraction of
the three acoustical modes). The vibrational spectra
of C_2H_6 and C_2D_6 have been found to be consistent with
the crystal structure recently determined by x-ray analysis
and the above prediction, except that only two of the three
predicted infrared-active translations have been observed,[23]
and that in a few cases fewer components are resolved for
the internal modes.

Table 2. Structural parameters for Free Ethane Molecule
and Molecule in Crystal.

	Gas[a]	Crystal[b]
r (C=C)	1.5335 Å	1.532 Å
r (C-H)	1.0955 Å	1.096 Å
< (H(1)-C-H(2))	107.76°	107.1°
< (H(1)-C-H(3))	107.76°	111.4°
< (H(2)-C-H(3))	107.76°	108.3°
< C-C-H(1)	111.10°	109.5°
< C-C-H(2)	111.10°	111.8°
< C-C-H(3)	111.10°	108.8°
δr (CH-CD)	.0019 Å	
δ<(HCC-DCC)	-.010°	
δr (CC-^{13}CC)	.00014 Å	
r (CC)	-5×10^{-5} Å for each successive deuterium substitution.	

[a]Gas phase values and δ's from Reference 40.

[b]From Reference 27.

Table 3. Correlation table for INTERNAL modes of solid ethane.

Molecular Point Group D_{3d}	Site Group C_i	Factor Group C_{2h} [a]	
ν_1, ν_2, ν_3 3A$_{1g}$	9A$_g$	9A$_g$	R
$\nu_{10}, \nu_{11}, \nu_{12}$ 3E$_g$		9B$_g$	R
ν_4 A$_{1u}$	9A$_u$	9A$_u$	IR
ν_5, ν_6 2A$_{2u}$		9B$_u$	IR
ν_7, ν_8, ν_9 3E$_u$			

[a] R and IR indicate Raman and infrared activity, respectively.

Table 3.   Continued. **Correlation table for EXTERNAL modes of Solid ethane .**

Molecular Point group D_{3d}	Site group C_i	Factor group [a] C_{2h}

R_z A_{2g} $3\,A_g$ $3\,A_g$ R

$R_{(x,y)}$ E_g $3\,B_g$ R

T_z A_{2u} $3\,A_u$ $3\,A_u$ IR

(1-acoustic)

$T_{(x,y)}$ E_u $3\,B_u$ IR

(2-acoustics)

[a] R and IR indicate Raman and infrared activity, respectively.

C. Theoretical Approach to the Calculation of Molecular
    Crystal Vibrations

In the following discussion, two theoretical descrip-
tions of the vibrations in molecular crystals are reviewed.
The first, which is a semiclassical treatment and follows
closely the work of Taddei et al.[41] was used to calculate
the external frequencies of ethanes in solid phase II.
The second, called the vibration exciton technique[42] and
developed by Davydov,[43] assists in the discussion of
experimental data for both pure and mixed crystals of the
partially-deuterated ethanes.

1. Calculation of Crystal-Vibrational Frequencies

In the conventional theory of lattice dynamics developed
by Born and Huang[44] the potential energy function of a
molecular crystal is divided into two parts:

$$U = V_o + V_e \, , \tag{1}$$

where V_o represents the intramolecular part, i.e., the
internal energy of all molecules in the crystal, and V_e
is the intermolecular potential energy and is the collection
of all terms which refer to more than one molecule.

For a piece of crystal large enough to fulfill the
cyclic boundary conditions, the infinitesimal linear

displacements of the atoms are described in terms of the
normal coordinates of the molecule and the external dis-
placement coordinates. The external displacement co-
ordinates are the Eckart-mass-weighted translational and
torsional coordinates.

As usual in the vibrational problem, the potential
energy is expanded in a Taylor series about the equilibrium
configuration in terms of the internal and external co-
ordinates,

$$U = \frac{1}{2} \sum_{\alpha\mu} [\sum_n^{3N-6} (\partial^2 V_0 / \partial Q^2_{\alpha\mu n})_0 Q^2_{\alpha\mu n}$$

$$+ \sum_{\beta\nu} \sum_{\ell m}^{3N} (\partial^2 V_e / \partial Q_{\alpha\mu\ell} \partial Q_{\beta\nu m})_0 Q_{\alpha\mu\ell} Q_{\beta\nu m}] , \qquad (2)$$

where μ, ν label the molecule in the unit cell, α, β
the unit cell and ℓ, m, n the external and internal co-
ordinates. The first (3N-6) coordinates are the internal
coordinates for a non-linear molecule, and the last six
coordinates are the external coordinates.

The force field of the free molecule may be assumed
for V_0 if the equilibrium configuration of the molecule
is not deformed severely in the crystal. However, V_0
in principle should be the intramolecular potential rela-
tive to the molecule in the site, and uncoupled to the
other molecules in the lattice. It should also be noted

that the second derivative of V_o is taken with respect to the internal normal modes only.

The form of V_e will be specified later. The second derivative of the intermolecular potential energy is expressed with respect to both the internal coordinates and the external coordinates. The first derivatives of V_o and V_e have been assumed to be zero.[45] These terms may be excluded only when the interaction terms between the intramolecular and intermolecular potentials are actually negligible and if V_e has a minimum for the observed crystal structure. The neglect of the third and higher derivatives of the potentials obviously confines such a treatment to the harmonic approximation.

The problem may now be simplified by expressing equation (2) in terms of the symmetry coordinates $Q_{\nu m}$ ($\underset{\sim}{K}$) which belong to the irreducible representation of the translational group. These symmetry coordinates are given as follows:

$$Q_{\nu m} (\underset{\sim}{K}) = L^{-1/2} \sum_{\beta} Q_{\beta \nu m} \exp (2\pi i \underset{\sim}{K} \cdot \underset{\sim}{r}_{\beta}) , \qquad (3)$$

where L is the number of unit cells in the crystal, $\underset{\sim}{r}_{\beta}$ is a position vector connecting the βth cell with an arbitrary reference cell which will be labeled 1, and $\underset{\sim}{K}$ is the wave vector.

The potential energy in terms of these symmetry

coordinates becomes,

$$U = \frac{1}{2} \sum_k \sum_\mu \left[\sum_\ell \lambda_\ell Q^*_{\mu\ell}(\underset{\sim}{K}) Q_{\mu\ell}(\underset{\sim}{K}) + \sum_\nu \sum_{\ell m} F^{\nu m}_{\mu\ell}(\underset{\sim}{K}) Q^*_{\mu\ell}(\underset{\sim}{K}) Q_{\nu m}(\underset{\sim}{K}) \right] \tag{4}$$

where,

$$F^{\nu m}_{\mu\ell}(\underset{\sim}{K}) = \sum_\beta \left(\partial^2 V_e / \partial Q_{1\mu\ell} \partial Q_{\beta\nu m} \right)_0 \exp(-2\pi i \underset{\sim}{K} \cdot \underset{\sim}{r}_\beta) . \tag{5}$$

The frequencies of the crystal normal modes $\nu(\underset{\sim}{K})$ can be calculated by solving the secular equation:

$$\left| F^{\nu m}_{\mu\ell}(\underset{\sim}{K}) - [\lambda(\underset{\sim}{K}) - \lambda_\ell] \delta_{\mu\nu} \delta_{\ell m} \right| = 0 \tag{6}$$

where $\lambda(\underset{\sim}{K}) = 4\pi^2 \nu^2(\underset{\sim}{K})$ and $\lambda_\ell = 4\pi^2 \nu_\ell^2$. The ν_ℓs are the frequencies of the free molecule.

The form of the intermolecular potential energy, V_e, must be specified in order to evaluate $F^{\nu m}_{\mu\ell}(\underset{\sim}{K})$. When only pairwise interactions are considered,

$$V_e = \frac{1}{2} \sum_{\alpha\beta} \sum_{\mu\nu} V^{\beta\nu}_{\alpha\mu}, \quad \mu \neq \nu \text{ when } \alpha = \beta . \tag{7}$$

Here $V^{\beta\nu}_{\alpha\mu}$ is the pairwise interaction between the μth molecule

in the αth unit cell and the νth molecule in the βth unit cell. Therefore, in terms of Equation (7),

$$F_{\mu\ell}^{\nu m}(\underset{\sim}{K}) = \sum_{\beta} \exp(-2\pi i \underset{\sim}{K} \cdot \underset{\sim}{r}_{\beta})(\partial^2 V_{1\mu}^{\beta\nu}/\partial Q_{1\mu\ell}\partial Q_{\beta\nu m})_o$$

$$\beta \neq 1$$

if $\mu = \nu$

$$+ \delta_{\mu\nu} \sum_{\beta} \sum_{\tau} (\partial^2 V_{1\mu}^{\beta\tau}/\partial Q_{1\mu\ell}\partial Q_{1\mu m})_o$$

$$\beta \neq 1$$

if $\mu = \tau$ \hfill (8)

The molecule-molecule interactions are usually expressed as a sum of atom-atom interactions,

$$V_e = \frac{1}{2} \sum_{\alpha\beta} \sum_{\mu\nu} \sum_{ij} V_{\alpha\mu i}^{\beta\nu j}(r_{\alpha\mu i}^{\beta\nu j}) \quad , \hfill (9)$$

where i labels the atoms belonging to molecule $\alpha\mu$, and j the atoms belonging to molecule $\beta\nu$. The interatomic distance between atoms i and j is given by $r_{\alpha\mu i}^{\beta\nu j}$. In terms of the atom-atom potentials, the second derivatives in Equation (8) are given by:

$$
\left(\frac{\partial^2 V^{\beta\nu}_{1\mu}}{\partial Q_{1\mu\ell} \partial Q_{\beta\nu m}} \right)_o = \sum_{ij} \left\{ \left(\frac{\partial^2 V_{ij}}{\partial r_{ij}^2} \right)_o \left(\frac{\partial r_i}{\partial Q_{1\mu\ell}} \cdot \frac{\partial r_{ij}}{\partial r_i} \right) \right.
$$

$$
\left(\frac{\partial r_j}{\partial Q_{\beta\nu m}} \cdot \frac{\partial r_{ij}}{\partial r_j} \right) + \left(\frac{\partial V_{ij}}{\partial r_{ij}} \right)_o \left[\left(\frac{\partial r_i}{\partial Q_{1\mu\ell}} \cdot \frac{\partial r_{ij}}{\partial r_i} \right) \left(\frac{\partial r_j}{\partial Q_{\beta\nu m}} \cdot \frac{\partial r_{ij}}{\partial r_j} \right) \right] \right\} ,
$$

$$
(10)
$$

where for simplicity, $V^{\beta\nu j}_{\alpha\mu i}$ and $r^{\beta\nu j}_{\alpha\mu i}$ have been replaced
by V_{ij} and r_{ij}, respectively. Taddei, et al.[41,46] have
pointed out that traditionally the second term in the above
equation has been ignored. They have calculated the lattice
frequencies of benzene with and without this term. The
inclusion of this "first derivative" term caused a 2% to
15% reduction in the calculated lattice frequencies, showing
that the effect of this term is not negligible. Kobayashi[47]
also points out that his calculation indicates that the
effect of inclusion of the linear terms on the normal fre-
quencies of polyethylene crystals is non-negligible for the
librational lattice modes (it lowers the frequencies by as
much as 20 cm^{-1}), while its effect is not drastic for the
translational lattice modes or for the correlation splitting
of the internal modes. Agreement between the observed
and calculated frequencies of the lattice modes is improved
significantly by inclusion of the linear terms. Therefore,
this term was included in the calculation of lattice

frequencies of the solid ethanes.

The solutions of the above secular equation [Equation (6)] will give the frequencies of the crystal normal modes over the entire Brillouin zone. However, K selection rules make it possible to observe only the optically-active vibrations, that is vibrations with $K = 0$, via infrared absorption and Raman scattering. It should be noted that K arises from the translational symmetry of the crystal; therefore if the translational symmetry is destroyed it may no longer be a "good" quantum number.

As noted earlier, the intermolecular potential is usually specified as the sum of molecule-molecule pairwise interactions which are expressed as a sum of atom-atom interactions. The atom-atom interaction potential for hydrocarbons is often expressed as a Buckingham potential (exp-6):

$$V_{ij} = B \exp(-Cr_{ij}) - Ar_{ij}^{-6} , \qquad (11)$$

and sometimes includes Coulombic interactions (exp-6-1):

$$V_{ij} = B \exp(-Cr_{ij}) - Ar_{ij}^{-6} + Q_i Q_j r_{ij}^{-1} \qquad (12)$$

where r_{ij} is the nonbonded interatomic distance, <u>i.e.</u>,
the interatomic distance between atom i of molecule α and
atom j of a molecule other than α in the crystal. A, B
and C are adjustable parameters which are obtained by
refinement to non-spectroscopic crystal properties such as
heats of sublimation and crystal lattice energies. The
parameters Q_i and Q_j are point charges on atoms i and j,
respectively.

The actual calculations of the crystal frequencies of
the ethanes were made using program TBON, a computer pro-
gram written by Taddei and Bonadeo.

2. <u>Vibrational Exciton Technique</u>

Over the past 30 years two complementary theoretical
approaches have been taken to solve the problem of Frenkel
excitons.[48] The first, the Halford-Hornig approach, is
almost purely group theoretical in nature. The second ap-
proach, called the Davydov theory,[43] is a technique for
obtaining general crystal energy levels. The following
discussion is a review of the modified form of Davydov's
theory given by Bernstein <u>et</u> <u>al</u>.[19] to be used in the
qualitative discussion of static and dynamic effects in
molecular crystals, <u>i.e.</u>, the splitting and shifts of
modes in the solid state in comparison to those of the
free molecule (see also Reference 49, Chapter 6).

The above-mentioned technique first quantizes the local, molecular modes (tight-binding formalism[50]), and then forms delocalized wave functions for the whole crystal. In the limit of the tight-binding (Frenkel) approximation, the zeroth-order crystal states, representing localized vibrational excitation f on a particular molecule at a given site nq in the crystal, is given by:

$$\psi_{nq}^{f} = \phi_{nq}^{f} \prod_{nq \neq n'q'} \phi_{n'q'}^{o} \quad , \tag{13}$$

where n labels the unit cell, q labels the site in the unit cell, f refers to the fth excited state of the molecule, and ϕ_{nq} is a crystal site function. It is assumed that the various f states do not mix and that the localized excitation functions are orthogonal, _i.e._,

$$\langle \psi_{nq}^{f} | \psi_{n'q'}^{f'} \rangle = \delta_{nn'} \delta_{qq'} \delta_{ff'} \quad . \tag{14}$$

Then, from these functions one can generate the one-site exciton functions (excitons in which any amount of excitation is on a single molecule) in the Bloch representation,

$$\psi_{q}^{f}(\mathbf{K}) = L^{-1/2} \sum_{n=1}^{N} \exp(i\mathbf{K} \cdot R_{nq}) \psi_{nq}^{f} \quad , \tag{15}$$

where N is the total number of molecules in the crystal and R_{nq} denotes the position of the center of a molecule located at the qth site in the nth unit cell with respect to a common origin.

$$\underset{\sim}{R}_{nq} = \underset{\sim}{r}_n + \underset{\sim}{\tau}_{nq} \quad , \qquad (16)$$

with $\underset{\sim}{r}_n$ being the vector from an arbitrary crystal origin to the origin of the nth unit cell and $\underset{\sim}{\tau}_{nq}$ a vector from the origin of the unit cell to the molecule in the qth site in the same unit cell.

It is convenient to divide the Hamiltonian, H, into a one-site Hamiltonian H^o and an intersite interaction Hamiltonian H';

$$H = H^o + H' \quad , \qquad (17)$$

where

$$H^o = \sum_{n=1} \sum_{q=1}^{\sigma} H^o_{nq} \qquad (18)$$

and

$$H' = \sum_{nq \neq n'q'} H'_{nq,n'q'} \quad . \qquad (19)$$

The $H'_{nq,n'q'}$ terms represent the pairwise interactions of the molecules in the crystal.

The eigenfunctions of H^o_{nq} are just the crystal site functions ϕ_{nq} introduced in Eq. (13). H^o_{nq} is (considered to be) the Hamiltonian of the free molecule whose nuclear framework has been distorted to match that of the molecule in the crystal. Using the one-site exciton functions of Eq. (13) as zero-order functions, the first-order Hamiltonian matrix element for the excited states of crystalline ethane, corresponding to the fth excited state of the molecule, are:

$$L^f_{qq'}(\underset{\sim}{K}) = \sum_{n'=1}^{N} \exp[(i\underset{\sim}{K})(\underset{\sim}{R}_{nq}-\underset{\sim}{R}_{n'q'})]<\psi^f_{nq}|H|\psi^f_{n'q'}> . \quad (20)$$

Separating the $\underset{\sim}{K}$-independent terms from the $\underset{\sim}{K}$-dependent terms,

$$L^f_{qq'}(\underset{\sim}{K}) = (\varepsilon^f+D^f)\delta_{qq'} + L^f_{qq'}(\underset{\sim}{K}) , \quad (21)$$

where

$$\varepsilon^f = <\psi^f_{nq}|H^o_{nq}|\psi^f_{nq}> = <\phi^f_{nq}|H^o_{nq}|\phi^f_{nq}> \quad (22)$$

is the $\underset{\sim}{K}$-independent free-molecule excitation energy, and

$$D^f = \langle\psi^f_{nq}|H'|\psi^f_{nq}\rangle = \sum_{nq \neq n'q'} \langle\phi^f_{nq}\phi^o_{n'q'}|H'|\phi^f_{nq}\phi^o_{nq}\rangle \qquad (23)$$

is the $\underset{\sim}{K}$-independent contribution to the environmental shift.

The $\underset{\sim}{K}$-dependent term consists of both a diagonal part,

$$L^f_{qq}(\underset{\sim}{K}) = \sum_{n \neq n'} \exp[i\underset{\sim}{K}(\underset{\sim}{R}_{nq}-\underset{\sim}{R}_{n'q'})]\langle\psi^f_{nq}|H'_{nq,n'q'}|\psi^f_{nq}\rangle ,$$
$$(24)$$

which represents the interactions of the translationally-equivalent molecules, and off-diagonal parts,

$$L^f_{qq'}(\underset{\sim}{K}) = \sum_{n,n'} \exp[i\underset{\sim}{K}(\underset{\sim}{R}_{nq}-\underset{\sim}{R}_{n'q'})]$$

$$\langle\psi^f_{nq}|H'_{nq,n'q'}(1-\delta_{qq'})|\psi^f_{n'q'}\rangle , \qquad (24)$$

representing the interactions of the translationally in-equivalent molecules in the crystal.

Band Energies - The crystal excitation energy, for a
particular value of $\underset{\sim}{K}$, now can be found by solving a
$\sigma \times \sigma$ determinant of H. For the ethane crystal where
$\sigma = 2$, the crystal energies would be:[49]

$$E^f(\underset{\sim}{K})^{\pm} = \epsilon^f + D^f + \frac{1}{2}[L^f_{qq}(\underset{\sim}{K}) + L^f_{q'q'}(\underset{\sim}{K})]$$

$$\pm \frac{1}{2}\{[L^f_{qq}(\underset{\sim}{K}) - L^f_{qq'}(\underset{\sim}{K})]^2 + 4[L^f_{qq'}(\underset{\sim}{K})]^2\}^{1/2} \quad , \quad (25)$$

where $E^f(o)^+$ and $E^f(o)^-$ are the energies of the two Davydov
components for the internal vibration f, separated by

$$\{[L^f_{qq}(\underset{\sim}{K}) - L^f_{qq'}(\underset{\sim}{K})]^2 + 4[L^f_{qq'}(\underset{\sim}{K})]^2\}^{1/2} \quad .$$

This splitting, which may be viewed as an effect of the
crystal field, is a dynamic effect, since it depends upon
the transfer of excitation between different molecules.
For

$$\underset{\sim}{K} = 0 \qquad L^f_{qq}(\underset{\sim}{K}) = L^f_{q'q'}(\underset{\sim}{K}) \equiv L^f_{qq} \quad .$$

Therefore,

$$E^{f\pm} = \varepsilon^f + D^f + L^f_{qq} \pm L^f_{qq'} \qquad (26)$$

or

$$E^{f\pm} = \varepsilon^f + D^f + L^f_q , \qquad (27)$$

where

$$L^f_q = L^f_{qq} \pm L^f_{qq'} \quad .$$

Alternatively,

$$\Delta E^{f\pm} \equiv E^f(\mathcal{K}) - E^\circ = \varepsilon + D + L^f_q(\mathcal{K}) \quad . \qquad (28)$$

Here, $E^f(\mathcal{K})$ and E° are, respectively, the excited and ground state energies of the crystal; $\varepsilon = \varepsilon^f - \varepsilon^\circ$, where ε^f and ε° are the excited and ground-state energies of a molecule at the site; $D = D^f - D^\circ$ is a $\mathcal{K}$-independent band-shift term. Eq. (28) can be rewritten as

$$\Delta E^{f\pm} = \varepsilon^- + L^f_q + \Delta \quad , \qquad (29)$$

where

$$\Delta = \varepsilon - \bar{\varepsilon} + D \quad .$$

In Eq. (29) the quantity $\bar{\varepsilon}$ is just the gas-phase
excitation energy and Δ is the site-shift term or gas-to-
ideal mixed crystal shift; D is the static field term and
involves no resonance interaction among the molecules in
the crystal. For a better understanding, some of these
energy contributions for mixed crystals and for $\underset{\sim}{K} = 0$
states of neat crystals are illustrated schematically in
Figure 2 for both degenerate and non-degenerate gerade
states of crystalline ethane. In Figure 2a Q is referred
to as the quasi-resonance shift and accounts for any
resonance interactions between the guest and host in the
dilute-mixed crystal. R is the resonance shifting caused
by interactions of translationally-equivalent molecules, and
equals L_{qq}^{f}. This term may be experimentally determined by
finding the difference between the mixed-crystal frequency
and the mean of the $\underset{\sim}{K} = 0$ doublet, assuming quasi-resonance
effects to be negligible. T is one-half the exciton band
width and is the same as $L_{qq'}^{f}$. It reflects the resonance
contributions directly related to interactions of the
translationally-inequivalent molecules in the crystal.

It should be noted that the shifts in neat crystals, in
isotopic mixed crystals, and in chemically mixed crystals
are often all of similar size. The effect of resonance
interactions is nearly lost in the second case and completely
lost in the latter case, indicating that the resonance
interactions must provide a relatively minor contribution
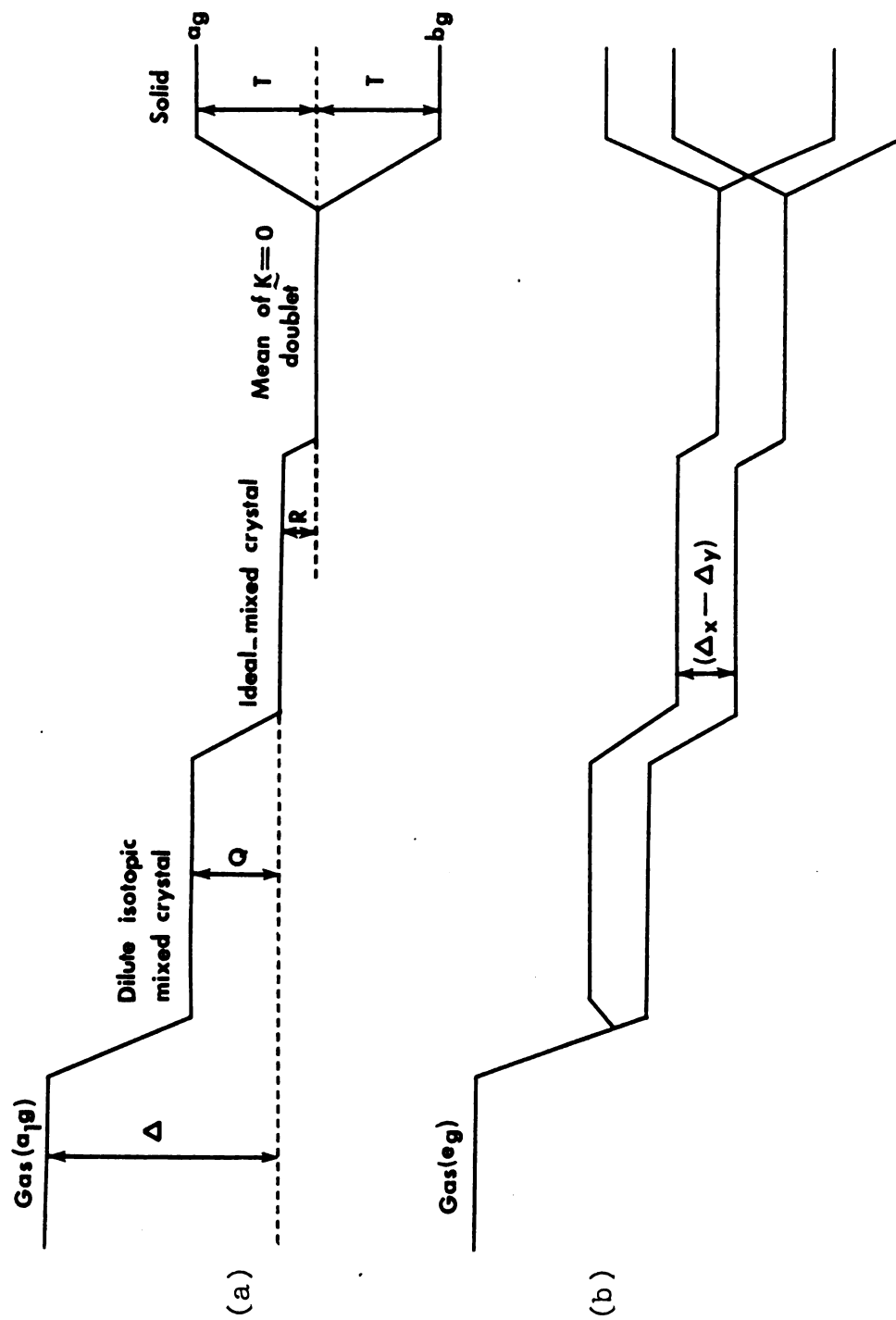
Figure 2. Schematic exciton structure of Raman-active bands in crystalline ethane.

to the shift. Therefore, the static and dynamic effects can be separated experimentally by observing the spectra of isotopic dilute mixed crystals, where it is $\bar{\epsilon} + \Delta$, not $\bar{\epsilon} + \Delta + L^f(o)$, that determines the position of the guest energy levels in the ideal case.

Site-Group Splitting - Another type of splitting which is observed in the spectra of molecular crystals like C_2H_6 is site-group, or static-field splitting. This is caused by the destruction of molecular degeneracies when the gas phase molecular symmetry is lowered in the crystal. Bernstein et al.[19,29] have suggested that the site-group splitting be defined phenomenologically as the splitting obtained for the guest in an ideal-mixed crystal, where there exist no resonance interactions between the molecules in the crystal. The ideal-mixed crystal is defined as one in which:

(a) The guest is infinitely dilute,

(b) Guest and host differ only by isotopic substitution,

(c) Guest and host have the same symmetry and dimension,

(d) Quasi-resonance interactions between guest and host (Q in Figure 2) are negligible, and

(e) The effect of isotopic substitution on Δ can be neglected.

In the ideal mixed crystal, therefore, the site-group splitting of a degenerate gas-phase band will be quantitatively identical to the difference in the Δ terms of the originally degenerate components. Symbolically this can be written as $(\Delta_x - \Delta_y)$ where x and y designate the degenerate components (see Figure 2b).

In the neat crystal there are additional resonance contributions to the splitting of free-molecule degenerate states; i.e., once degeneracy has been removed by static-field interactions, the degenerate levels may be further coupled by the dynamic ($\mathbf{K}$-dependent) interactions or by quasi-resonance interactions in the mixed crystal. The essence of the above statement is that whenever both site group and factor group splitting are expected together, the total effect cannot be treated as a simple superposition of the two independent effects. A separation of the two effects would be justified as a first approximation only if:

    (a)   The site-group interaction is at least an order of magnitude larger than the resonance interaction; and

    (b)   the site-group components are of different symmetry; or

    (c)   the resonance interactions are much larger than the site-group splitting.

Except for the first two cases, the so-called site-group splitting in a neat crystal will contain contributions not only from the phenomenological site-group splitting in the ideal mixed crystal, but also from resonance interactions.

The Orientational Effect - The effect of the crystal site on degenerate molecular states was considered in the last section. However, another site effect, referred to as Orientational "splitting" may be observed for non-degenerate modes in the spectra of dilute mixed crystals of partially deuterated ethanes in comparison to mixed C_2H_6/C_2D_6 crystals. This arises because the guest molecules can have different specific orientations with respect to the environmental field of the host; i.e., the guest molecule can orient itself in more than one way in this field, and the differently oriented vibrational transitions may have different "static" energies which appear as a "splitting" in the experimental spectrum. This is illustrated in Figure 3 for a dilute mixed crystal of C_2H_5D in C_2H_6 (or C_2HD_5 in C_2D_6). However, of the six distinct translationally-inequivalent orientations, 3(a) and 3(b) are energetically equivalent on the C_1 site of the host as are 3(c) and 3(d), and 3(e) and 3(f). This is easily understood by examining the nearest neighbor interactions. The orientational splitting therefore depends upon the site symmetry of the host. If the C_2H_5D (or C_2HD_5) guest
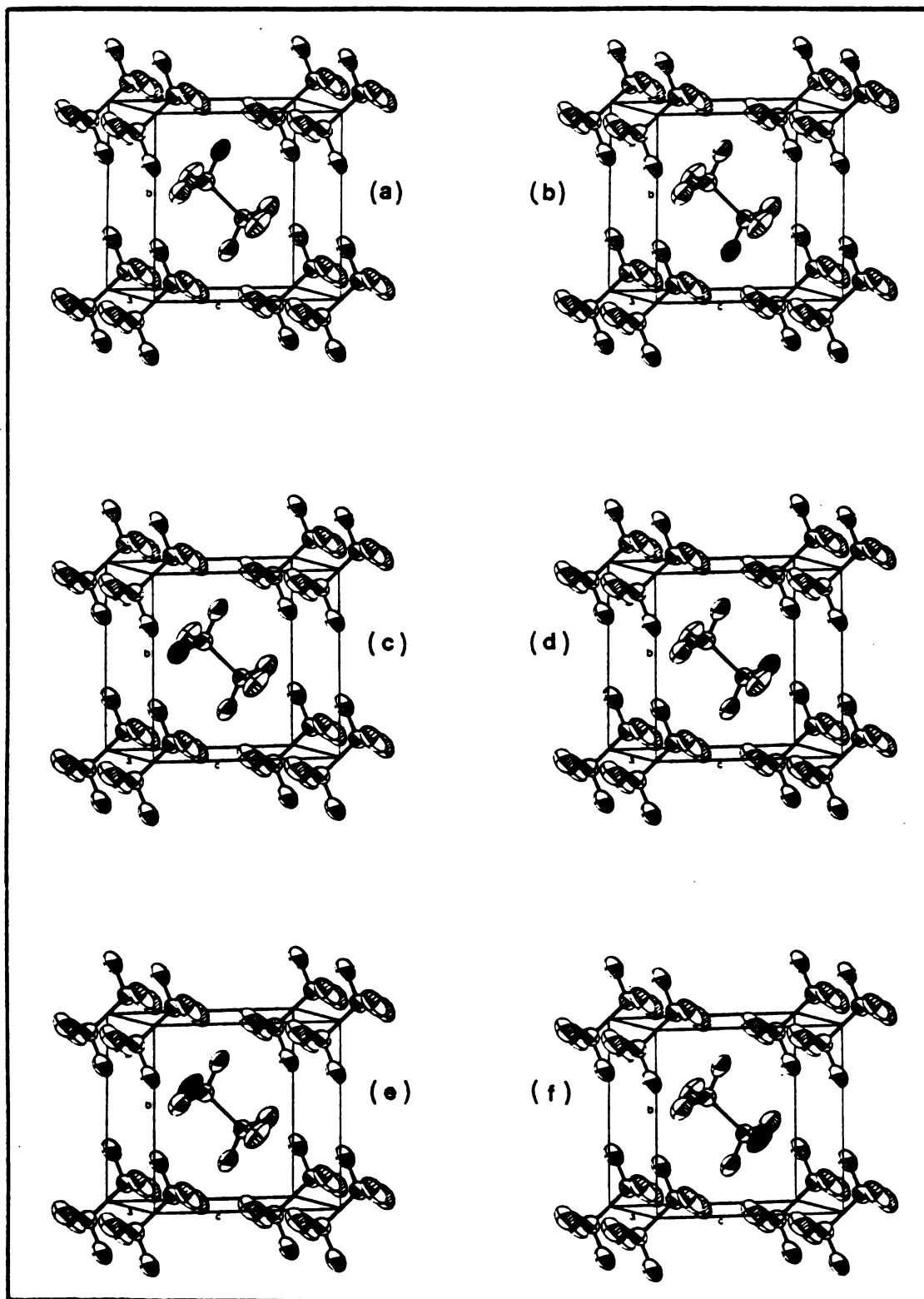
Figure 3 — The orientations of C_2H_5D in C_2H_6.

molecule resides on a C_1 site (which in a rigorous mathematical sense would apply, for example, to dilute mixed crystals of the d_1-isotope in the d_5-isotope), obviously the six orientations 3(a) - 3(f) would be energetically-inequivalent and a sextet is expected for the non-degenerate guest modes. Thus the number of components observed in the spectrum for a given vibration is an indication of the "effective" site symmetry.

The orientational effect has been observed for a number of isotopically-substituted molecules, including the partially deuterated ethylenes in our laboratory[17] and the partially deuterated benzenes by Bernstein.[29] Bernstein mentions in his report that the orientational "splitting" observed in mixed crystals occurs also in a neat crystal, but usually serves to broaden the exciton structure.

A group theoretical method described by Kopelman[51] may be used to determine the number of translationally-inequivalent orientations and the number of energetically-inequivalent orientations which exist for a given isotope. The number of energetically-inequivalent orientations which exist for the different partially-deuterated ethanes in a C_i or C_1 site are tabulated in Table 4.

As was pointed out earlier, the site splitting and orientational effect are similar and both are static effects. Therefore, the orientational "splitting" is also equivalent to the difference between Δ's in the dilute-mixed

Table 4. Number of Energetically-Inequivalent Orientations for C_2H_6 Isotopes in Sites of C_i and C_1.

Substituted Compound	Molecular Symmetry	No. of Orientations In Site of	
		C_i	C_1
Ethane-d_1 and-d_5	C_s	3	6
Ethane-1,2-d_2 and 1,1,2,2 d_4	C_2	3	6
	C_{2h}	1	3
Ethane 1,1-d_2 and 1,1,1,2-d_4	C_s	3	6
Ethane 1,1,1-d_3	C_{3v}	1	2
Ethane 1,1,2-d_3	C_s	3	6
	C_1	6	12

isotopic crystals.

It should be noted that partial deuteration of ethane destroys not only the D_{3d} symmetry of the free C_2H_6 molecule, but also results in the destruction of the translational as well as the C_i site symmetry of the crystal lattice, because in the partially-deuterated ethanes the molecules assume translationally-distinct orientations in the crystal. However, the disordered crystals may show an "effective" C_i site. This can be understood if one ignores the substituents on the C-C frame, and notes that the same crystal structure as the parent C_2H_6 is retained assuming negligible changes in the lattice parameters upon deuteration. One goal of this research was to ascertain whether the effective site symmetry in the partially-deuterated ethane crystals was C_1 or C_i.

CHAPTER III

EXPERIMENTAL

Research grade ethane (C_2H_6) was obtained from MG Scientific Gases and had a stated minimum purity of 99.99%. The $-d_1$, $-1,1-d_2$, $-1,1,1-d_3$, $-d_5$ and $-d_6$ isotopic species of ethane were obtained from Merck, Sharp and Dohme of Canada; their minimum isotopic purities were stated to be 96.34 atom %D, 98 atom % D, 98 atom %D, 99 atom %D and 99 atom %D, respectively. All samples were used without further purification. The mass spectrum of each compound was obtained using electron bombardment beam energies of 15 eV, 20 eV and 70 eV, but no additional information on impurities could be determined.

The gas phase samples were sprayed onto the cold cell substrate for both Raman and infrared experiments. The vapor-deposition technique was used because it is more convenient and controllable than growing polycrystalline samples from a drop of liquid (a technique sometimes employed in such studies), in that it allows samples of different thickness to be studied in the infrared and samples of good scattering quality to be obtained for Raman investigation. Both the back pressure and flow rate of the

sample were found to be important and critical in obtaining deposits of high scattering quality for Raman investigation. When the samples were deposited and a needle valve was used to control the flow in such a way that more sample was deposited on one side of the cold substrate, the sample looked snowy and very good scattering was obtained from that side. To get such a deposit, one starts to open the needle valve slowly until the beginning of the (white) condensate on the substrate is observed. Then the flow of the sample should be increased and controlled to maintain more deposition on one side. If the flow is slower than it should be, then a uniform deposit is obtained which has poorer scattering quality. The Raman samples were deposited at low temperature ($\sim$20°K) and then annealed at approximately 70°K for 15-30 minutes prior to recooling for spectroscopic observation. Annealing was important to be sure that the sample was in the stable ordered solid phase of ethane, the phase we were interested in studying. Annealing above 75°K (the melting points of the ethanes[52] are $\sim$90°K) produced solid samples with many cracks and of poor scattering quality. The infrared samples were deposited at about 70°K and maintained at that temperature for 5-10 minutes for annealing, and then slowly cooled for spectroscopic observation.

The dilute mixtures were made by mixing predetermined amounts of gas phase samples of the guest and host. A

high vacuum line with calibrated volumes was used, and the pressure of the gases was measured with a mercury manometer. The amount of the mixture made was such that it would yield a back pressure similar to that of the pure samples.

Instrumentation

An Air Products model CS-202 or CSA-202 Displex cryogenic helium refrigerator system was used for cooling the samples. Typical temperatures were between 16-23°K when the spectra were recorded, as measured by a gold (0.07% iron) vs. chromel thermocouple imbedded in the cold substrate. The higher temperature limit usually applied for the Raman experiments. The higher temperature is believed to be caused by the size of the Raman cell and the fact that the cell and shroud were not nickel plated. The temperature of the samples was controlled with either a cryodial model ML 1400 automatic temperature regulator or an Air Products temperature controller with calibrated platinum resistor for temperature sensing.

For IR experiments, $C_s I$ was used for the outer windows and the cold substrate. Quartz was used for the outer windows and copper for the substrate in the Raman work. Thin sheets of indium were placed between any two parts of the cryostats required to be in good thermal contact.

The Raman cell which was used has been described previously by Elliott and Leroi.[15] It is a closed cell which enabled evacuation independent to that of the shroud. The vacuum in the sample cell was about 2×10^{-5} torr before the cell was cooled and the sample deposited.

The following spectrometers were employed:

A Perkin-Elmer Model 225 IR grating spectrometer (4000-200 cm^{-1}), with resolution better than 1 cm^{-1} above 500 cm^{-1} and between 1-2 cm^{-1} below 500 cm^{-1}. Reported frequencies should be accurate to ± 1 cm^{-1}.

A Raman spectrometer comprised of a Jarrell-Ash model 25-100 double Czerny-Turner monochromator coupled with a thermoelectrically-cooled RCA C31034 Photomultiplier tube and a spectra physics Model 164 Ar^+ ion laser as the excitation source. Both the 5145 Å and 4880 Å lines of the Ar^+ ion laser were used as exciting lines for all Raman experiments in order to distinguish laser-fluorescence lines. In some cases the lattice spectra were also observed with the 4765 Å line of the argon-ion laser as the exciting line in order to positively eliminate interference from laser-fluorescence lines. The resolution in the Raman spectra was 1 cm^{-1} or better for the fundamentals and lattice modes.

Most of the reported infrared and Raman frequencies are believed to have an accuracy of ± 1 cm^{-1}, especially

for those of sharp and strong bands; for poorly resolved bands this accuracy is ± 2 cm^{-1}. However, for very broad bands in both the infrared and Raman the accuracy may fall to ± 3 to ± 5 cm^{-1}, as well as for overtones and combination bands.

CHAPTER IV

RAMAN PHONON MODES IN CRYSTALLINE C_2H_6, C_2D_6

AND PARTIALLY DEUTERATED ETHANES

A. Phonons in Disordered Crystals

It was pointed out in Chapter II that isotopic substi-
tuion in molecular ethane causes the molecular point group
symmetry, D_{3d}, of the parent (C_2H_6) molecule to be lost
with the formation of lower molecular symmetries. There-
fore, isotopically substituted molecular ethanes, C_2H_5D,
CH_3CD_3, C_2HD_5 . . ., etc. can assume several different
relative orientations upon solidification, and crystals
of these molecules are translationally disordered. This
might be a disaster in the interpretation of the experi-
mental results, because the mutual exclusion of the lattice
phonon modes is expected to be destroyed in the absence
of C_i site symmetry, and the "$\underset{\sim}{K}$-selection rule" may no
longer be applicable due to lack of translational symmetry.

Recently there has been much interest in the study of
phonons and excitons of heavily doped mixed crystals.
More studies, however, have been centered on excitons
rather than phonons.

Phonons of simple disordered systems of heavily doped isotopic mixed crystals like: benzene-h_6:benzene-d_6;[53] naphthalene-h_{10}:naphthalene-d_{10};[54] durene-h_{14}:durene-d_{14}[55] have attracted investigators the most. Their studies of the mixed crystals have provided information regarding the nature of phonon bands, the validity of the separation between librational and translational motions, line broadening, band mixing, and localization vs. delocalization in the mixed crystals. It has been observed that the phonon states of isotopic-mixed crystals are in the amalgamation limit;[53,56] that is, the same number of phonon bands are observed for mixed crystals as in the pure crystal, while the corresponding phonon bands shift almost linearly as a function of the concentration, between the positions of the two pure constituents. It appears as though the two substances are completely amalgamated to yield another new crystal with perfect periodicity. The mixed crystal can then be regarded as a virtually perfect crystal.

Hong and Kopelman[53] have shown, in their coherent potential approximation for interacting bands in the weak perturbation limit (virtual crystal limit[57,58]), that the phonon energies of the mixed isotopic crystals can be expressed as follows:

$$\omega = \omega_A/(1-C_B\Delta^f) \quad , \tag{30}$$

where ω_A is the frequency of the pure host and C_B is the mole fraction concentration of the guest. The parameter Δ^f is called the perturbation strength of the band and is defined as $(\eta_A^f - \eta_B^f)/\eta_A^f$, where f designates the degree of freedom (i.e., R_x, R_y, R_z, T_x, T_y, T_z) and η is the mass (for translations) or moment of inertia (for librations). If Δ^f is very small, Equation (30) can be rewritten as

$$\omega = \omega_A(1 + \frac{1}{2} C_B \Delta^f) \quad , \quad (31)$$

which predicts a linear dependence of the frequencies on the guest concentration. The weak perturbation assumption holds perfectly in substitutionally disordered systems, where the intermolecular force constants of the mixed crystals are the same as those of the pure crystal. It follows that, in substitutionally disordered systems:

(a) The K-selection rule is still valid;

(b) all the phonons are delocalized; and

(c) the normal coordinates described in the mass- or moment-of-inertia-weighted coordinate system remain unchanged in going from the pure host crystal to the pure guest crystal.

It can be concluded, then, that the spectroscopic activity of the lattice modes should remain unchanged. Thus, mutual exclusion would be retained if the pure crystal has

a centrosymmetric site symmetry. No significant changes in the phonon band widths are predicted in the virtual crystal limit. However, the relative intensity of the phonon modes may be altered relative to the pure crystal if Δ^f is different for different degrees of freedom. Hong and Kopelman[53] have indicated in their theoretical development that within the virtual crystal limit, the total intensity of the Raman spectra of the mixed crystal is equal to that of the pure crystal, but since Δ^f is usually different for each rotation, this would lead to mixing of intensities among different Raman bands. However, the infrared spectrum of mixed crystals should have the same intensity pattern as that of the pure crystal because Δ^f is always equal for all the translations.

Whitfield[16] has demonstrated that the neat, partially deuterated ethylene solids can be considered as isotopic-mixed crystals. Certainly this is true for partially-deuterated ethanes too, where the nearest neighbor atoms are either hydrogens or deuteriums as in a mixture of $C_2D_6:C_2H_6$. Thus the intermolecular interactions are quite similar to those in a mixture of C_2H_6 and C_2D_6. The fact that the phonon energies of isotopic mixed crystals are mass-dependent leads to the conclusion that an analogy can be drawn between the percent deuteration of a partially deuterated ethane and the concentration of the guest in a $C_2D_6:C_2H_6$ mixed crystal. For example, solid CH_3CD_3

is in many respects analogous to a mixed crystal containing equimolar C_2H_6 and C_2D_6.

Since in the virtual crystal limit the force constants and "effective" symmetry, i.e., the spectroscopically observed symmetry, of the crystal remain unchanged, the phonon frequencies of the partially deuterated crystals in this limit can be calculated assuming they are pure crystals. Therefore, the semi-classical method of calculating the phonon frequencies (TBON) discussed in Chapter II should still apply. The crystal symmetry and potential function remain the same for each ethane unit; only the masses of the molecules are different.

B. The Potential Function of Ethane

During the last decade there has been a great deal of interest in the normal vibrations of molecular crystals.[49] The intermolecular forces in crystals are of particular importance because of their close relation to the physical properties of solids.

In most cases, as was mentioned in Section C-1 of Chapter II, it is assumed that the intermolecular potential can be approximated as the sum of pairwise interactions between non-bonded atoms, each being expressed by an empirical or semi-empirical function.[59-61] This type of intermolecular force field has been used extensively in previous normal coordinate treatments of various molecular

crystals such as crystalline benzene,[41,62] poly-
ethylene,[47,63,64], <u>etc</u>.

Several atom-atom potentials have been proposed re-
cently, and their derivations have been extensively dis-
cussed, especially by Kitaigorodskii[59] and Williams.[60,61,65,66]
In particular, Williams has collected a large number of ex-
perimental data for entire classes of molecules and has
obtained several potential functions by simultaneous fitting
of crystal structures, heats of sublimation, and elastic
constants.

Several such potential functions have been used in the
calculation of the lattice frequencies of ethane in order
to determine which potential best fits the observed lattice
frequencies. Table 5 lists the parameters of the potentials
tested. The calculations were based on the use of a fore-
shortened bond length of C-H equal to 1.026 Å (reduced
from the gas phase value by 0.07 Å). This was required
for a consistent application of Williams' potentials,
because in deriving the parameters from crystal data,
Williams had to shift the location of the repulsion-attrac-
tion center by 0.07 Å toward the C atom along the C-H
bond.[67] The choice of 6 Å for truncation of the inter-
action radius was made because it is sufficient to ensure
the convergence of the calculated frequencies to a constant
value.[68] The unit cell dimensions from the x-ray work by
Van Nes and Vos[27] were used without any refinement for

Table 5 — Nonbonded Potential Parameters*, Where $V_{ij} = -Ar^{-6} + Bexp(-Cr) + Q_iQ_jr^{-1}$

Set	C····C				C····H				H····H				Ref.
	A	B	C	Q_iQ_j	A	B	C	Q_iQ_j	A	B	C	Q_iQ_j	
I	506	47460	3.60	0	127	12640	3.67	0	32	2145	3.74	0	61
II	505	61900	3.60	0	128	11000	3.67	0	32.3	2629	3.74	0	61
III	187	47810	3.60	0	266	14580	3.67	0	-19.4	1628	3.74	0	61
IV	443.2	68821	3.611	0	150	9772.8	3.669	0	44.14	3429.8	3.787	0	41
V	566.7	78658.8	3.610	0	127.6	8809.9	3.669	0	26.5	2260.3	3.738	0	41
VI	568	83630	3.60	0	125	8766	3.67	0	27.3	2654	3.74	0	61
VII	514	69600	3.60	0	141	9421	3.67	0	38.8	4000	3.74	0	61
VIII	511.5	71701.7	3.60	0	111.7	8508.6	3.67	0	24.4	2170.2	3.74	0	69
IX	535	74460	3.60	0	139	9410	3.67	0	36	4000	3.74	0	60
X	578.4	97896	3.60	.025	131.9	15155.3	3.67	-.025	30.11	2346.1	3.74	.025	66

*Units are kcal./mole(A&B), Ångstrom(C) and electron^2(Q_iQ_j).

minimum crystal energy.[72]

Potential functions I, II and III were obtained by Williams[61] from a least-squares fit of observed and calculated crystal data of aliphatic hydrocarbons only. Potential IX was obtained by a least-squares fit of observed and calculated crystal data for aromatic hydrocarbons,[60] while potentials VI, VII and VIII were obtained by least squares refinement between the observed and calculated crystal structures of both saturated and aromatic hydrocarbons.[61,69] Potential functions IV and V have been obtained by Taddei, et al.[41] by a least-squares refinement of potential functions VI and IX to obtain the best agreement between the calculated and observed lattice frequencies of benzene, whereas potential X recently obtained by Williams[66] from 18 saturated and aromatic hydrocarbon crystal structures, includes an optimum net point charge of .159 $\bar{e}$ on the hydrogen and carbon atoms.

Each interaction potential was used to calculate the lattice frequencies of ethane and the results compared to the observed values. The results are tabulated in Table 6 which includes also the standard deviations. The best agreements with the observed librational frequencies are obtained with potential functions I, II and VI. The agreement for translations is best with potentials V and VIII; however, the low frequency librational modes calculated with these potentials fit more poorly the experimental

Table 6. The Observed and Calculated Lattice Frequencies (cm^{-1}) of Solid (II) Ethane.

						Potential Set					
Librations Obs.	I	II	III	IV	V	VI	VII	VIII	IX	X
77	74	78.5	84.5	71.5	69	77	92	70.5	93.5	83
98.5	82	83	86	75	73	80.5	93	74.5	95	83
102	99	102	106.5	98	92	100	118	92	120	113.5
117	110.5	119	122	118	108.5	119	142	108.5	144	118.5[a]
120	124	131.5	140	126	118	129	156	118.5	159	134.5
131.5	130	141	147.5	140.5	128.5	141	171.5	128	173.5	138.5
Translations										
83[b]	75.5	76.5	77	74	69.5	75	87	70	88	92
101[b]	94	93	93.4	88	84.5	92	104	85	106	107
	107.5	110	111	108.5	101	110	127.5	101	129	115.[a]
rms[c]	8.01	9.02	11.85	9.97	10.61	9.18	25.42	9.92	27.22	14.42

[a] These could be interchanged, since they have contribution from both librational and translational modes.
[b] From Reference 23.
[c] root-mean-square error, rms = $\{\Sigma[(\nu_{exp}-\nu_{calc})^2/n]\}^{1/2}$.

values compared to the predictions of potentials I, II
and VI. As a result, the overall agreement for both trans-
lational and librational frequencies is best with potential
functions I, II and VI, as is clear from the calculated root-
mean-square error shown in Table 6. Although potential
I fits the observed lattice frequencies of C_2H_6 better
than II, and II is slightly better than VI, it was found
that the reverse is true for C_2D_6 and the partially-
deuterated species. The best potentials for C_2H_6 were
used to calculate the lattice frequencies of C_2D_6. The
calculated and observed frequencies of C_2D_6 are listed in
Table 7. Comparison of the standard deviation for the
observed and calculated librational and translational
frequencies of C_2D_6 indicates that potential II is pre-
ferred to I and VI with the agreement being poorest for
potential I. Therefore it was concluded that potential
II is superior among the potentials tested, and that po-
tentials VI and I are the next best potentials for the
crystalline ethanes.

It may be noted that recently Eggers and Wisnosky have
been involved in similar calculations for crystalline
ethane.[28] They employed a different program and their con-
clusions differ from those drawn above. Prior to the
calculation of the normal mode frequencies they performed
an energy minimization calculation for the crystal struc-
ture, which leads to a structure slightly different from

Table 7. The Observed and Calculated Lattice Frequencies
(cm^{-1}) of Solid (II) C_2D_6.

Observed Librations	I	II	VI	VIII
57	57.5	61	59	54
81	68	69	67	62
84.5	83.0	85.5	84	77
98.5	85.0	92	91.5	83
----	96	101	100	91
103	99.5	109	109	98.5
Translations				
----	69.0	70	69.0	63
76.5[a]	85.5	84.5	84.	77.5
91.5[a]	98.0	100.5	100.5	92
rms	9.02	7.99	8.38	10.71

[a]From Reference 23.

the experimental one. They have tested only three poten-
tial functions (here numbered VI and VIII, and one of
Williams' Coulombic potentials).[68] They selected the
Coulombic potential as the best intermolecular interaction
function for ethane, based on the fairly good agreement
with the translational lattice modes and the slightly
better fit to the splitting observed for the internal
modes. It is unlikely that this is the best choice.
From Table 6 it may be noted that the Coulombic potential
gave poor agreement, on the average, with the observed
librations and translations. It is not safe to choose
the best potential on the basis of only three models. In
contrast, a broad range of potential functions were used
in the calculations reported here, and the transferability
of potential II, which was obtained by a least-squares
refinement to the crystal data of aliphatic hydrocarbons,
in calculating the lattice frequencies of the (aliphatic
hydrocarbon) ethane crystal is not suprising. The claim
that potential II is the best one, and the rejection of
the Coulombic one in the calculation of the lattice fre-
quencies of ethane is supported by a statement by Wil-
liams[65] that "the Coulombic contribution to the lattice
energies of aliphatic hydrocarbons (n-pentane, n-hexane,
n-octane) is less than 1%, while it reaches a value of 29%
of the total lattice energy of benzene.

As a final point, it should be mentioned that potential

II is not necessarily the best overall potential function for crystalline ethane; an examination of how well the various potentials predict the internal mode frequencies is required for a better judgment.

Only two of the three expected infrared-active translations of C_2H_6 and C_2D_6 have been observed.[23] The energies of these phonons are 83 cm^{-1} and 101 cm^{-1} for ethane-h_6 and 76.5 and 91.5 cm^{-1} for ethane-d_6. The third optically active translational mode has been calculated to be at lower frequency (see Tables 6 and 7). Potential VIII also provided the best agreement for the translational frequencies of C_2D_6 (Table 7). Therefore the translational frequencies for all isotopic species of ethane were calculated using potential VIII; they are tabulated in Table 8. It is to be noted that potential VIII predicts the exact value of

Table 8. Calculated Translational Frequencies (cm^{-1}) of Ethanes From Potential Set VIII.

d_0		d_1	d_2	d_3	d_4	d_5	d_6	
Obs.[a]	Calc.						Obs.[a]	Calc.
---	70	68.5	67.5	66.5	65.5	64.5	---	63
83	85	84	82.5	81.0	80.0	79.0	76.5	77.5
101	101	99.5	98.0	96.5	95.0	94.0	91.5	92

[a]From Reference 23.

the highest translational frequency of both C_2H_6 and C_2D_6, while the second highest calculated translational frequency for C_2H_6 and C_2D_6 is higher by 2 and 1 cm^{-1} than the observed ones, respectively. This is certainly expected to be true for isotopic species of ethane as well.

C. The Librations of the Ethanes

The Raman spectra in the lattice region of the stable phase of ethane-d_0, ethane-d_6 and several partially deuterated species are shown in Figures 4 and 5. Six bands for C_2H_6, and at least five bands for C_2H_5D, CHD_2CH_3, CH_3CD_3, C_2HD_5 and C_2D_6 were observed, with a second-highest frequency band of C_2H_5D, CHD_2CH_3 and C_2HD_5 appearing as shoulders. A comparison of the observed and calculated (from potentials II and VI) librational frequencies of ethane-d_0, -d_1, -$1,1$-d_2 and d_5 was used to estimate the "missing" band for CH_3CD_3 and C_2D_6. The situation is complicated because the librational modes which lie second and third-highest in ethane-d_0 "cross" positions with increasing deuteration, according to the eigenvector distribution (see Table 10). For CH_3CD_3 these two modes are predicted at 110.5 cm^{-1} and 105 cm^{-1} by potential II, and their eigenvectors are mixed. However, if the difference between the calculated and observed frequencies of these two vibrations from C_2H_6, C_2H_5D, $1,1$-$C_2H_4D_2$ and C_2HD_5
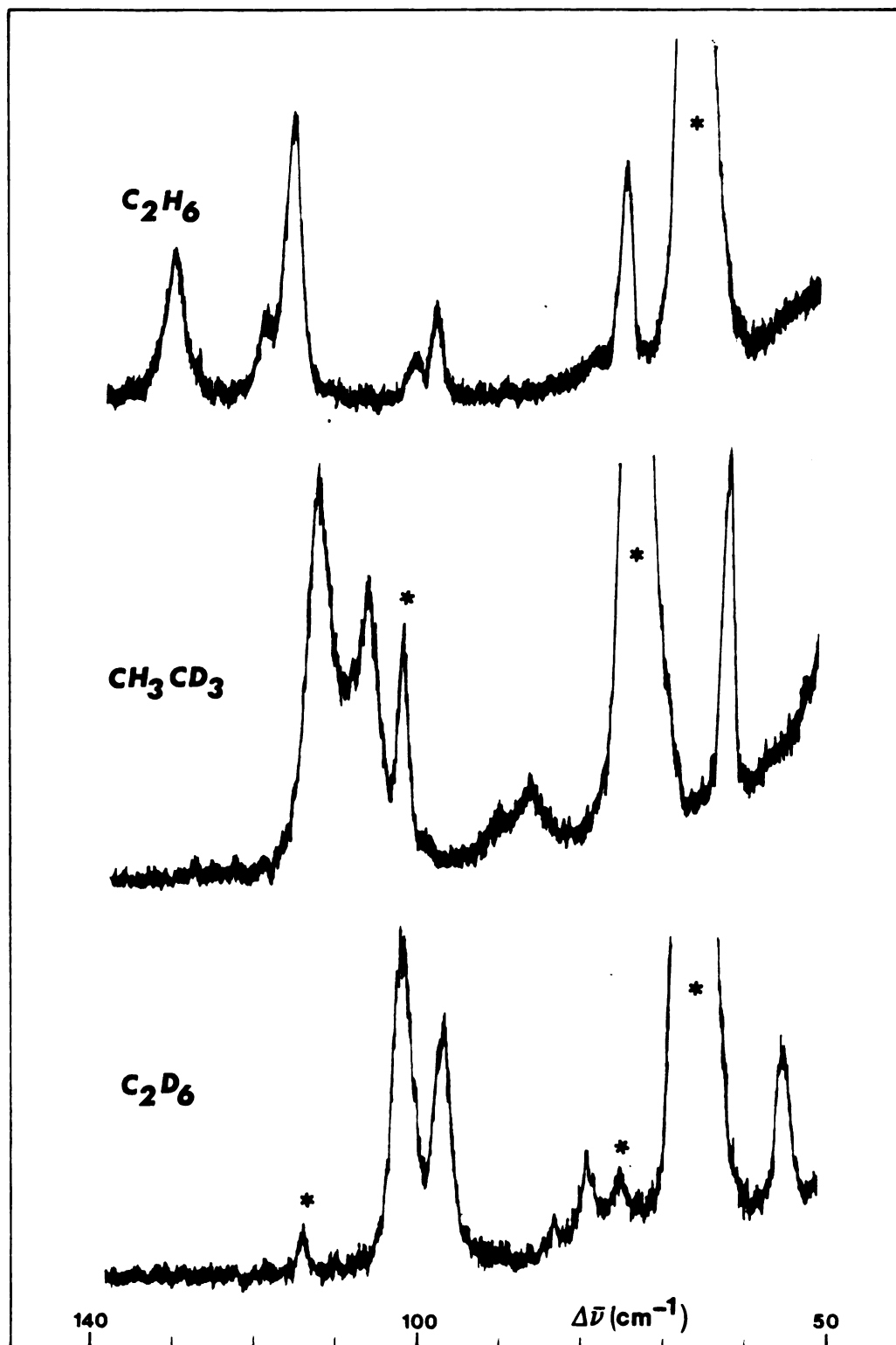
Figure 4 — The Raman lattice region of C_2H_6, CH_3CD_3 and C_2D_6. The peaks marked with an asterisk are laser-fluorescence lines.
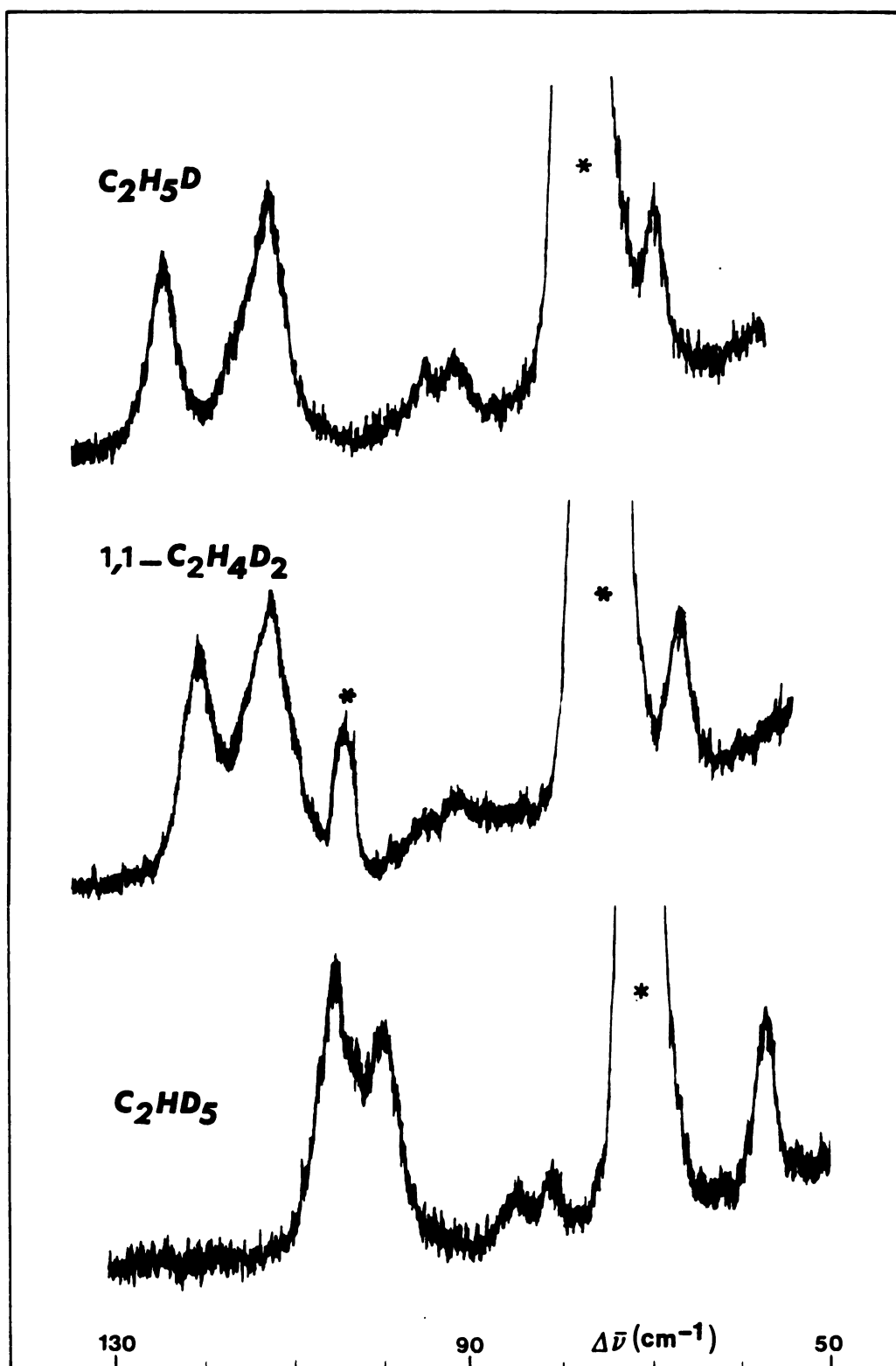
Figure 5 — The Raman lattice region of solid (II) C_2H_5D, $1,1-C_2H_4D_2$ and C_2HD_5; the peaks marked with an asterisk are laser fluorescence lines.

are interpolated to CH_3CD_3 then both can be expected to lie near 108 cm^{-1}. A band is indeed observed in CH_3CD_3 at 108.5 cm^{-1} (see Table 9), which is relatively stronger in comparison to the other librational intensities than one might expect from the other isotopic ethanes. Perhaps it encompasses both of the bands expected in this range. In C_2D_6 the two vibrations retain the distinctive normal mode distribution found for C_2H_6, the expected correlation being (in cm^{-1}), 120 (d_0): 92 (d_6) and 117 (d_0): 101 (d_6). Extrapolation of the frequencies observed for the other ethanes suggests that the former would lie in the 97-100 cm^{-1} range and the latter would fall between 98 and 101 cm^{-1}. Again a single band is observed for C_2D_6 in this region, at 98.5 cm^{-1}, which may belong to both librational modes.

The frequencies of the lattice modes of the partially-deuterated ethanes were calculated using interaction potential II. It was assumed that deuteration causes only a change in the mass of the molecule and that the symmetry of the lattice remains unchanged. The slight changes in bond lengths and bond angles upon deuteration were also neglected, since these should have only a minor effect on the calculated frequencies. The calculated and observed librational frequencies are given in Table 9. The agreement between the calculated and observed values is as good as that for ethane-d_0 and ethane-d_6.

Table 9. The Observed and Calculated Librational Frequencies (cm^{-1}) of Ethanes.[a]

C$_2$H$_6$		C$_2$H$_5$D		1,1-C$_2$H$_4$D$_2$		CH$_3$CD$_3$		C$_2$HD$_5$		C$_2$D$_6$	
Obs.	Cal.	Obs.	Cal.	Obs.	Cal.	Obs.	Cal.	Obs.	Cal.	Obs.	Cal.
77	78.5	71.5	74.5	67.5	71	64.5	68	58.5	63	57	61
98.5	83	95	80	92	77.5	89	75	82.5	71	81	69
102	102	98	98.5	95	95.5	92	92.5	87	87.5	84.5	85.5
117	119	113	114.5	112	110		105	100.5	96	98.5	92
120	131.5	116	122	115	115.5	108.5	110.5	103.5	104		101
131.5	141	125.5	133	120.5	127	113.5	121	107	112.5	103.5	109

[a]Calculations based on potential set II.

The crystal normal coordinates obtained from TBON for the librations of the crystalline ethanes are given in Table 10. The eigenvectors provide a direct measure of the degree of mixing of molecular rotations or of translations in each normal mode. It is to be noted that mixing of the translational and rotational degrees of freedom was strictly forbidden, since the frequencies were calculated assuming centrosymmetric site symmetry for each ethane crystal. The eigenvectors listed in Table 10 show that in most cases it is impossible to think of a crystal normal mode as being a pure rotation around a given principal molecular axis. In fact, it is seen from Table 10 that some modes are mixed by more than 20%, and even up to 50% (the highest and the lowest frequency modes). However, the relative contribution of each rotation to each normal coordinate remains essentially unchanged in going from C_2H_6 to C_2D_6, except for the eigenvectors for the second- and third-highest frequencies of C_2H_6, which "mix" and "cross" at $C_2H_4D_2$ and $C_2H_3D_3$.

The calculated and observed librational frequencies are plotted against the number of deuterium atoms per molecule in Figures 6 and 7, respectively. A virtually linear dependence between the frequencies and number of deuteriums are predicted for the four lowest frequency vibrations in Figure 6. (Note that the fifth lowest frequency of ethane d_3-d_6 corresponds to the fourth lowest frequency

Table 10.   The Crystal Normal Coordinates of the Librations
            of the Ethanes.

Crystal	$\nu_{calc.}$ $(cm^{-1})^a$	R_x	R_y	R_z
C_2H_6	78.5	.63	−.03	.77
	83	.11	−.11	−.99
	102	.11	.99	.05
	119	.24	−.97	.03
	131.5	.96	.24	.10
	141.	.77	−.11	.63
C_2H_5D	74.5	.66	−.03	−.75
	80	.12	−.01	−.99
	98.5	−.11	−.99	−.06
	114.5	.39	−.92	.05
	122	.91	.39	.11
	133	−.74	.12	−.66
$C_2H_4D_2$	71	.69	−.02	−.72
	77.5	.13	−.01	−.99
	95.5	−.11	−.99	−.08
	110	.61	−.79	.09
	115.5	.78	.62	.10
	127	.72	−.13	.69
$C_2H_3D_3$	68	.71	−.02	−.70
	75	−.14	.01	.99
	92.5	−.11	−.99	−.09
	105	.81	−.57	.12
	110.5	−.57	−.82	−.07
	121	.70	−.14	.70

Table 10. Continued.

Crystal	$\nu_{calc.}$ $(cm^{-1})^a$	R_x	R_y	R_z
$C_2H_2D_4$	65	-.73	.01	.69
	73	.15	.01	.99
	90	-.11	-.99	-.10
	100.5	-.90	.42	-.14
	107	-.41	-.91	-.05
	116.5	.68	-.15	.72
C_2HD_5	63	-.74	.01	.67
	71	-.16	.01	.99
	87.5	-.11	-.99	-.11
	96.0	-.93	.32	-.16
	104	-.32	-.95	-.04
	112.5	.66	-.15	.73
C_2D_6	61	-.75	.01	.66
	69	.17	-.01	-.98
	85.5	-.11	-.99	-.11
	92	-.95	.27	-.17
	101	-.26	-.96	-.04
	109	.65	-.16	.74

[a]Calculations based on potential set II.
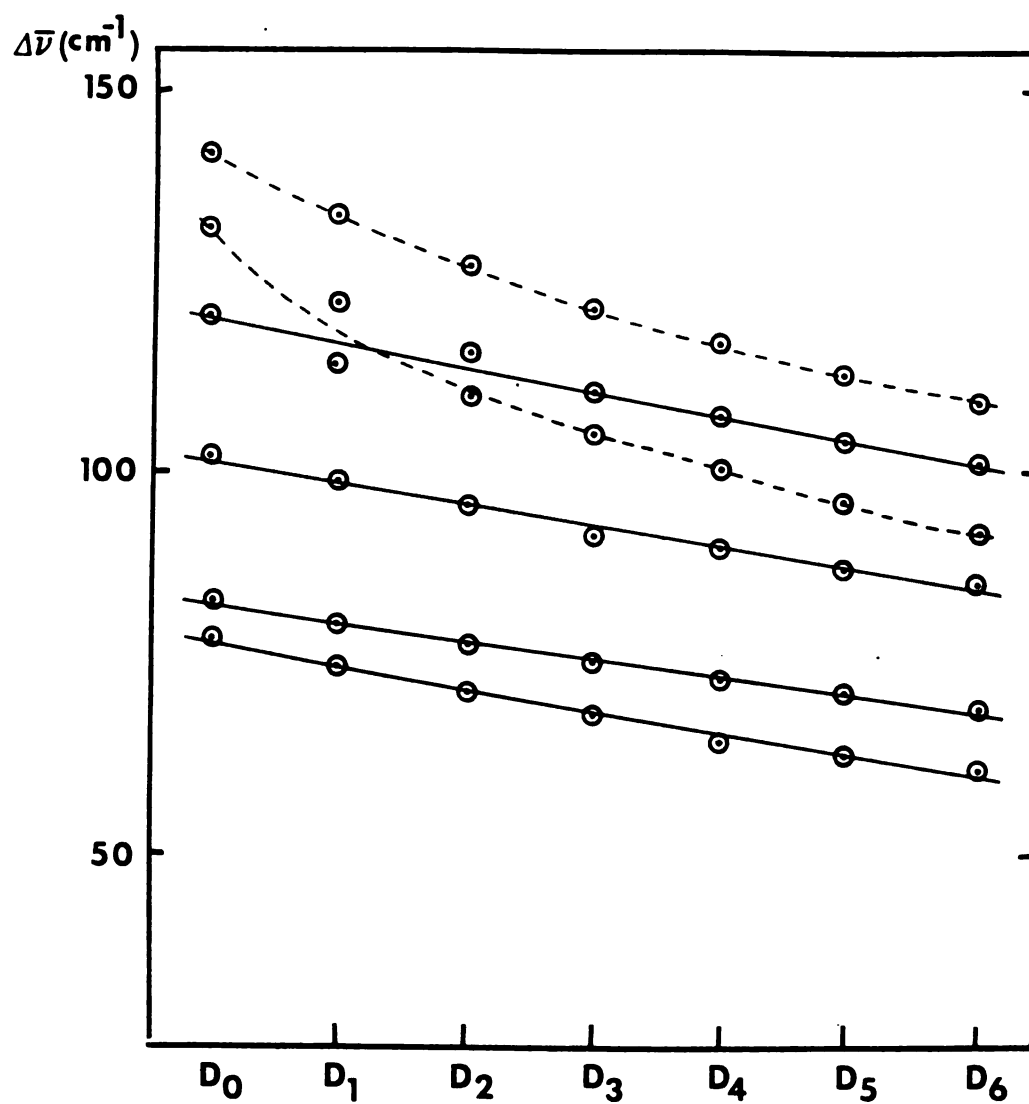
Figure 6._The calculated librational frequencies versus the number of deuterium atoms.
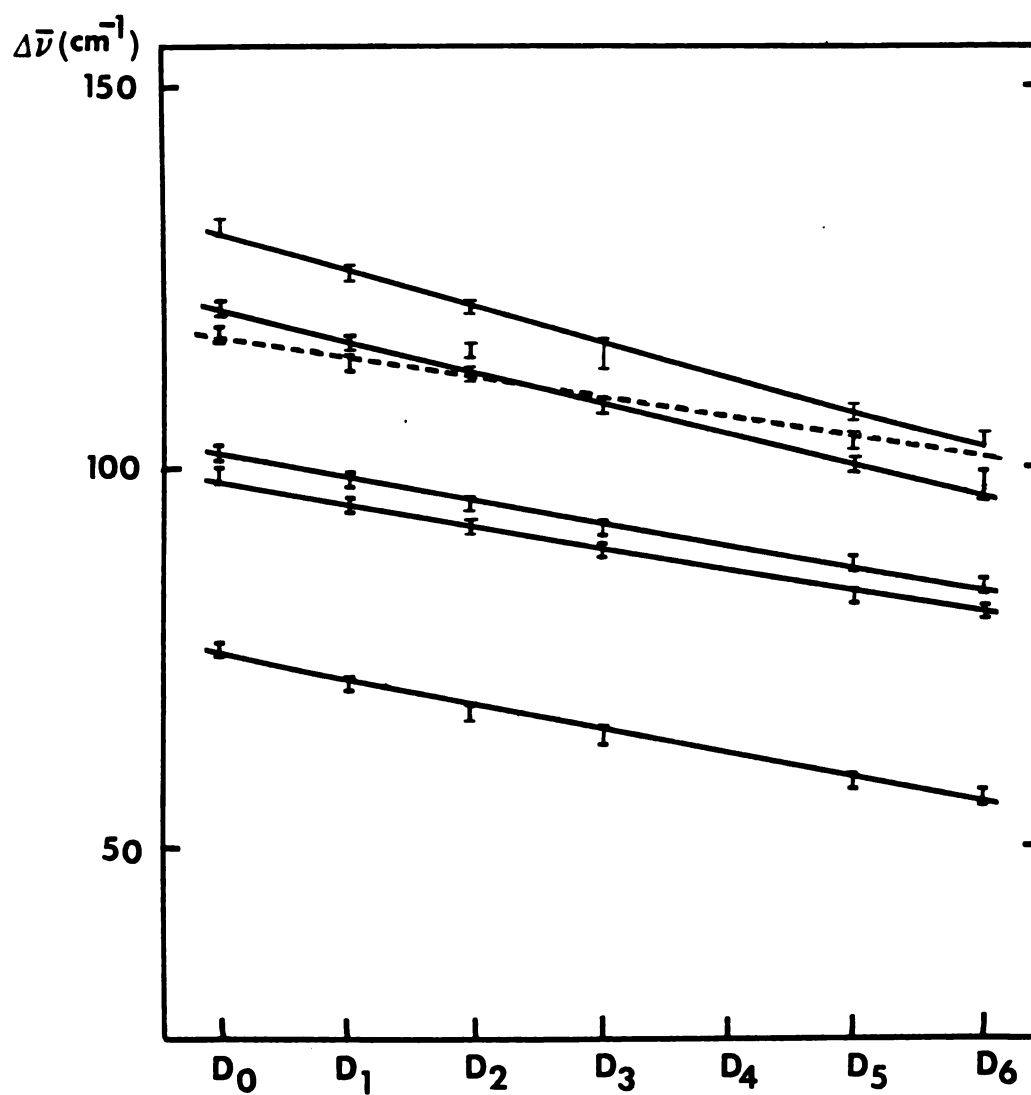
Figure 7 _The observed librational frequencies versus the number

of deuterium atoms.

of ethane d_0-d_2.) This is expected also on the basis of the low perturbation strengths calculated from moment-of-inertia data ($\Delta^{R_y} = \Delta^{R_z} = -.44$), and Equation (31). Therefore, the frequency dependence on the percentage deuteration should be described by Equation (31) for these bands. Non-linear behavior is predicted for the two highest frequency bands of ethane-d_0 and their counterparts in the deuterated species, suggesting that Equation (30) should describe the curves for these bands.

The perturbation strengths, Δ^f, of the calculated frequencies are given in Table 11 along with the experimentally observed values of Δ^f, and those calculated for pure rotations about the principal axes from the moments-of-inertia of C_2H_6 and C_2D_6. The Δ^f's of the calculated frequencies were determined by calculating the perturbation strength for each point with Equation (30), and then finding the average Δ^f for the band. (The averages, in fact, were very close to those calculated for the CH_3CD_3 bands.) The experimental perturbation strengths were found by determining the slopes of the lines shown in Figure 7 and using Equation (31) to determine Δ^f. If one wishes to draw a line straight through the points of the two highest frequency bands, it is necessary to increase the uncertainty of the peaks at 113.5 cm^{-1} for CH_3CD_3 and 98.5 cm^{-1} for C_2D_6 to ±2.5 and ±2 cm^{-1}, respectively, even though the experimental uncertainty is closer to ±1 cm^{-1}.

Table 11. Perturbation Strengths of the Ethane Librations.

$$\Delta^{R_x} = -.99 \qquad \Delta^{R_y} = -.44 \qquad \Delta^{R_z} = -.44$$

Libration (C_2H_6) cm^{-1}	$\Delta^f_{(exp)}$[a]	$\Delta^f_{(calc)}$[b]
77	-.41	-.65
98.5	-.34	-.45
102	-.36	-.42
117	-.36	-.40
120	-.48	-1.02
131.5	-.63	-.67

[a]From Figure 7.

[b]From Figure 6.

The values of the experimentally-determined perturbation strengths are consistent with those expected for rotational motions ($\Delta^f_{translation}$ = -0.2), given in Table 11. The greater experimental uncertainty of the measured value of the second-highest frequency band may account for the somewhat larger discrepancy. As also is indicated by the normal coordinate calculation, the Δ^f's for the four lowest frequency (C_2H_6) librations are primarily motions about the y and z principal rotational axes of the molecule. However, it will be noticed from Table 10 that the lowest and highest frequency bands are in fact strong mixtures of rotations about the x- and z-axes. This mixing accounts for the strong intensity of these bands relative to expectations based on the oriented gas model[71] for librations primarily around the C-C axis.

The fact that only five or six Raman-active phonons are observed for the partially deuterated ethanes, and their energies vary smoothly with the degree of deuterium substitution, indicates that the librational motions of the ethane crystals are amalgamated. Furthermore, the applicability of Equation (31) to five of the modes, and of Equation (30) to the sixth, shows that solid ethane can be treated in the virtual crystal limit. This conclusion is supported by the close agreement between the experimental perturbation strengths and those calculated on the basis of the virtual crystal approximation. The virtual

crystal limit implies that the partially-deuterated mole-
cules form substitutionally disordered crystals. Moreover,
this implies that the effective lattice symmetry of the
partially-deuterated ethane crystals is the same as that
of the C_2H_6 and C_2D_6 lattice, and that the intermolecular
force constants remain unchanged.

The relative intensities of the Raman lattice modes
of crystalline ethane and deuterated species are shown in
Figure 8. No significant changes in the relative intensi-
ties of the librations are observed for the partially-
deuterated ethanes, although this is permitted by the
virtual crystal theory, since for ethane $\Delta^{R_x} \neq \Delta^{R_y} = \Delta^{R_z}$.
The apparent higher intensity of the highest frequency
mode in CH_3CD_3, C_2HD_5 and C_2D_6 is believed to be due to
some contribution from an "unobserved" component (the
second highest frequency band) in the above crystals. At
the same time, Figure 8 nicely shows the smooth decrease
of librational band energies with the degree of deuterium
substitution, as is expected. It is also interesting to note
that the lowest and the highest energy librational bands,
which according to the normal coordinate calculation both
have contribution from rotation about x and z principal
axes, move faster to lower frequency than other modes in
the deuterated species.
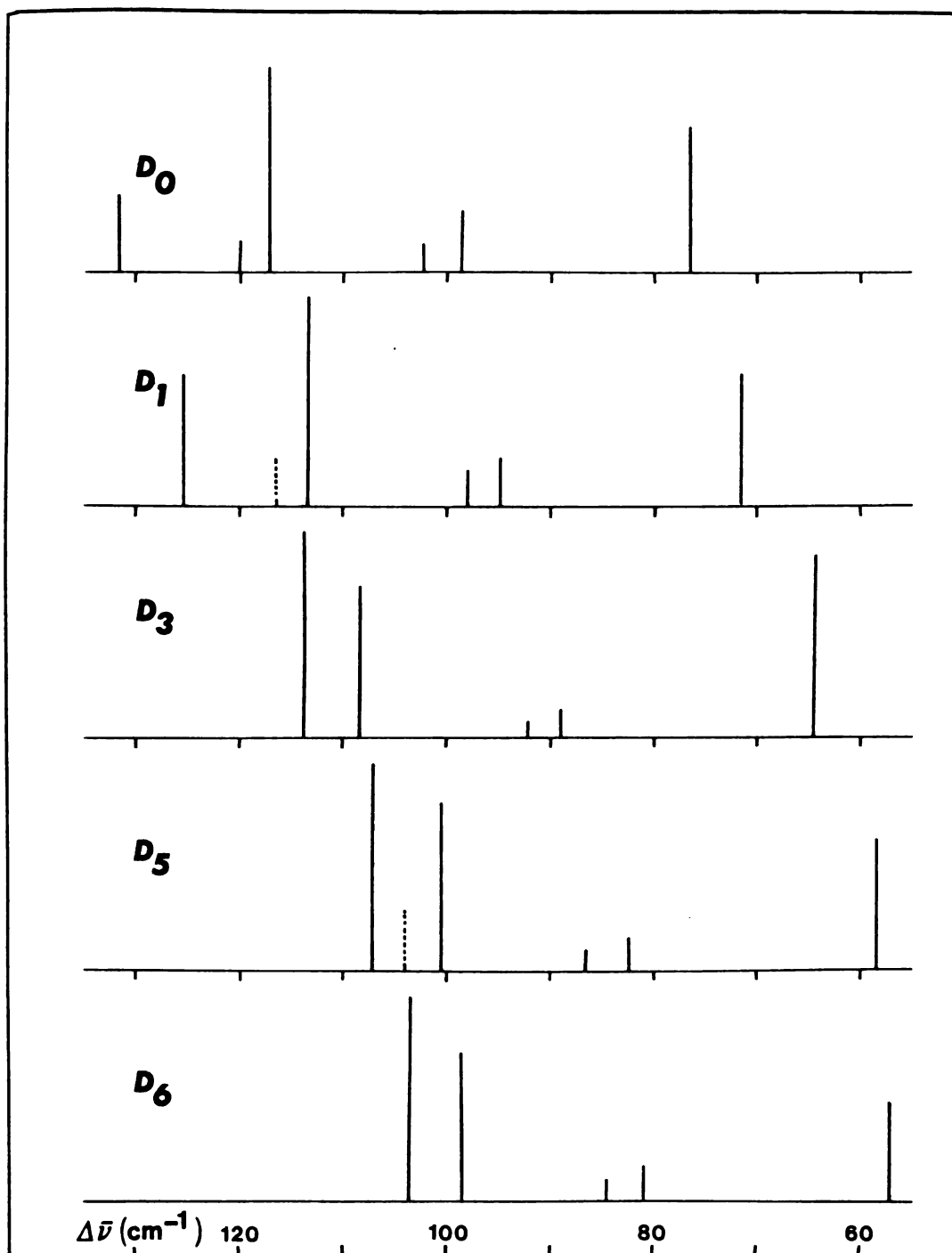
Figure 8 _ The Raman lattice modes of crystalline C₂H₆ and deuterated species.

Relative intensities within each species are denoted by the vertical lines. Shoulders in the experimental spectra are indicated by dotted lines.

D. <u>Raman Phonon Modes in the Metastable Solid Phase of</u>

    <u>Ethanes</u>

In the course of this research we were notified by
Eggers[70] of a newly-found phase for ethane, called the
metastable phase, indicating its behavior. A complete
description of this phase and the conditions under which
it is obtained in pure form are given elsewhere.[39] After
learning of the existence of such a phase we noticed that
some of our earlier spectra belonged to either the pure
metastable phase or to a mixture of both crystalline phases.
The spectra of the metastable phase show many regions of
marked difference from those of the stable phase (II),
especially in the lattice region, where the location,
relative intensities and the number of phonon bands are
different. This fortunate difference in the Raman lattice
region then permitted us to check for purity of the ordered
stable phase (II), which was the primary subject of the
present investigation. Because our main interest was the
study of the ordered stable phase (II) of the ethanes,
here we only show, in Figures 9 and 10, examples of the
Raman lattice region of the pure metastable phase of CH_3CD_3
and C_2HD_5, and of a mixture of metastable and stable phases
of C_2H_6 and C_2D_6. The spectra were taken at 23°K for
C_2H_6, CH_3CD_3 and C_2HD_5, and at 30°K for C_2D_6; the annealing
temperature was 38°K for C_2H_6 and about 50°K for the other
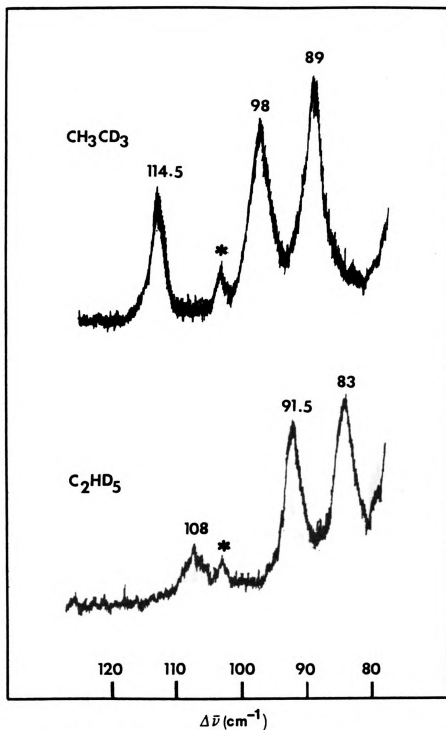
Figure 9 —The Raman lattice region of CH_3CD_3 and C_2HD_5 in metastable phase. The peaks marked with an asterisk are laser-fluorescence lines.
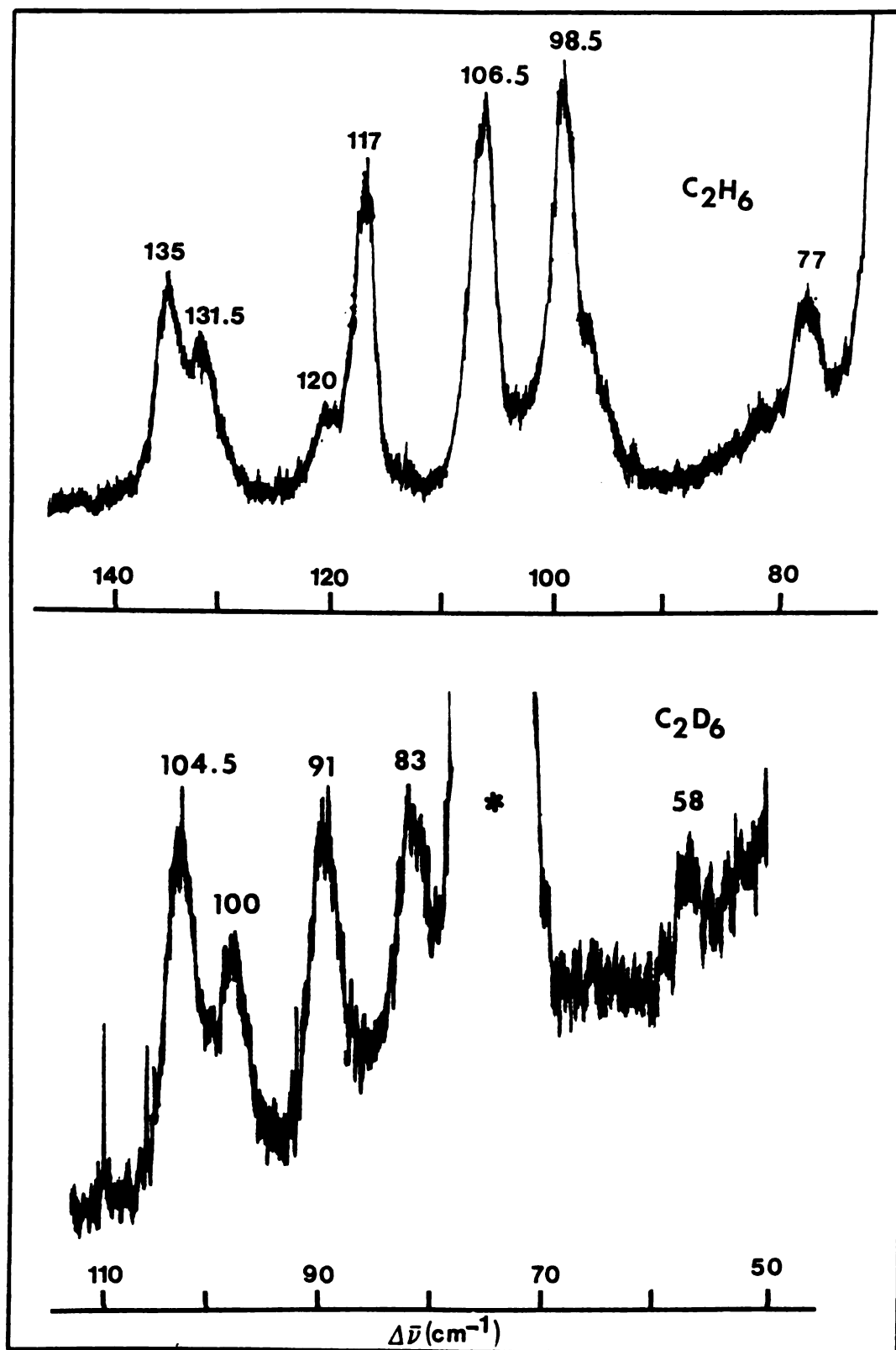
Figure 10 — The Raman lattice region of C_2H_6 and C_2D_6 in the

Presence of both stable and metastable Phases.

The peak marked with an asterisk is a laser-fluorescence line.

three crystals.

The metastable phase, as exemplified in Figure 9, shows three bands in the Raman lattice region, two bands of essentially equal intensity separated by about 8 cm^{-1} and a less intense peak at higher frequency. It was noted, from the comparison of the stable and metastable phase spectra, that the two intense peaks in the metastable phase have similar components in the stable phase, but of weak intensity, separated by 3-4 cm^{-1}, and that the third band corresponds to the highest-frequency band in the lattice region of the stable phase. Therefore, the presence of the metastable phase can be distinguished by the two intense peaks described above. Table 12 below lists the librational frequency modes of C_2H_6, C_2D_6, CH_3CD_3 and C_2HD_5 in the metastable solid phase.

Table 12. The Librational Lattice Frequencies (cm^{-1}) of Ethanes in the Metastable Phase.

C_2H_6	CH_3CD_3	C_2HD_5	C_2D_6
98.5	89	83	83
106.5	98	91.5	91
135	114.5	108	104.5

E. <u>Conclusions</u>

The following conclusions have been drawn in this chapter:

(a) The interaction potential II, which has been obtained by a least-squares refinement to the crystal data of aliphatic hydrocarbons, is the best overall potential function for ethane. This also confirms the transferability of such an interaction potential to other aliphatic hydrocarbons.

(b) The librations of the ethanes are amalgamated and can be described in the virtual crystal limit. This implies that:

(1) The effective lattice symmetry of the partially-deuterated ethane crystals is the same as the lattice symmetry of the C_2H_6 and C_2D_6 crystals; therefore $\underline{K}$ is still a "good quantum number" and the effective site symmetry is C_1.

(2) The intermolecular force constants and the lattice normal coordinates remain unchanged in going from the C_2H_6 to the C_2D_6 crystal.

(3) The bands observed in the Raman phonon region are the librations - no interference from the translations was observed, consistent with a C_1 site.

(c) The observed Δ^f's predict a mixing of the rotations about the principal axes, as does the frequency calculation.

CHAPTER V

THE ORIENTATIONAL EFFECT, A MEANS FOR PROBING
THE SITE SYMMETRY OF THE PARTIALLY-DEUTERATED
CRYSTALLINE ETHANES

A. <u>Theory</u>

In the previous chapter it was shown that mutual ex-
clusion for the lattice vibrations of the partially-deuter-
ated ethanes is retained, and it was concluded that the
lattice vibrations of these crystals experience an "ef-
fective" C_i site symmetry. In this context "effective"
means that the electronic distribution of the neighbors,
but not their isotopic composition, governs the inter-
molecular interactions. Thus it can be said that the
molecules cannot distinguish between hydrogens and
deuteriums on the neighboring molecules.

A knowledge of the "effective" site symmetry is neces-
sary for the interpretation of the spectra of the internal
modes of the neat partially-deuterated ethanes because the
orientational effect may complicate these modes, and the
number of energetically inequivalent orientations depends
on the site symmetry. However, the orientational effect
may also be used to probe the "effective" site symmetry

of the partially-deuterated crystals.

The discussion in Chapter II showed that the number
of orientational components observed for the guest modes
of a dilute isotopic mixed crystal is governed by the site
symmetry of the host as well as the guest point-group sym-
metry. A group theoretical procedure as described by
Kopelman[51] can be used to determine the number of orienta-
tional components expected for the partially-deuterated
ethanes in sites of C_1, C_i or any other symmetry. Our
approach in Chapter II, however, was of a more straight-
forward and physical nature. The results for the number
of energetically inequivalent orientational components
determined for a C_1 or C_i site were listed in Table 4.

All of the partially-deuterated ethanes can be used
as probes of the site symmetries of the other partially
deuterated ethanes. CH_3CD_3 shows no orientational
"splitting" in a site of C_i symmetry, because of its higher
point-group symmetry, viz. C_{3v}. However, it is seen from
Table 4 that three components for each (nondegenerate) mode
of C_2H_5D, $1,1-C_2H_4D_2$ and C_2HD_5 as guest molecules diluted in
C_2H_6, C_2D_6 or any deuterated species of ethane are expected
if the effective site symmetry is C_i, while six components
should be observed in sites without any symmetry (C_1).

B. Experimental

The orientational effect was studied on transitions
of C_2H_5D, $1,1-C_2H_4D_2$ and C_2HD_5 (see Figures 11-18).
Tables 13-15 list the observed guest frequencies of the
following dilute-mixed crystals of the partially-deuterated
ethanes:

Experiment Number	Guest/host
1	C_2HD_5/C_2H_5D
2	$\begin{cases} C_2H_5D/CH_3CD_3 \\ 1,1-C_2H_4D_2/CH_3CD_3 \end{cases}$
3	$\begin{cases} C_2H_5D/C_2HD_5 \\ 1,1-C_2H_4D_2/C_2HD_5 \end{cases}$

Experiments 1, 2 and 3 were utilized to probe the effective
site symmetry of ethane-d_1, -d_3 and -d_5, respectively.
At the same time, experiments 2 and 3 provided information
about the effect of the host and guest molecules on the
magnitude of the orientational "splitting", δ_{OE}, of certain
vibrational modes.

There are some general observations to be made about
the data obtained. First, in no case were more than the
three components expected on the basis of C_1 site sym-
metry observed for the guest fundamental bands. However,
only in a few cases were three bands resolved. Second,
in most cases, doublets were observed, often with an
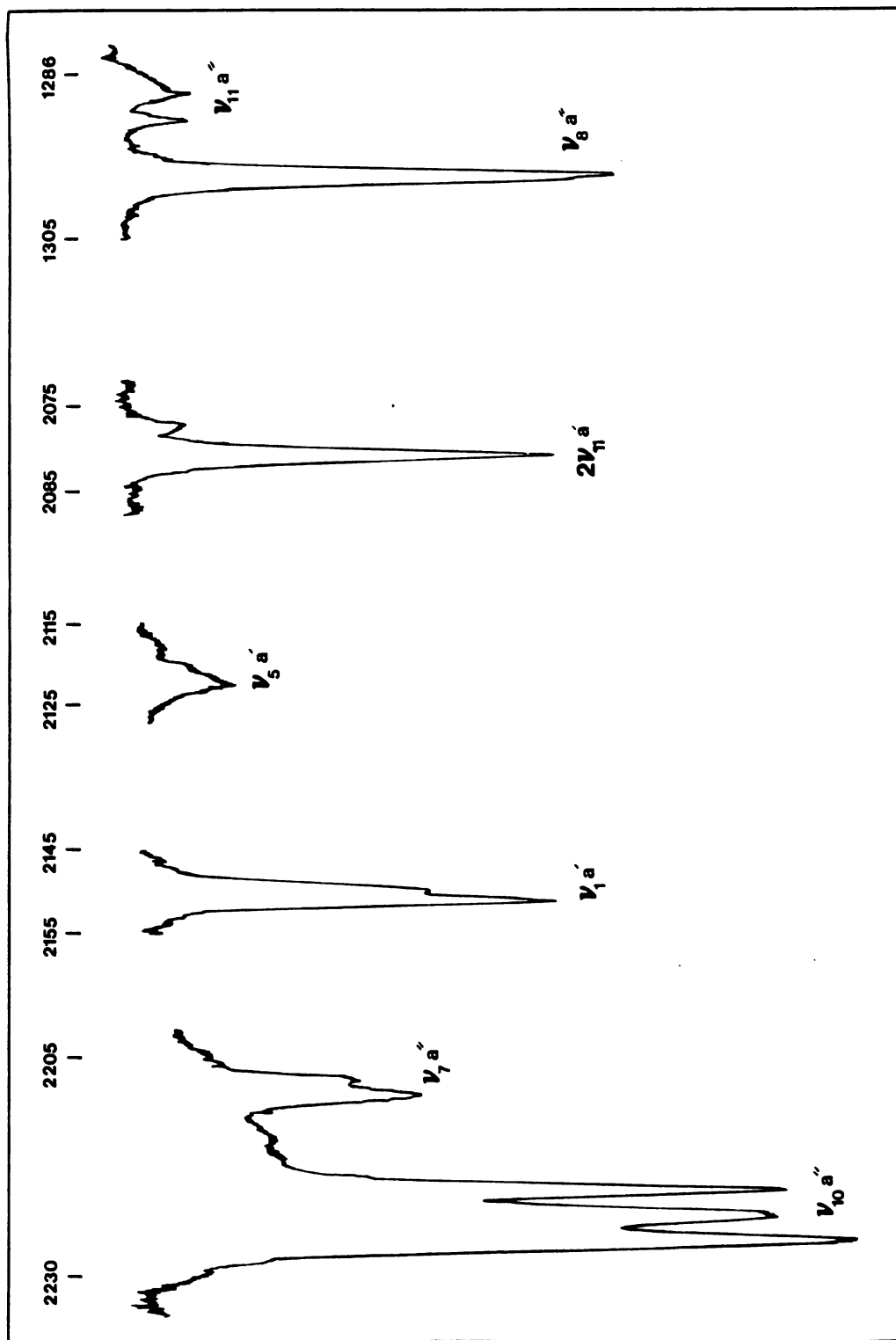
Figure 11. Part of the infrared spectrum of 3% C_2HD_5/C_2H_5D; ν_1, ν_5, ν_7 (a"), ν_8 (a"), ν_{10} (a' and a") and ν_{11} (a") of C_2HD_5.
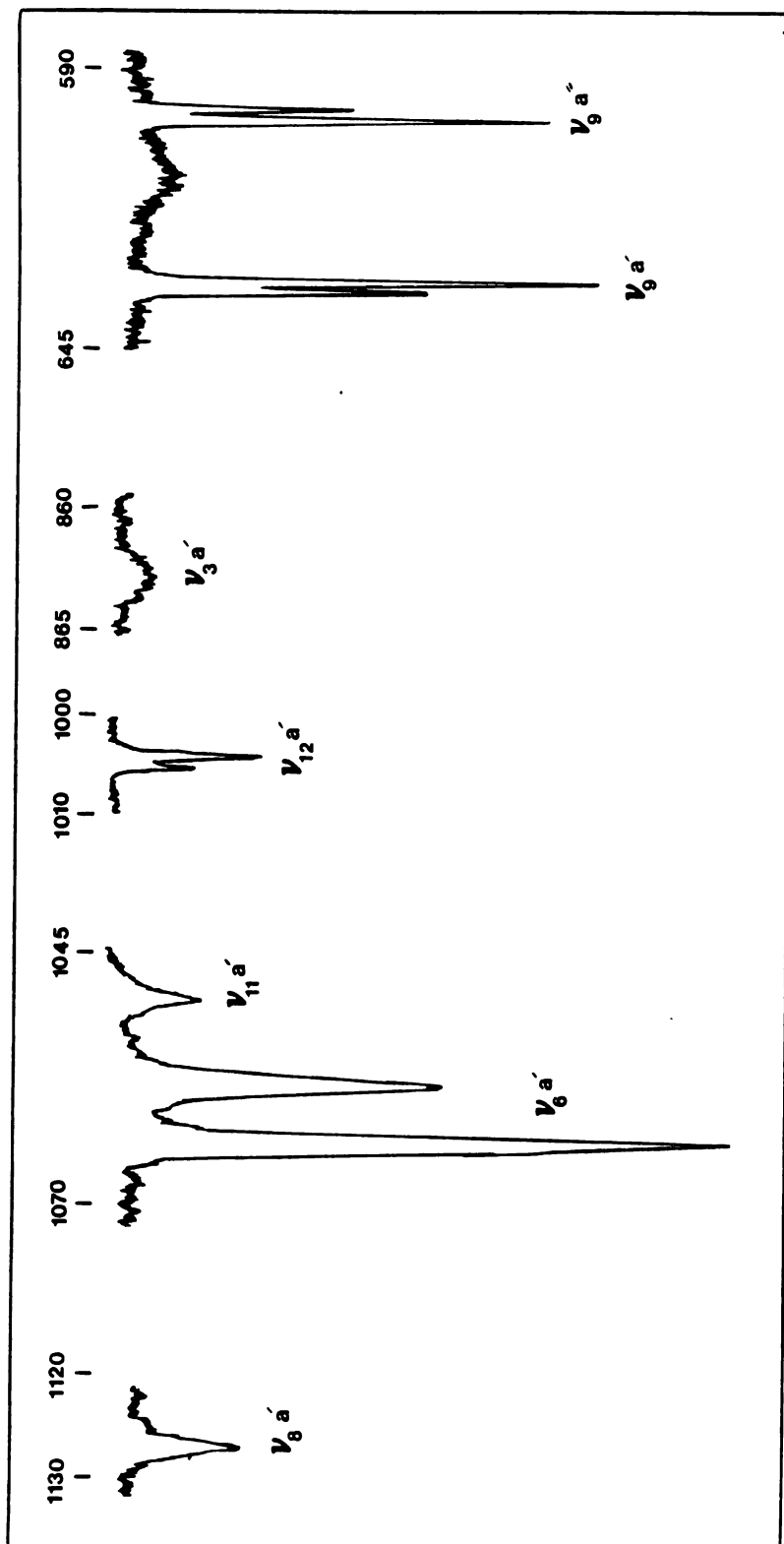
Figure 12. Part of the infrared spectrum of 3% C_2HD_5/C_2H_5D; ν_3, ν_6, ν_8 (a'), ν_9(a' and a") ν_{11} (a') and ν_{12} (a') bands of C_2HD_5.
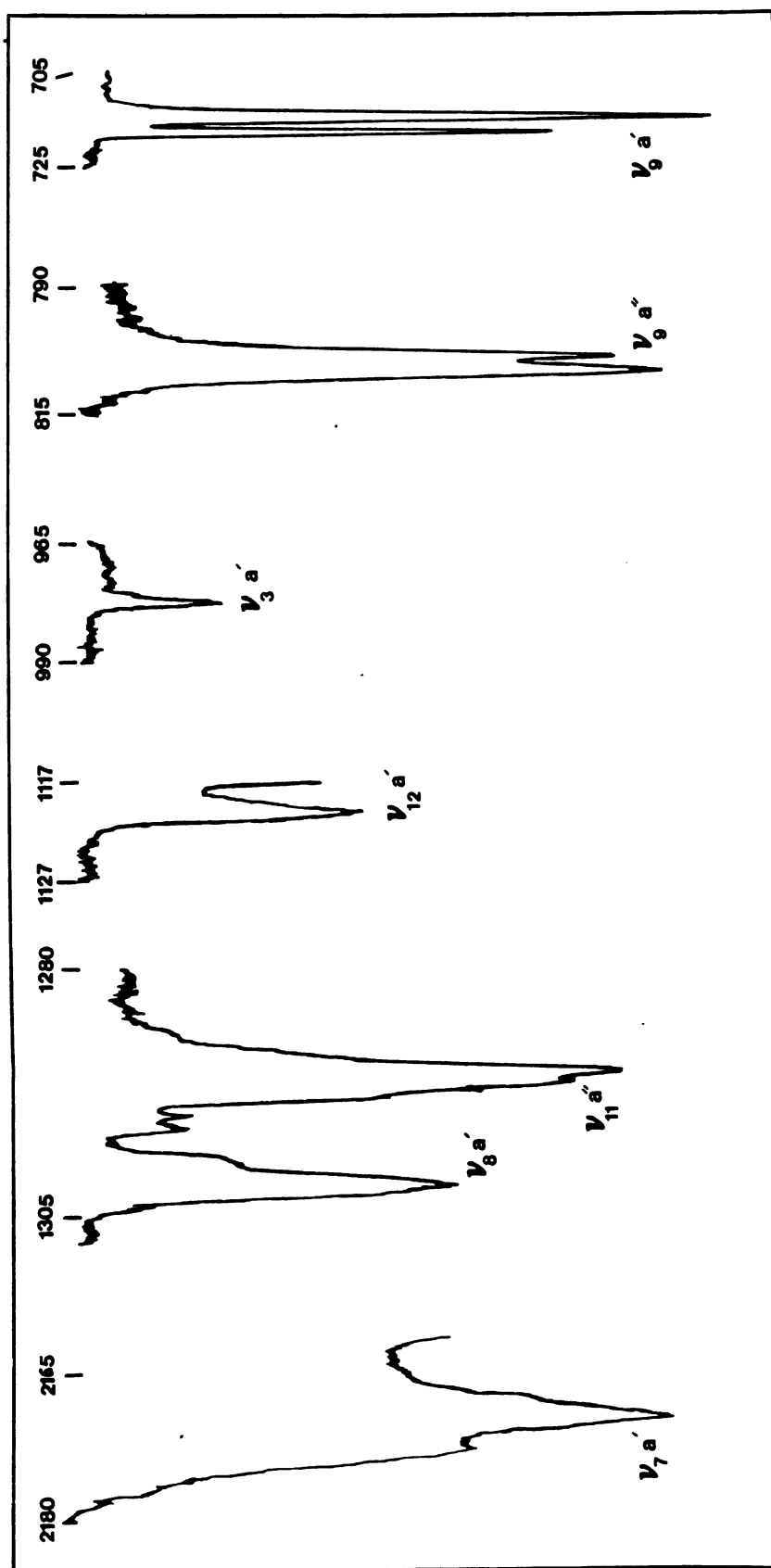
Figure 13. Part of the infrared spectrum of 3% C_2H_5D /CH_3CD_3; ν_3, ν_7 (a'), ν_8 (a'), ν_9 (a', a"), ν_{11} a" and ν_{12} a' bands of C_2H_5D.
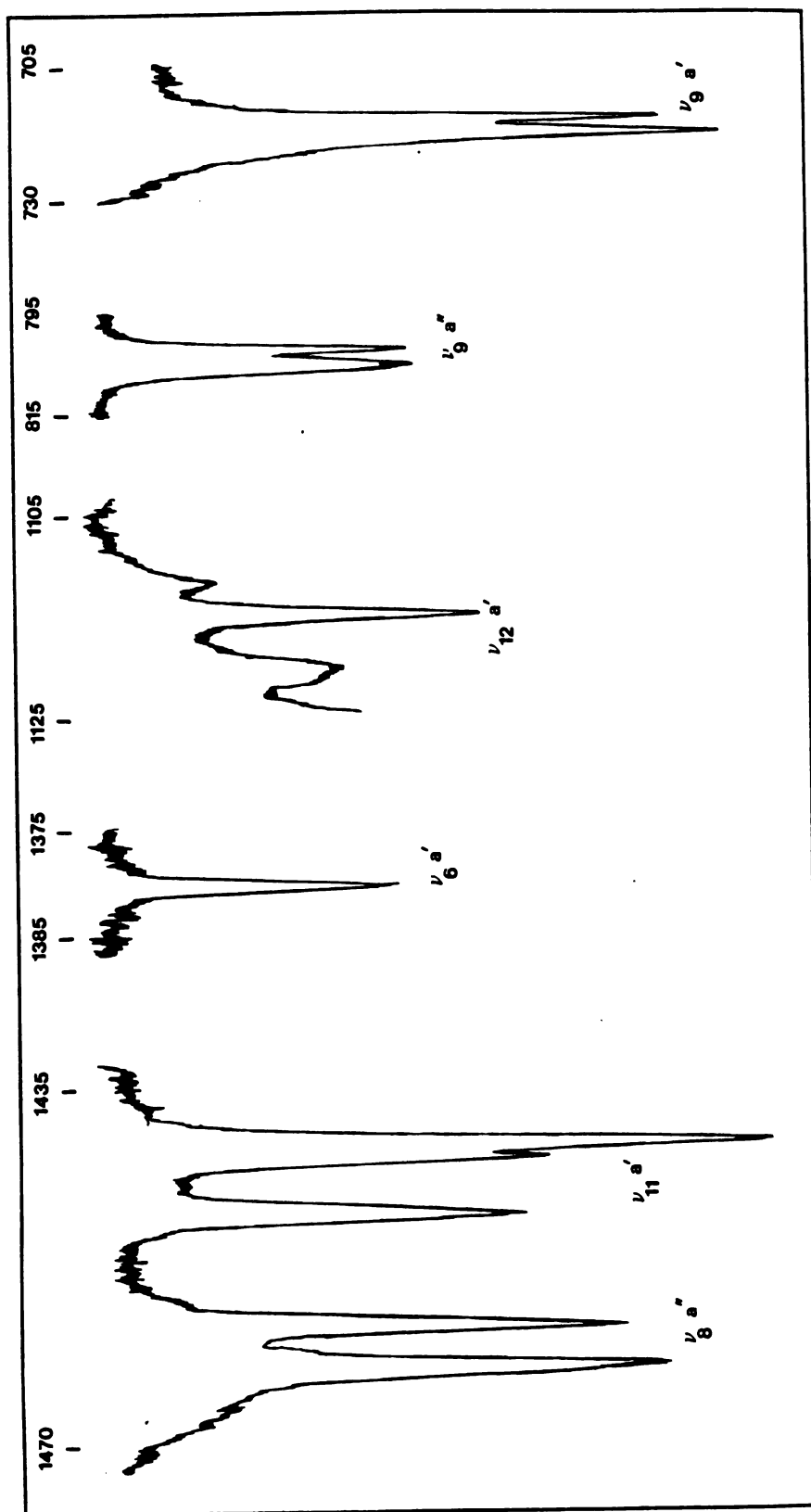
Figure 14. Part of the infrared spectrum of 3% C_2H_5D/C_2HD_5; ν_6, ν_8 (a"), ν_9 (a' and a"), ν_{11} (a') and ν_{12} (a') bands of C_2H_5D.
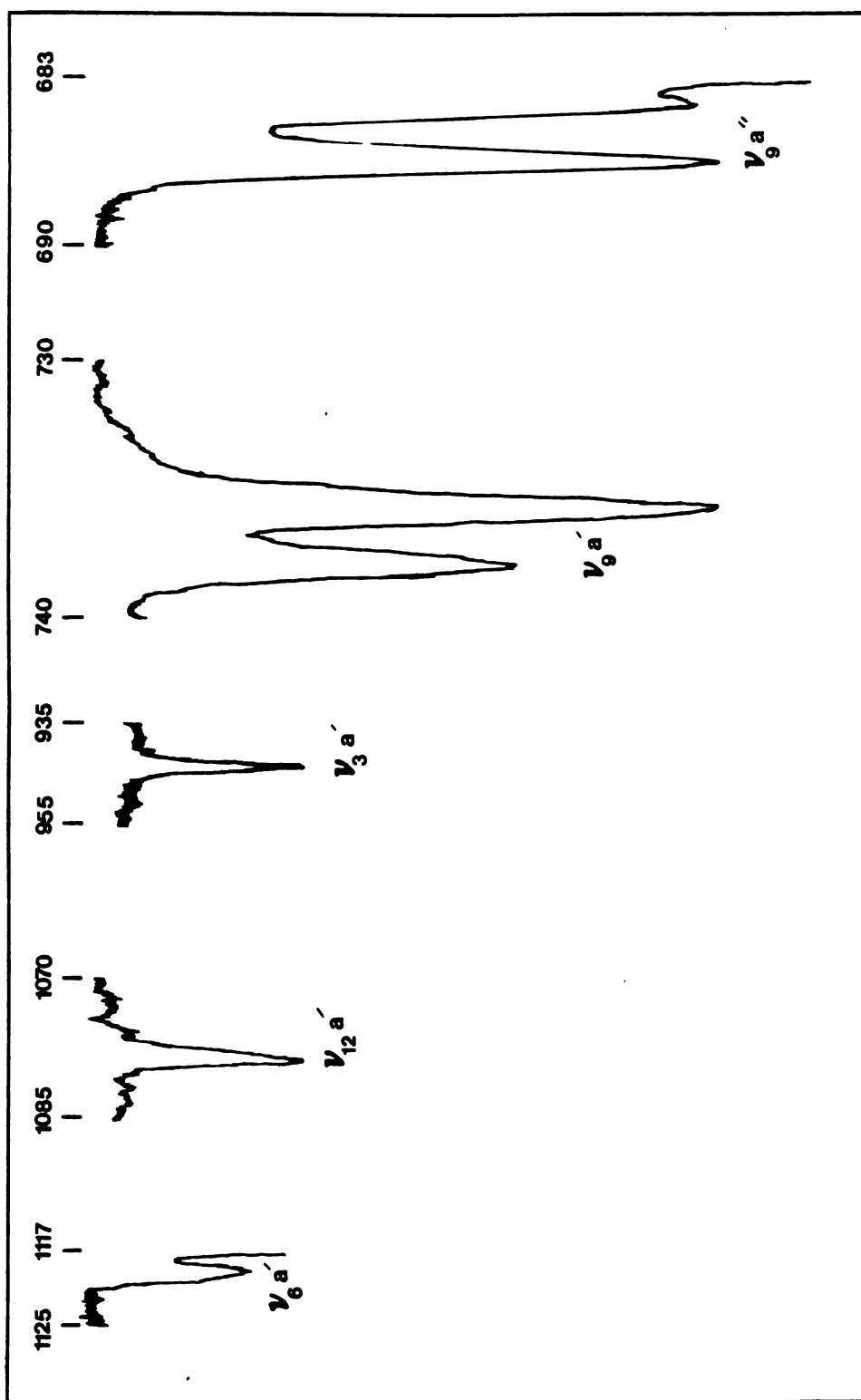
Figure 15. Part of the infrared spectrum of 1.5% 1,1-$C_2H_4D_2$/CH_3CD_3; ν_3, ν_6, ν_8 (a') ν_9 (a' and a"), and ν_{12} (a') of 1,1-$C_2H_4D_2$.
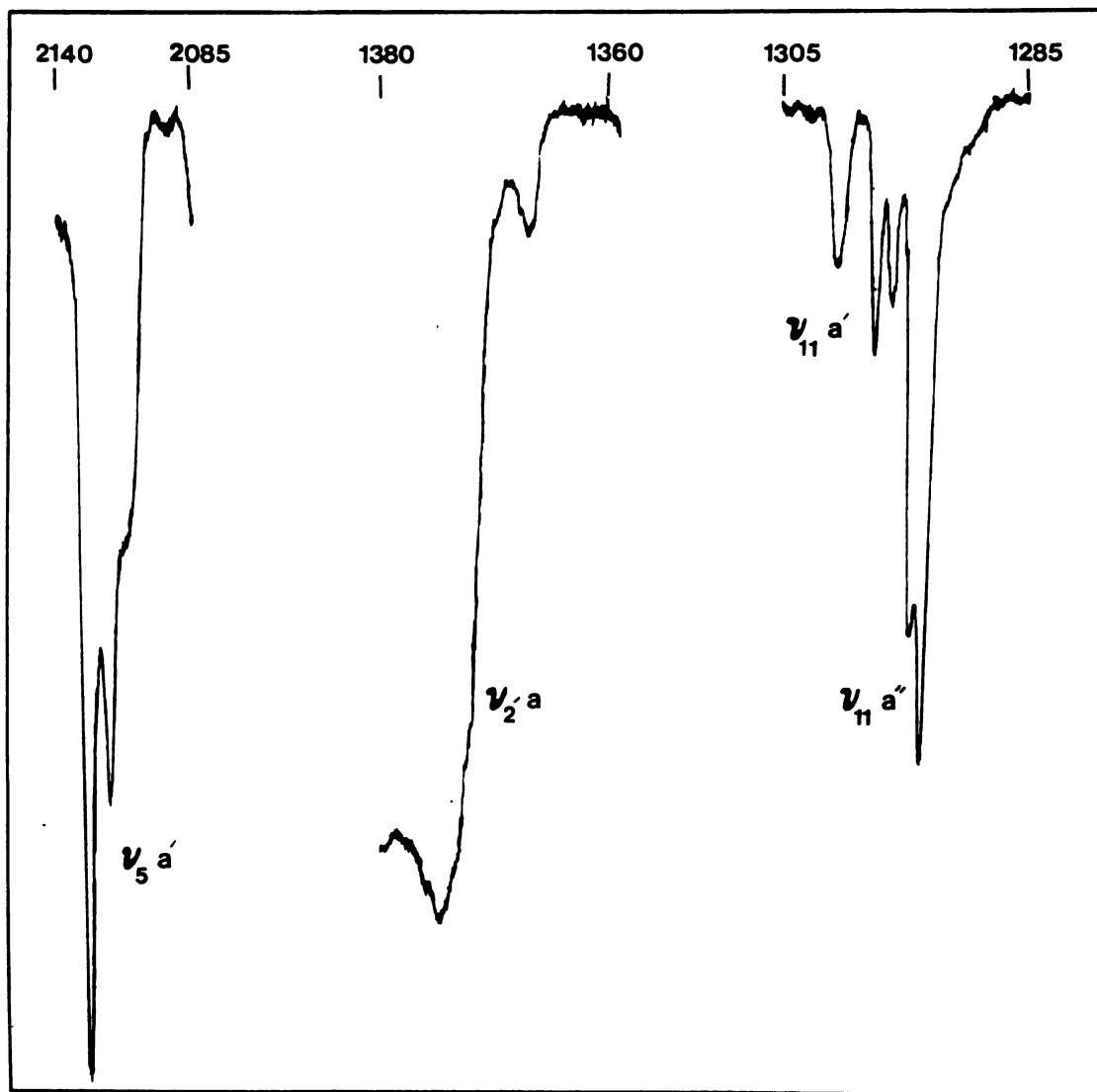
Figure 16. Part of the infrared spectrum of 1.5% 1,1-$C_2H_4D_2$/
CH_3CD_3; ν_2, ν_5 and ν_{11} (a' and a") bands of
1,1-$C_2H_4D_2$.
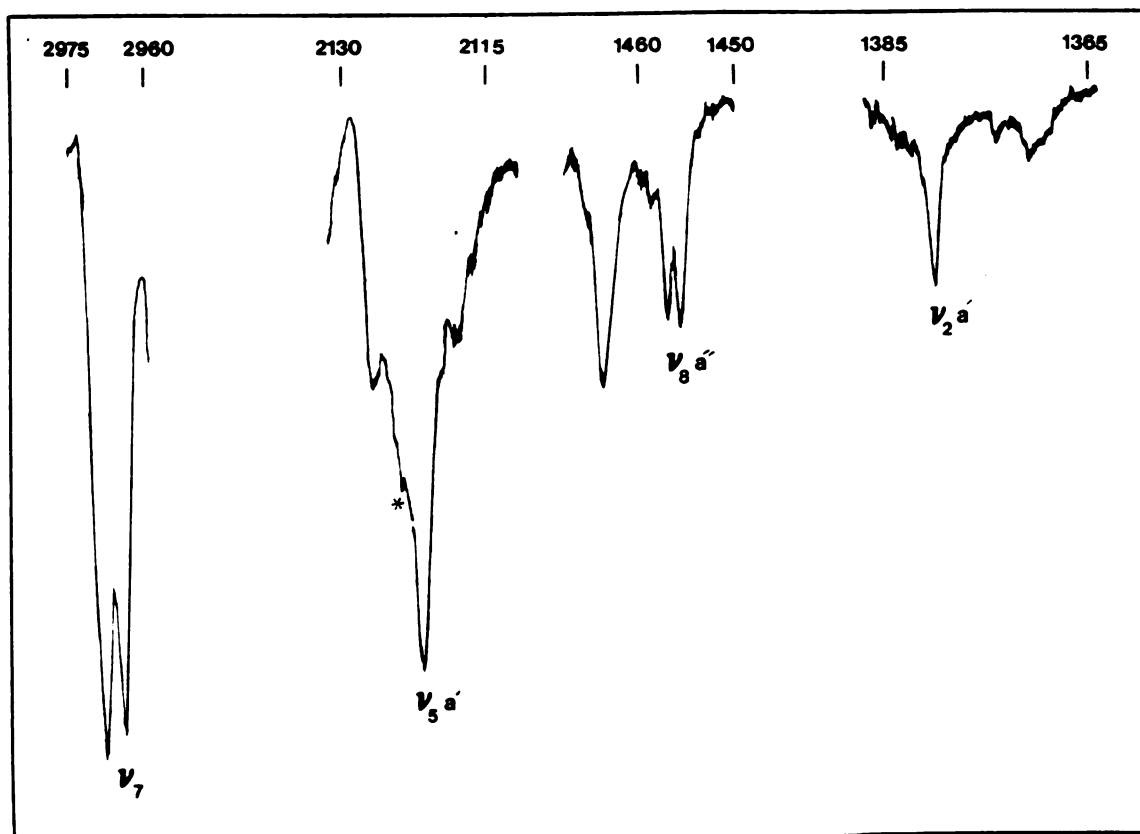
Figure 17. Part of the infrared spectrum of 4% 1,1-$C_2H_4D_2$/
C_2HD_5; ν_2, ν_5, ν_7 (a' and a") and ν_8 (a")
bands of 1,1-$C_2H_4D_2$. The peak marked with an
asterisk is due to the ν_5 band of the host.
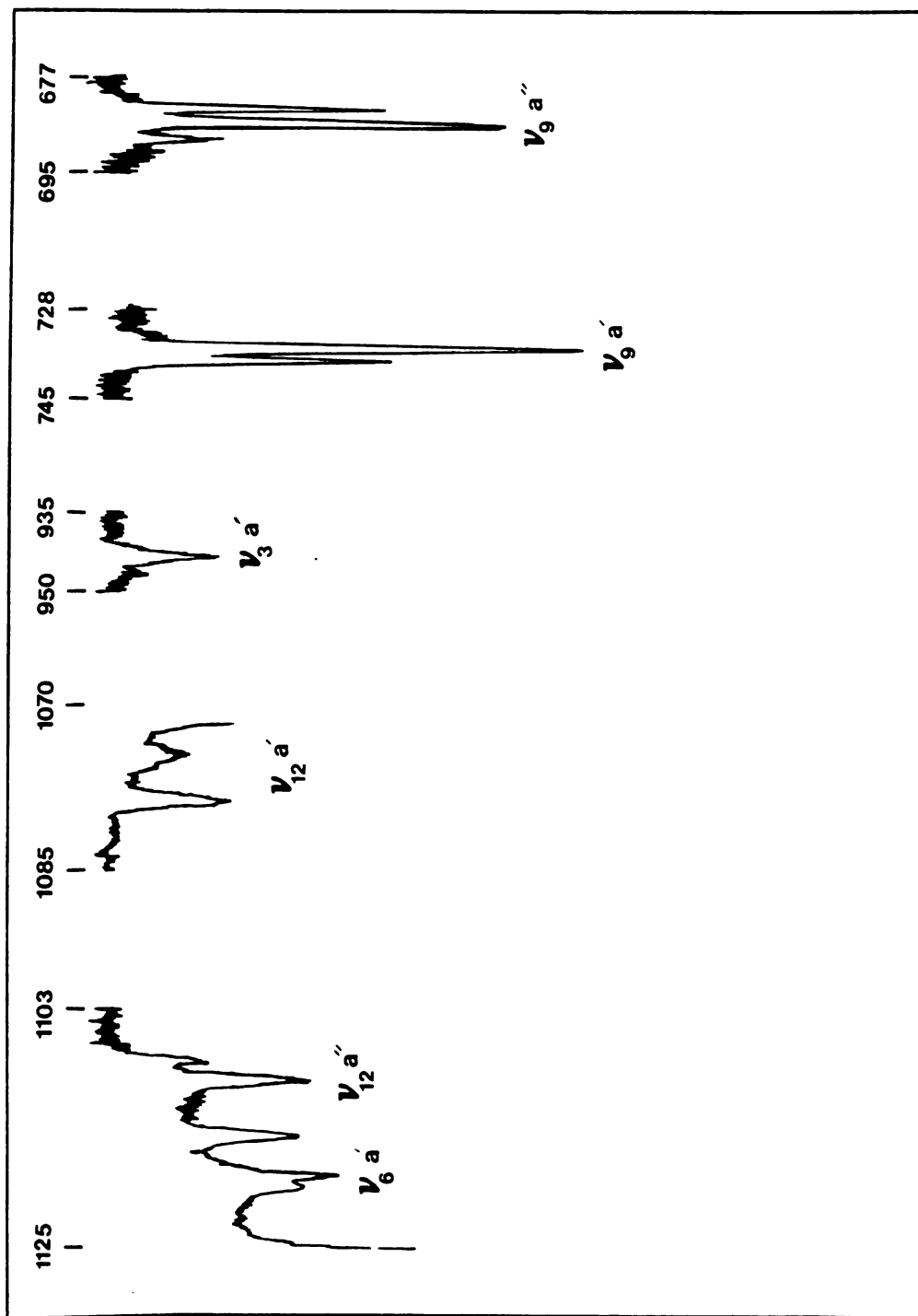
Figure 18. Part of the infrared spectrum of 4% 1.1-$C_2H_4D_2/C_2HD_5$; ν_3, ν_6, ν_9 (a' and a") and ν_{12} (a' and a") bands of 1,1-$C_2H_4D_2$.

Table 13. Observed C_2HD_5 Fundamentals in the Infrared
Spectrum of a 3% C_2HD_5/C_2H_5D Mixed Crystal.

Assignment[a]	Wavenumber (cm^{-1})	Assignment	Wavenumber (cm^{-1})
ν_1 a'	2150.5 (ms)	ν_{10} a'	2255 (w)
	2149.3 (m,shld)		
ν_3 a'	862.8 (vw)	a"	2225.2 (s)
			2222.6 (s)
ν_5 a'	2121.5 (w)		2219.8 (s)
ν_6 a'	1067 (ms)		
	1063.7 (s)	ν_{11} a'	1057.9 (w)
ν_7 a"	2208.8 (m)	a"	1291.0 (w)
	2207.0 (m, shld)		1287.8 (w)
ν_8 a'	1127.3 (mw)	ν_{12} a'	1005.8 (w)
a"	1297.6 (s)		1003.8 (mw)
ν_9 a'	598.0 (ms,sh)		
	600.2 (s, sh)		
a"	631.9 (s, sh)		
	633.6 (ms, sh)		

[a]The a' and a" assignments in this and the following tables
are from the gas phase assignment.

Table 14. Observed Infrared Fundamental Frequencies (cm^{-1})
of C_2H_5D Diluted in CH_3CD_3 and C_2HD_5.

Assignment	2% C_2H_5D in CH_3CD_3	3% C_2H_5D in C_2HD_5
ν_3 a'	977.2 (m)	977.5 (w)
ν_6 a'		1379.8 (ms)
ν_7 a'	2172.5 (m,shld)	
	2169.5 (s)	
a"		2968 (vs)
ν_8 a'	1303 (ms)	
	1301 (w,shld)	
a"		1461.5 (s)
		1458.0 (s)
ν_9 a'	717.2 (s)	717.1 (s)
	714.0 (s)	714.2 (s)
a"	805.2 (s)	805.5 (ms)
	802.4 (s)	802.1 (ms)
ν_{11} a'		1447.2 (ms)
		1441.9 (ms, shld)
		1440.5 (s)
a"	1292.2 (s, shld)	
	1291.0 (s)	
ν_{12} a'	1119.5 (ms)	1119.8 (mw)
		1114.7 (ms)
		1111.6 (w)

Table 15. Observed 1,1-$C_2H_4D_2$ Fundamentals in the Infrared Spectra of 1.5% 1,1-$C_2H_4D_2$/CH_3CD_3 and 4% 1,1-$C_2H_4D_2$/C_2HD_5 Mixed Crystals.

Assignment	1.5% 1,1-$C_2H_4D_2$/CH_3CD_3 Wavenumber (cm^{-1})	4% 1,1-$C_2H_4D_2$/C_2HD_5 Wavenumber (cm^{-1})
ν_2 a'		1379.9 (m)
	1374.8 (s)	1374.4 (w)
	1367.2 (w)	1370.0 (mw)
ν_3 a'		946.0 (w)
	943.1 (w)	943.2 (mw)
ν_5 a'	2128.5 (s)	2125.5 (ms)
	2120.0 (s)	2120.4 (s)
	2113.0 (ms, shld)	2117.0 (ms)
ν_6 a'	1118.5 (m)	1119.2 (mw)
		1118.2 (m)
		1114.5 (m)
ν_7 a'		2968.2 (vs)
a"		2964.8 (vs)
ν_8 a'	1482.0 (vw)	1482.5 (vw)
	1479. (w)	1479.8 (mw)
ν_8 a"		1463.2 (ms)
		1457.0 (m)
		1455.6 (m)

Table 15. Continued.

Assignment	1.5% 1,1-$C_2H_4D_2$/CH_3CD_3 Wavenumber (cm^{-1})	4% 1,1-$C_2H_4D_2$/C_2HD_5 Wavenumber (cm^{-1})
ν_9 a'	737.4 (ms)	737.7 (ms)
	735.3 (s)	735.5 (s)
a"		688.6 (m)
	686.6 (s)	685.8 (s)
	684.5 (ms)	683.2 (ms)
ν_{11} a'	1300.2 (mw)	
	1297.0 (mw)	
	1296.0 (mw)	
a"	1293.0 (s)	
	1293.7 (s)	
ν_{12} a'	1077.5 (m)	1078.6 (m)
		1074.5 (mw)
a"		1109.5 (m)
		1107.7 (mw)

intensity ratio of 2:1, and in some cases singlets were recorded. In the latter case the bands were usually weak (compare, for example, the ν_3 band of the three species in dilute mixed crystals) and that is possibly one reason why they do not show "splitting". In cases where doublets or (stronger) singlets were observed it can be assumed that the orientational "splitting" is too small to allow the components to be observed, or that the resolution is hampered by the sample quality. In any event, the orientational components were resolved in many cases, and hence the determination of the site symmetries of the partially-deuterated ethanes by way of the orientational effect should be applicable. The observed orientational "splittings" varied from unresolved to 8.5 cm^{-1}.

It is to be noted that it is impossible for all bands in all dilute mixed crystals to compare isotopic guest or host effects on the magnitude of the orientational "splitting". Problems arise when guest bands are obscured by host bands (especially in the wavenumber ranges 1300-1400 cm^{-1} and 2800-3000 cm^{-1}) or the guest bands are difficult to assign due to the presence of extraneous impurities (other than the guest molecules) and/or the presence of host overtones and combination bands. The frequency region lower than approximately 1200 cm^{-1} was considered best to most definitively observe the guest modes of the dilute mixed crystals (ν_9 for example).

The presence of doublets and triplets in dilute-mixed crystal spectra clearly indicate an "effective" centrosymmetric site symmetry. Table 16 lists the magnitude of the orientational "splitting", δ_{OE}, for vibrational modes of ethane-d_1, 1,1-d_2 and -d_5 in dilute-mixed crystals. The ν_9 (a') and ν_9 (a") fundamentals are the only modes which were observed in all dilute-mixed crystals. They show doublets in all cases, with an intensity ratio often close to 2:1. The intensity difference between the two components is possibly due to the third, unresolved orientational component. It can be seen that the effect of host or guest isotopic substitution on the orientational "splitting" is negligible; however, the orientational effect is different for different vibrational modes.

The following bands have shown a different number of orientational components in different hosts:

ν_3 (1,1-$C_2H_4D_2$) - exhibits two components in the C_2HD_5 host, at 943.2 cm^{-1} and 946 cm^{-1}, but shows only one component, at 943.1 cm^{-1} in the CH_3CD_3 host. The absence of the higher frequency component in CH_3CD_3 is believed to be due to its weakness and the poorer sample quality.

ν_6 (1,1-$C_2H_4D_2$) - shows three components in the C_2HD_5 host, at 1119.2 cm^{-1}, 1118.2 cm^{-1} and 1114.5 cm^{-1}, but shows only one component, at 1118.5 cm^{-1}, in the CH_3CD_3 host. Undoubtedly the two unobserved lower frequency bands are hidden by the ν_6 band of the CH_3CD_3 host.

Table 16. Orientational "splitting", δ_{OE}, of Partially Deuterated Ethane Guests in Dilute-Mixed Crystals.[a]

	D_5/D_1	D_1/D_3	D_1/D_5	$1,1\text{-}D_2/D_3$	$1,1\text{-}D_2/D_5$
ν_1	1.2	---	---	---	---
ν_2	---	---	---	7.6	5.5, 4.4.
ν_3	0	0	0	0	2.8
ν_5	0	---	---	8.5, 7.0	5.1, 3.4
ν_6	3.3	---	0	0	3.7, 11.0
ν_7 a'	---	3.0	---	---	0
a"	1.8	---	0	---	0
ν_8 a'	0	2.0	---	3.0	2.7
a"	0	---	3.5	---	6.2, 1.4
ν_9 a'	2.2	3.2	2.9	2.1	2.2
a"	1.7	2.8	3.4	2.1	2.6, 2.6
ν_{10} a'	0	---	---	---	---
a"	2.6, 2.8	---	---	---	---
ν_{11} a'	0	---	5.3, 1.4	3.2, 1.0	---
a"	3.2	1.2	---	0.7	---
ν_{12} a'	1.2	---	5.1, 3.1	0	4.1
a"	---	---	---	---	1.8

[a]Zeros in the Table indicate unresolved bands; no entry (-) means that the guest band could not be observed in the dilute-mixed crystal.

ν_9 (1,1-$C_2H_4D_2$) - shows three components in the C_2HD_5 host, at 688.6 cm^{-1}, 685.8 cm^{-1} and 683.2 cm^{-1}, but shows only two components, at 686.6 cm^{-1} and 684.5 cm^{-1} in the CH_3CD_3 host. Probably the better sample quality in the former case enables three components to be observed.

ν_{12} (1,1-$C_2H_4D_2$) - shows two components in the C_2HD_5 host, at 1078.6 cm^{-1} and 1074.5 cm^{-1}, but shows only one component, at 1077.5 cm^{-1} in the CH_3CD_3 host. This discrepancy is also possibly due to the poorer sample quality in the latter case, where a very weak but indistinct band is seen around 1073 cm^{-1} in the CH_3CD_3 host.

ν_2 (1,1-$C_2H_4D_2$) - shows three components in the C_2HD_5 host, at 1379.9 cm^{-1}, 1374.4 cm^{-1} and 1370 cm^{-1}, but shows only two components, at 1374.8 cm^{-1} and 1367.2 cm^{-1} in the CH_3CD_3 host. Obviously the high frequency band is hidden by ν_2 of the CH_3CD_3 host.

C. Site Shifts

The experimental site shifts Δ can be determined from the tables of data as $E_{gas} - E_{mixed\ crystal}$. Of particular interest are whether or not such shifts are present, what trends in the shifts can be determined as a function of vibrational state, and what the host or guest isotope effects are on these shifts. However, it must be noted that the contribution of various symmetry coordinates (that is the atomic motions) to any particular fundamental

vibration will change upon deuteration. Thus a strict comparison between different molecules may not be possible. These changes, however, are expected to have a more pronounced effect on the band width of the vibrations, which arise from dynamic interaction between the molecules, and less effect on the static interactions; that is, the orientational "splittings" and the Δ's - the gas to crystal field shifts - should be less dependent on the potential energy distribution.

The inaccuracy of the gas phase data (see Chapter VII) gives rise to uncertainties in the site shift measurements in several cases. Therefore, only those vibrations for which it is believed these complications are minimized will be discussed in Table 17. The values tabulated for the site shifts are the mean Δ's measured from Raman and infrared experiments and/or in different hosts. A comparison of the host effect on the site shifts is not possible because not all experiments were done in the same host. Therefore, the above data give only a rough idea of the size of the site shifts for ν_1, ν_2, ν_3, ν_8 and ν_9 for the different isotopes of ethane. Generally the differences in the Δ's for a given vibrational mode between infrared and Raman spectra among different hosts varied between 0-3.0 cm^{-1}. Small site shifts for the ν_3 C-C stretching and ν_9 bending modes, which appear relatively constant for all isotopes, indicate small interaction with the surrounding field.

Table 17. Gas-to-Mixed Crystal Shifts of the Ethanes.

		d_0	d_1	$1,1\text{-}d_2$	d_3	d_5	d_6
$\Delta\nu_1$	CH(CD) str.	19.0	---	----	----	13.1	14.5
$\Delta\nu_2$	$CH_3(CD_3)$ def.	11.0	---	14.4	12.8	----	7.5
$\Delta\nu_3$	C-C str.	-0.1	0.5	0.9	2.0	3.2	0.7
$\Delta\nu_9(a')$	Bend.	0.6	1.4	2.4	0.7	-0.1	0.2
$\Delta\nu_9(a'')$	Bend		1.2	4.1		-1.8	
$\Delta\nu_8(a')$	$CH_3(CD_3)$ def	4.4	---	5.9	----	5.7	11.0
$\Delta\nu_8(a'')$	$CH_3(CD_3)$ def.		5.5	11.4	----	11.4	

In contrast, for the ν_1 CH(CD) stretching, and the ν_2 and ν_8 $CH_3(CD_3)$ deformation modes, larger site shifts (~15.5 cm^{-1}, ~11.0 cm^{-1} and $\sim6.0-11.0$ cm^{-1}, respectively) are observed which are not nearly as constant with isotopic substitution. The greater site shifts for the latter vibrations imply a greater interaction with the static field. It is seen from the given Δ values that the site shifts for vibrations involving deuterium motion rather than hydrogen motion tend to be smaller (compare for instance the Δ's of ν_1, ν_2 and ν_9). Generally a large site shift is expected to be observed for any given vibration which is perturbed by Fermi resonance interaction with a nearby band.

Although all the available data have not been interpreted in detail, it is possible to conclude from the above discussion that there is no significant isotope effect on the Δ term for the ground vibrational states of ethanes.

D. Conclusions

The following conclusions can be drawn from the observations of the guest modes of the dilute-mixed crystals of the partially-deuterated ethanes in each other.

The "effective" site symmetry of the partially-deuterated ethane crystals is C_1. Therefore the ethane molecules cannot distinguish between hydrogens and

CHAPTER VI

THE RAMAN SPECTRA OF NEAT CRYSTALLINE C_2H_6

C_2D_6 AND THEIR MUTUAL SOLID SOLUTIONS IN

THE INTERNAL REGION

The Raman and infrared spectra of solid (II) ethane

and C_2D_6 are consistent with the recent crystal structure

reported by Van Nes and Vos.[27] Observation of a maximum

of four components for the ν_9 (e_u) vibrational mode in the

ir spectrum (already reported by Eggers and Tejada[18])

indicates the existence of at least two molecules per unit

cell. The site symmetry of C_1 for crystalline ethane is

strongly supported, since the mutual exclusion rule holds

in the ir and Raman spectrum.

If the correlation diagram (Table 3) for C_2H_6 of

molecular symmetry D_{3d} on a C_1 site with C_{2h} factor group

symmetry is considered, one can see that all the degenerate

modes can be split at the site into two components as a

result of   reduction in symmetry of the molecule from D_{3d}

to the C_1 site symmetry. Furthermore, any of the funda-

mentals can be split by factor group coupling into two

components, one with symmetry "a" and the other of sym-

metry "b". Consequently one would expect to observe a

102

maximum of four resolved components for degenerate modes and two resolved components for non-degenerate modes in both the infrared and the Raman spectra of solid (II) ethane.

The observed Raman fundamental vibrational frequencies of C_2H_6, C_2D_6 and their dilute mutual solid solutions are listed in Tables 18 and 19. The observed spectra are shown in Figures 19-23. For two of the three nondegenerate g-modes two components are indeed observed for both C_2H_6 and C_2D_6, while for the third non-degenerate mode only a singlet has been resolved, with an apparent shoulder for the C_2H_6 crystal. Also, three components have been resolved for two of the degenerate g-modes in both compounds, while the third e_g vibrational mode appeared as a doublet. In the following we consider these vibrational modes and their components in more detail.

$\underline{\nu_1\ (e_{1g})}$ - This fundamental is observed as a single intense peak in the Raman spectra of both C_2H_6 and C_2D_6. However, a second component of moderate intensity is seen as a shoulder for C_2H_6 which could not be resolved. This, if not the second component of ν_1, might be assigned to an overtone of ν_8 in Fermi resonance with ν_1. Two moderately intense peaks in the Raman spectra of C_2D_6, at 2121 and 2141.6 cm^{-1}, are tentatively assigned to the overtones of ν_6 and ν_8. Single peaks on the low frequency side of the ν_1 a_u vibration of both compounds, at 2861.6 cm^{-1} (C_2H_6)

Table 18.   Observed Raman Fundamental Frequencies (cm^{-1})
of Pure Polycrystalline (solid II) Ethane and
its Dilute Solid Solution in C_2H_6.[a]

Assignment	Gas Phase[b]	Pure Crystalline	5% C_2H_6/C_2D_6
ν_1 a_{1g}	2899	2874 (vs)	2880.0
		2873.4 (m, shld)	
ν_2 a_{1g}	1400	1400.4 (m)	
		1374.8 (w)	1389
ν_3 a_{1g}	993	978.4 (w)[c]	
		992.0 (s, sh)	
		995.1 (s, sh)	994.0
ν_{10} e_g	2955	2959.5 (s)	2958.4
		2954.5 (s)	2955
ν_{11} e_g	1460	1433.0 (w)[c]	
		1445.3 (ms)	
		1448.9 (w)	
		1460.8 (s)	1456.0
ν_{12} e_g	1190	1190.2 (w)	
		1191.8 (w)	1191.0
		1198.3 (vw)	1197.1

Key to Table:

[a]v = very,   s = strong,   m = moderate,   w = weak,   sh = sharp
shld = shoulder.

[b]Gas phase values are from Reference 21(d) and 21(m).

[c]These frequencies are attributed to C-13 substituted molecules.

Table 19. Observed Raman Fundamental Frequencies (cm^{-1}) of Pure Crystalline Ethane-d_6 (solid II) and its Dilute Solid Solution in C_2H_6.

Assignment	Gas Phase[a]	Pure Crystalline C_2D_6	4% C_2D_6/C_2H_6
$\nu_1\ a_{1g}$	2083	2067.2 (vs)	2068.5
		2061.4 (vw)[c]	
$\nu_2\ a_{1g}$	1155	1145.25 (m)	
		1152.35 (w)	1147.5
$\nu_3\ a_{1g}$	843	823.7 (w)[c]	
		836.05 (s)	
		848.25 (s)	842.25
$\nu_{10}\ e_g$	2225	2210.9 (vs)	
		2215.2 (vs)	2212.95
		2217.3 (shld, ms)	2215.75
$\nu_{11}\ e_g$	1041	1041.40 (m)	
		1051.60 (m)	1048.3
		1057.15 (m)	
$\nu_{12}\ e_g$	970[b]	963.65 (w)	
		966.35 (m)	964.2

[a] Gas phase values from Ref. 21(g).

[b] From Reference 21(n).

[c] These frequencies are attributed to C-13 substituted molecules.
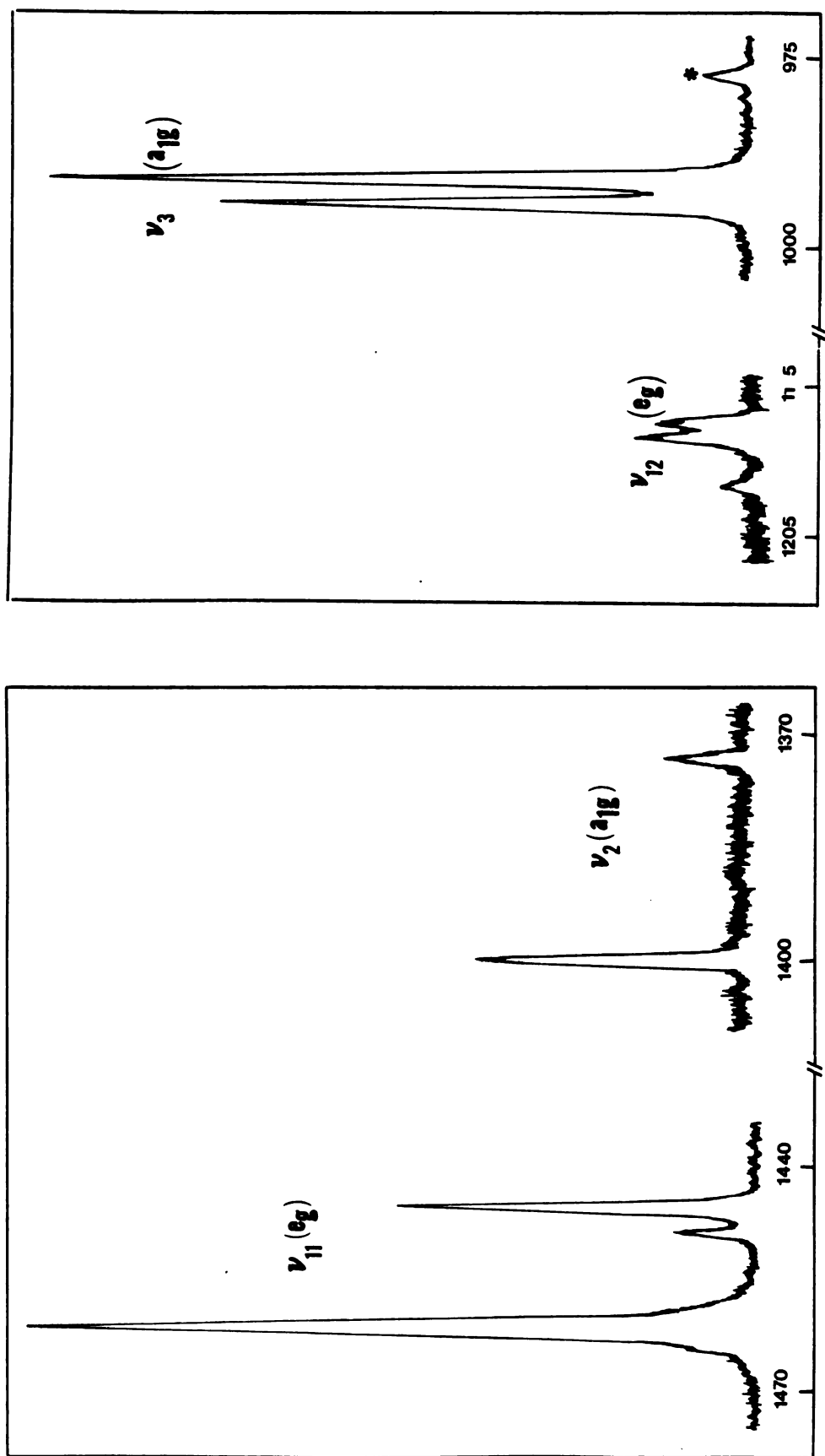
Figure 19. Part of the Raman spectrum of solid (II) ethane. The peak marked with an asterisk is attributed to ν_3 of C-13 substituted ethane molecules.
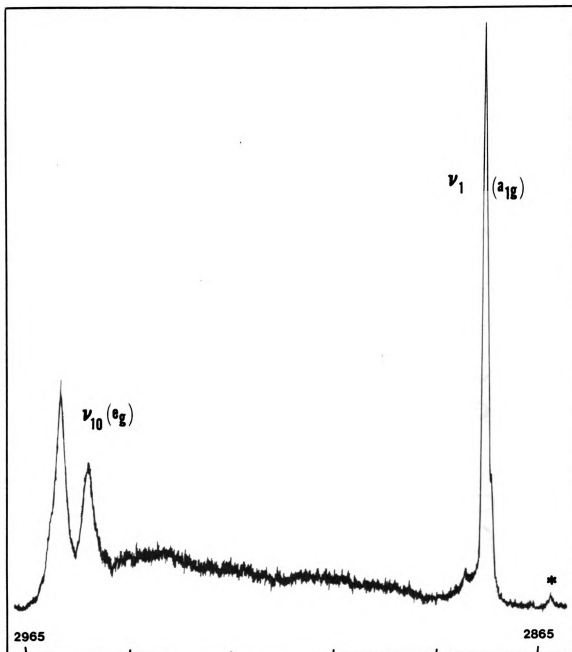
Figure 20. Part of the Raman spectrum of solid (II)
C_2H_6 (ν_1 and ν_{10}). The peak marked with an
asterisk is attributed to ν_1 of C-13 substi-
tuted ethane molecules.

Figure 21. The Raman spectrum of solid (II) C_2D_6. The peak marked with an asterisk is attributed to C-13 substituted ethane-d_6 molecules.

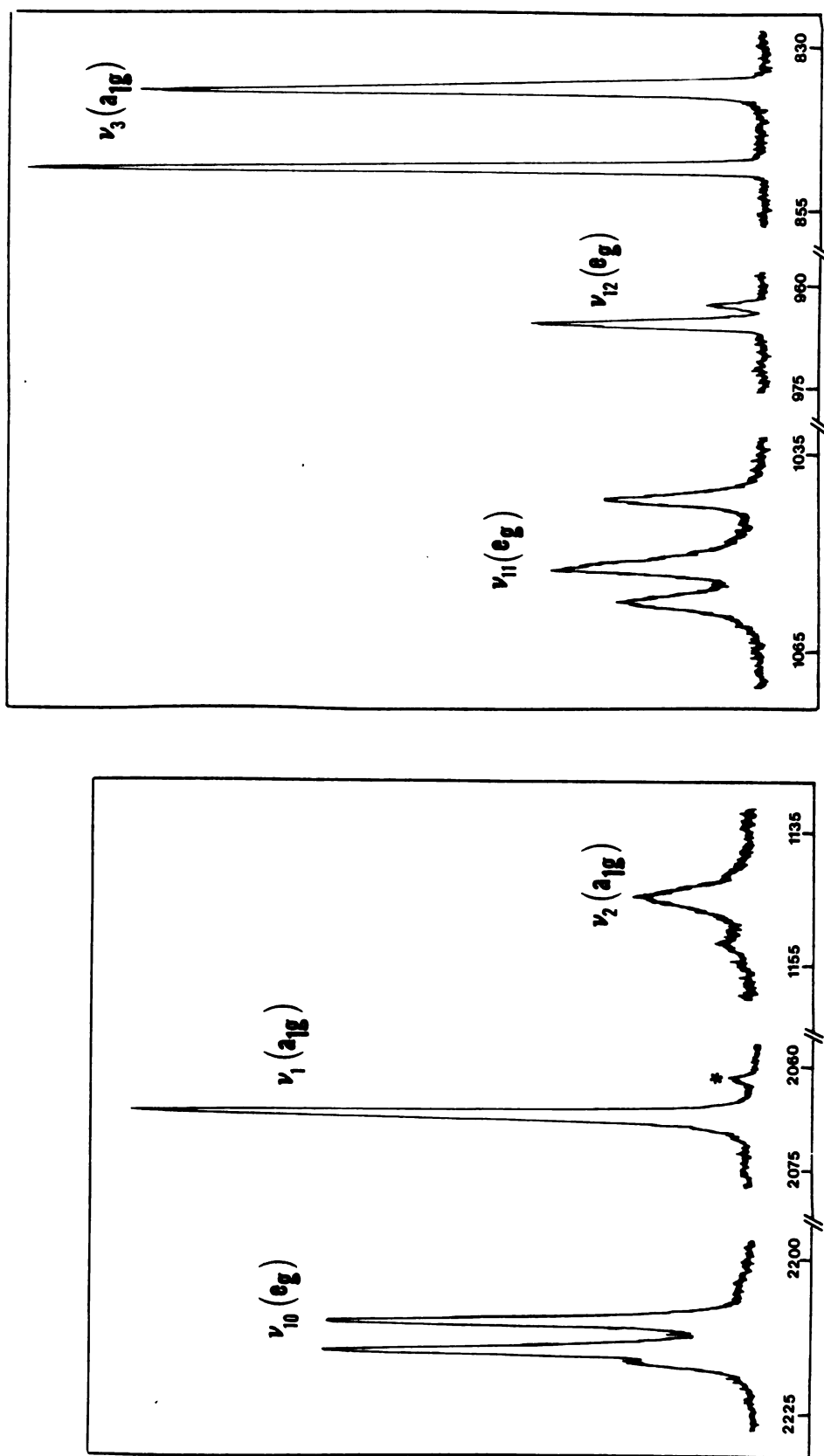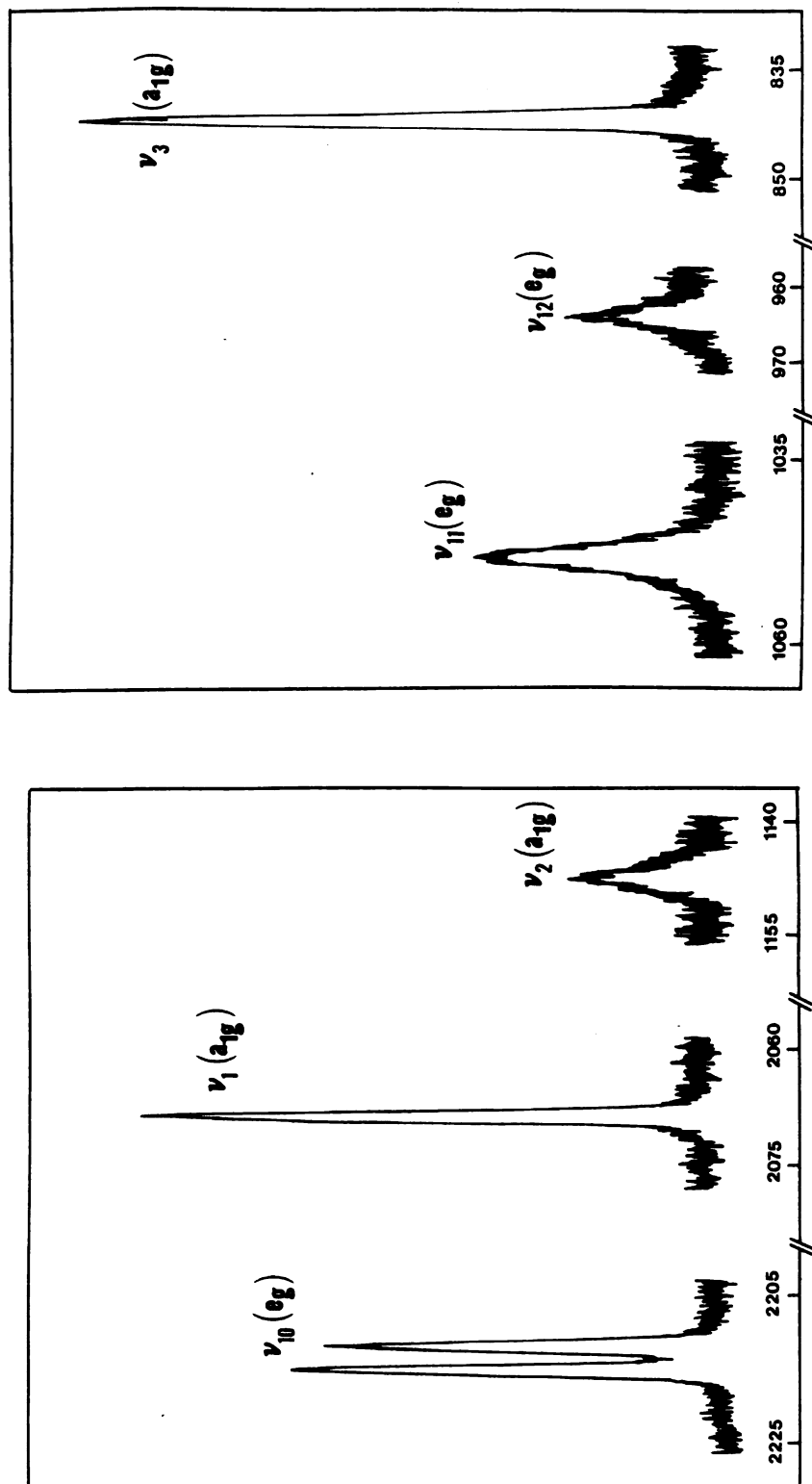Figure 22. The Raman spectrum of solid (II) ethane-d_6 in a 4% solution of C_2D_6 in C_2H_6.
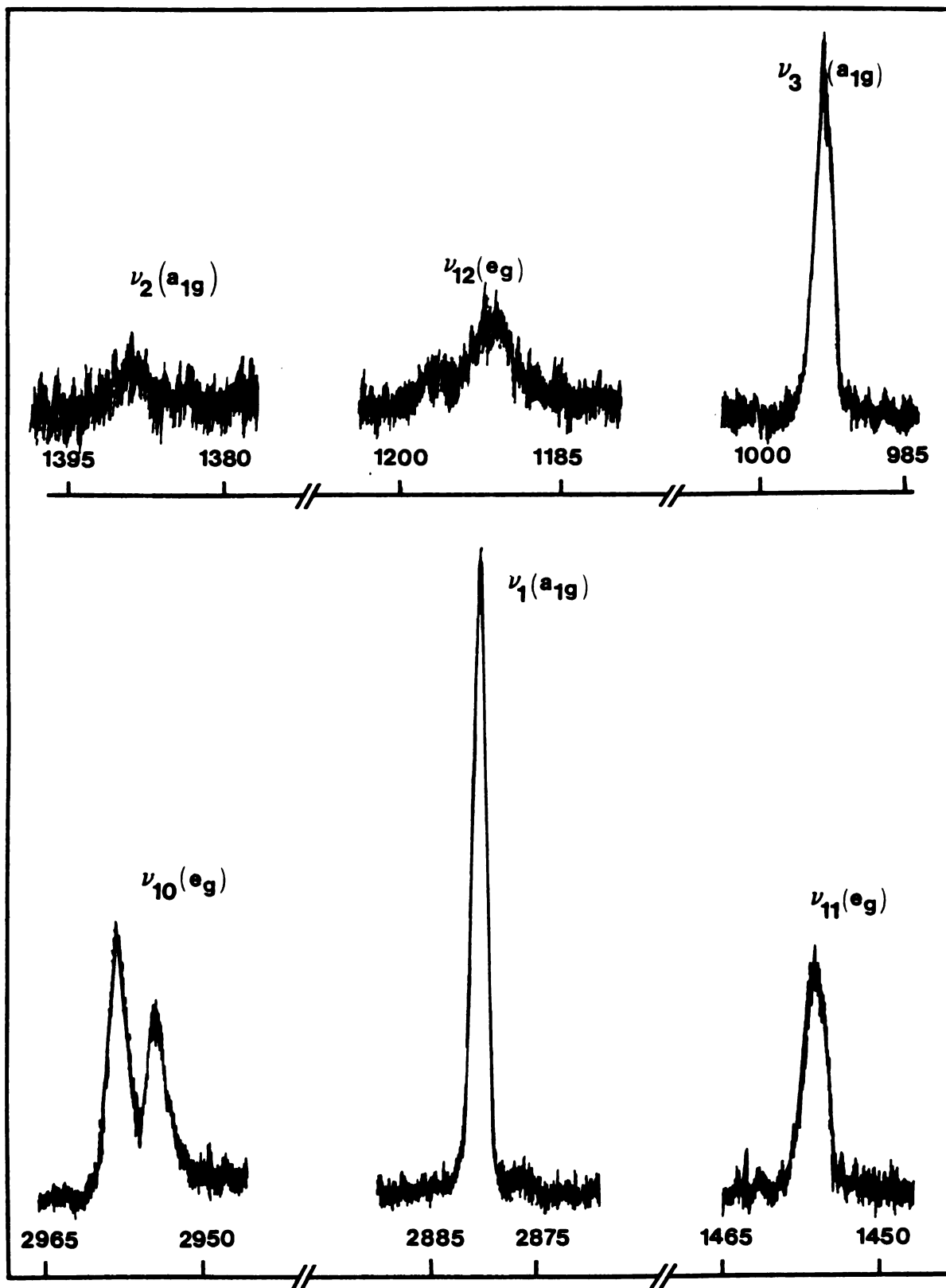
Figure 23. Part of the Raman spectrum of solid (II) ethane in a 5% solution of C_2H_6 in C_2D_6; ν_1, ν_2, ν_3, ν_{10}, ν_{11} and ν_{12} of C_2H_6.

and 2061.4 cm^{-1} (C_2D_6), are assigned to ν_1 of the corresponding molecule containing one C-13 atom. Their low intensity, 2.5% and 3% of the parent (C_2H_6 and C_2D_6, respectively) peak, is in good agreement with this assignment.

$\underline{\nu_2}$ $\underline{(a_{1g})}$ - This fundamental, a CH_3 deformation mode, appears with two components in both the C_2H_6 and C_2D_6 Raman spectra, one weak component and the other moderately intense. In the spectra of isotopically dilute solutions, the two components are replaced by a singlet in the region between the original pair of peaks, indicating the factor group origin of the components. The splitting of the components in C_2H_6 (25.6 cm^{-1}) is much larger than for C_2D_6 (6.1 cm^{-1}).

$\underline{\nu_3}$ $\underline{(a_{1g})}$ - An intense doublet is observed for ν_3, the C-C stretch, mode, in both cases, with no such splitting found in the mixed crystal. These observations are consistent with predictions from the correlations previously given. The ^{13}C-^{12}C stretch is seen at 978.4 (C_2H_6) and 823.7 (C_2D_6) cm^{-1} as a single satellite of ν_3 which exhibits correlation field splitting only. This feature may be considered to be the ν_3 stretch mode for a matrix-isolated species. These isotopic peaks have ∿2.2% of the intensity of the corresponding parent peak, are consistent with double the natural aboundance of ^{13}C (1.1%) and lie,

as expected, on the low frequency side of the factor group components of the host.

$\underline{\nu_{10}\ (e_g)}$ - ν_{10}, a CH(CD) stretch mode, is an e_g mode. Now, an e_g mode <u>may</u> exhibit both site and factor group splitting. However, C_2H_6 shows only two of the four expected components for ν_{10}, while in C_2D_6, three components are observed (two strong peaks and one of moderate intensity). The ν_{10}-spectra of isotopically dilute solutions of C_2H_6 in C_2D_6 and vice-versa, however, consist of two components of equal intensity at nearly the same frequency as the strong bands observed for the pure solids. These observations validate the site and factor group predictions postulated on the basis of the crystal structure, and exemplify the utility of mixed crystal spectra. Because the crystal structures of the pure host and guest are identical, the site symmetry is unchanged and thus the site splittings are unaffected. On the other hand, the neighboring molecules that interact with the guest species are now no longer identical oscillators, thus causing the resonance interactions which give rise to the correlation field splitting, to vanish.

$\underline{\nu_{11}\ (e_g)}$ - ν_{11}, a $CH_3(CD_3)$ stretch mode is also an e_g mode. This fundamental was observed with three components for both C_2H_6 and C_2D_6, although the pattern of intensities for the three peaks reveals obvious differences in the two

cases. For C_2D_6, the three components are all of comparable intensity, with the central peak slightly more intense. For C_2H_6, the three components consist of two more intense peaks and a weak one in between. However, in the spectra of the dilute solid solutions only a single peak, broader than in the pure spectra, could be resolved, thus providing no further information.

$\underline{\nu_{12}\ (e_g)}$ - The ν_{12} band, the Raman-active bending mode, consists of three components in the spectrum of C_2H_6, but only two components were observed for C_2D_6, with the intensities markedly different in the two cases. For C_2H_6, the three components consist of two moderately intense neighboring peaks and a weak component on the high frequency side. The corresponding C_2D_6 feature appears as a weak peak and a moderately strong higher frequency peak. However, in the spectra of the isotopic dilute solutions, this fundamental appears as a doublet for C_2H_6 and a singlet for C_2D_6 guests. The bands are somewhat broader than in the pure crystals, and thus one can be certain that the extra components observed for the pure solids are due to factor group splitting.

CHAPTER VII

THE INTERNAL MODES OF THE PARTIALLY-DEUTERATED ETHANES

A. Introduction

     It has been shown in Chapters IV and V that the crystals

of the partially-deuterated ethanes have an "effective" C_1

site symmetry. This leads to the existence of only one

energetically distinguishable orientation of the molecules

in the CH_3CD_3 crystals, and three energetically inequivalent

orientations in the C_2H_5D, $1,1-C_2H_4D_2$ and C_2HD_5 crystals

(see Table 4). This chapter is therefore divided into

three sections. Section B concerns the assignments of the

internal modes of CH_3CD_3 in neat crystals and in dilute

solid solutions in C_2H_6 and C_2H_5D hosts; Section C deals

with the observed fundamental vibrations of C_2H_5D, 1,1-

$C_2H_4D_2$ and C_2HD_5 neat crystals. A comment on the assign-

ments of the observed frequencies is in order. The free

molecules of the partially-deuterated ethanes are of lower

symmetry than the D_{3d} symmetry of ethane. Therefore,

fundamentals, overtones and combinations which were in-

active for the C_2H_6 and C_2D_6 crystals may now become active.

Fermi resonance may also become more prevalent in the

114

crystals of the partially-deuterated ethanes due to the
lower symmetry of the molecules. Moreover, the neat samples
contained some impurities, and natural abundance C-13 im-
purity was present in all the samples. Thus the spectra
of the neat partially-deuterated samples exhibit many bands
and assignment of these is at best tenuous. (A calculation
of C-13 harmonic shifts from the free molecule C-12 fre-
quencies of the partially-deuterated ethanes, using standard
normal coordinate analysis, has been under way, but was
not finished at the time when this thesis was completed.)

The assignments given in this chapter are based on gas
phase frequencies, relative intensities and observed dilute-
mixed crystal frequencies. Also, mutual exclusion was not
observed, so a comparison of infrared and Raman data aided
in the assignments. Only bands assigned as fundamentals
are presented in the wavenumber tables in this chapter,
together with their relative intensities.

B. The Internal Modes of CH_3CD_3

The CH_3CD_3 molecule is of interest among other isotopic
species of ethane, in that substantial symmetry remains
and thus it shows no orientational effect in dilute-
mixed isotopic crystals. The absence of the orientational
effect in the internal mode spectrum of CH_3CD_3 might lead
to an analogy between the internal modes of CH_3CD_3, C_2H_6

and C_2D_6. However, it must be noted that CH_3CD_3 is still disordered because of the existence of the translationally inequivalent orientations. Therefore the usefulness of the $\underset{\sim}{K} = 0$ selection rule may be questionable.

Unfortunately there have been only a few studies of the internal modes of disordered molecular crystals.[73-76] Most of these have dealt with isotopic mixed crystals whose modes are in the separate band limit,[56] and the goal has been to identify the nature of the splitting in the pure crystal spectrum. Little effort has been concentrated on the internal modes in the amalgamation limit.[56] However, studies of the phonons of the isotopic mixed molecular crystals have revealed the usefulness of $\underset{\sim}{K}$ in the amalgamation limit (see Chapter IV).

The most important parameter which determines to which type a given mixed crystal belongs is the ratio of the difference Δ of the energies of the host and guest to the width T of the energy band. When this ratio is large, the energy band is split into a number of bands which correspond approximately to the guest and host, and each band gives rise to its own absorption peak(s). This is the case in the separate band limit or persistence type.[56] The amalgamation limit, on the other hand, is achieved when this ratio is small; i.e., when the energy difference between the host and guest vibration is less than the bandwidth of the pure-crystal mode. A crystal containing molecules

in energetically-inequivalent orientations can be considered a mixture of different "pure crystals", each containing molecules in a simple orientation. The orientational "splitting" then corresponds (approximately) to the guest-host difference, Δ. Formally one can say that the energy difference between the orientational components of CH_3CD_3 is zero. That is, for each vibration all orientations have only one energy, and thus the energy difference is zero. Zero is certainly less than the bandwidth of the vibration, and thus the internal vibrations of these crystals are in the amalgamation limit.

Excitons are more localized than phonons, and thus the phonons of a crystal probe the periodicity of the lattice over a larger range than do the vibrational excitons. If $\mathcal{K}$ is a "good quantum number" for the phonons of a disordered solid in the amalgamation limit, it is likely to be a "good quantum number" for the vibrational excitons of the disordered (CH_3CD_3) solid in this limit as well. If $\mathcal{K}$ selection rules still apply to this disordered solid, then the bands should show the same number of Davydov components as do the corresponding bands of ethane and ethane-d_6. In other words, one would expect to observe a doublet for the non-degenerate modes and a maximum of a quartet for the degenerate modes in the infrared and Raman spectra of solid (II) CH_3CD_3. A breakdown of $\mathcal{K}$ selection rules would most likely lead to broad, structureless bands.

The observed fundamental vibrational frequencies of solid CH_3CD_3 are listed in Table 20. Tables 21 and 22 include the observed frequencies of CH_3CD_3 fundamentals in dilute mixed crystals of C_2H_6 and C_2H_5D. The mixed crystal spectra will aid both in the assignment of CH_3CD_3 fundamental bands and in finding the origin of the neat CH_3CD_3 band splittings. In the neat crystal, singlets were observed for all non-degenerate modes (except for the Raman spectrum of ν_3) and doublets were observed for the degenerate modes in both spectra (except for the IR spectrum of ν_{12}). If it is true that the CH_3CD_3 crystal still possesses a spectroscopically "effective" C_i site symmetry, like C_2H_6 and C_2D_6, then the "a" mode doublets, etc. would arise from Davydov interactions and they should disappear in the dilute-mixed crystals.

C-13 isotope shifts were observed for three of the twelve fundamentals of CH_3CD_3. It is to be noted that for this molecule two different C-13 species exist, each with 1.1% natural abundance. The Raman and IR spectra of the fundamental modes of neat crystalline CH_3CD_3, and of its dilute solid solutions in C_2H_6 and C_2H_5D hosts, are shown in Figures 24-32.

Table 20. Internal Fundamental Frequencies (cm^{-1}) of CH_3CD_3.[a]

Mode	Description	Neat Crystal	
		IR	Raman
ν_1 (a_1)	CH str.	2881.3 (vs)	2878.1 (vs)
		2876.0 (w)[c]	2874.8 (w)[c]
ν_2 (a_1)	CH_3 def.	1376.2 (m)	1387 (w)
		1380.5 (m)	
ν_3 (a_1)	C-C str.	902 (vw)	907 (s)
			898 (s)
			889.7 (w)[c]
ν_5 (a_1)	C-D str.	2078.7 (s, sh)	2077.8 (vs, sh)
		2070.5 (w)[c]	2070.6 (w)[c]
ν_6 (a_1)	CD_3 def.	1113.6 (m, asy)	1114.8 (m)
ν_7 (e)	CH str	2965.5 (vs)	2965.2 (s)
		2963.3 (vs)	2960.1 (s)
		2957.5 (m, shld)[c]	
		2955.0 (m, shld)[c]	
ν_8 (e)	CH_3 def.	1460.0 (m)	1462.3 (mw)
		1456.5 (m)	1453.9 (w)
ν_9 (e)	Bend.	681.5 (s)	
		674.3 (s)	
		672.1 (ms)[c]	
		667.4 (w)[c]	
ν_{10} (e)	C-D str.	2236.2 (s, sh)	2235.3 (s)
		2233.8 (s, sh)	2232.3 (s)

Table 20. Continued.

Mode	Description	Neat Crystal	
		IR	Raman
ν_{11} (e)	CD_3 def.	1109.0 (m)	1110.2 (w)
		1107.0 (m)	
ν_{12} (e)	Bend	1061.3 (shld)	1062 (w, asy)
		1059.0 (m)	
		1056.4 (m)	1054.2 (w)
		1052.8 (w, sh)	

Key to Table:

[a] v = very, s = strong, m = moderate, w = weak, sh = sharp, shld = shoulder, bd = broad, asy = asymmetric.

[b] Gas phase values from Reference 21(k).

[c] These frequencies are attributed to C-13 substituted molecules. However, see further comments in text.

[d] From Reference 77.

Table 21. Observed Frequencies of CH_3CD_3 Fundamentals in Dilute Mixed Crystals of CH_3CD_3/C_2H_6.

Assignment	3% d_3 in d_0 IR (cm^{-1})	4% d_3 in d_0 Raman (cm^{-1})
ν_1 a_1	1376.2 (ms)	
ν_3 a_1	902 (w)	902.3 (s)
		890.0 (vw)[a]
ν_5 a_1	2079.5 (vs, sh)	2079 (vs)
	2069.6 (w)[a]	
ν_6 a_1	1114.3 (ms, sh)	1115 (m)
ν_9 e	679.8 (s)	
	676.7 (s)	
	673.7 (w)[a]	
ν_{10} e	2235.8 (s)	2235 (s)
	2232.8 (s)	2232 (s)
ν_{11} e	1109.5 (m, sh)	1109 (w)
	1107.4 (m, sh)	
ν_{12} e	1060.5 (w)	
	1058.7 (vs)	1059 (ms)
	1056.5 (w)	

[a]These frequencies are attributed to C-13 substituted molecules.

Table 22. Observed Frequencies (cm^{-1}) of CH_3CD_3 Fundamentals in 2% CH_3CD_3/C_2H_5D.

Assignment	Infrared	Raman[a]
ν_3 a_1	902 (w)	902 (s)
ν_5 a_1	2079.5 (vs, sh) 2071.0 (w)[b]	2078.0 (vs)
ν_6 a_1	1113.9 (ms, sh)	----
ν_9 e	679.8 (s) 676.6 (s) 673.2 (w)[b]	
ν_{10} (e)	2236.6 (vs) 2233.3 (s)	2236 (s) 2232 (s)
ν_{11} (e)	1109.3 (m, sh) 1107.2 (m, sh)	---- ----
ν_{12} e	1060.6 (w) 1058.6 (vs) 1056.5 (w)	1058.0 (m)

[a]The ν_6 and ν_{11} bands of CH_3CD_3 are hidden by the C_2H_5D host bands in the Raman spectra.

[b]These frequencies are attributed to C-13 substituted molecules of CH_3CD_3.

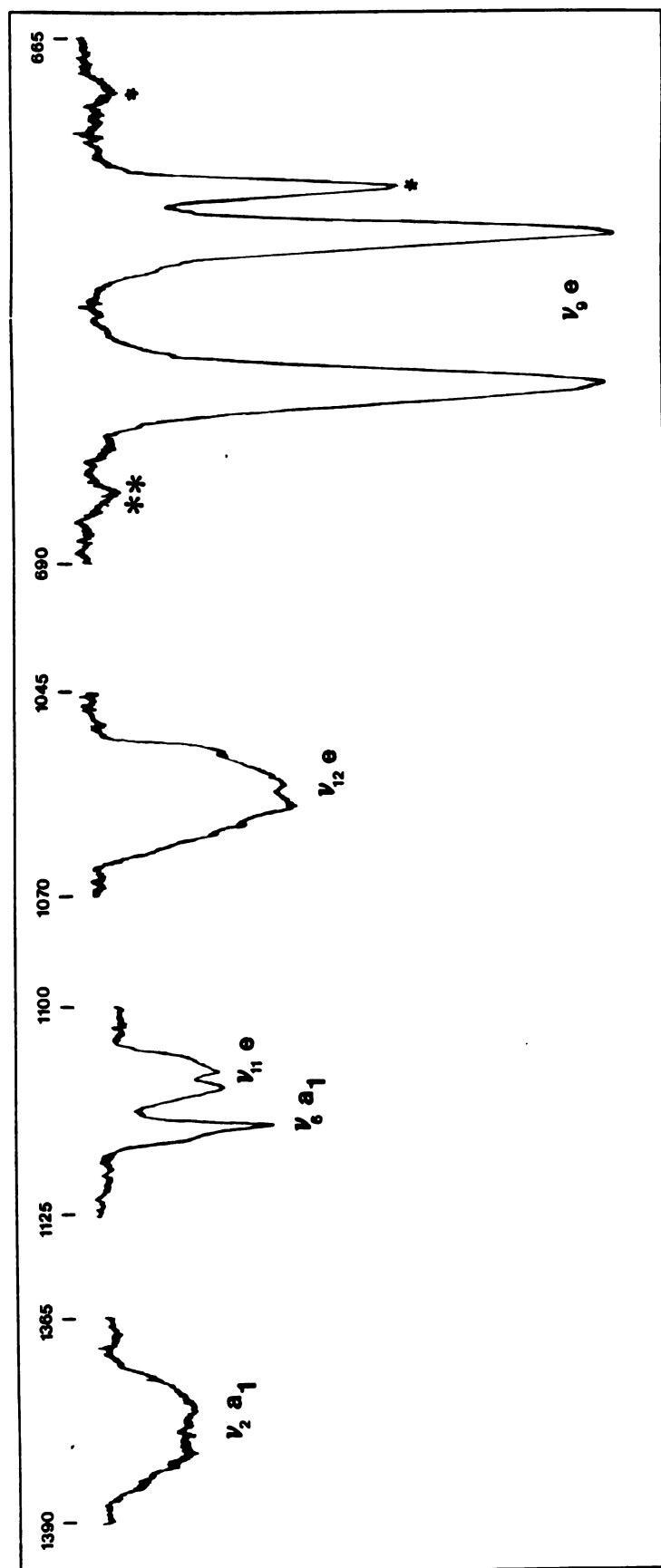Figure 24. Part of the IR spectrum of solid (II) CH_3CD_3; ν_2, ν_6, ν_9, ν_{11} and ν_{12}. The peaks marked with an asterisk are attributed to C-13 substituted molecules of CH_3CD_3 and that marked with the double asterisk is attributed to ν_9 (a") of $1,1-C_2H_4D_2$.

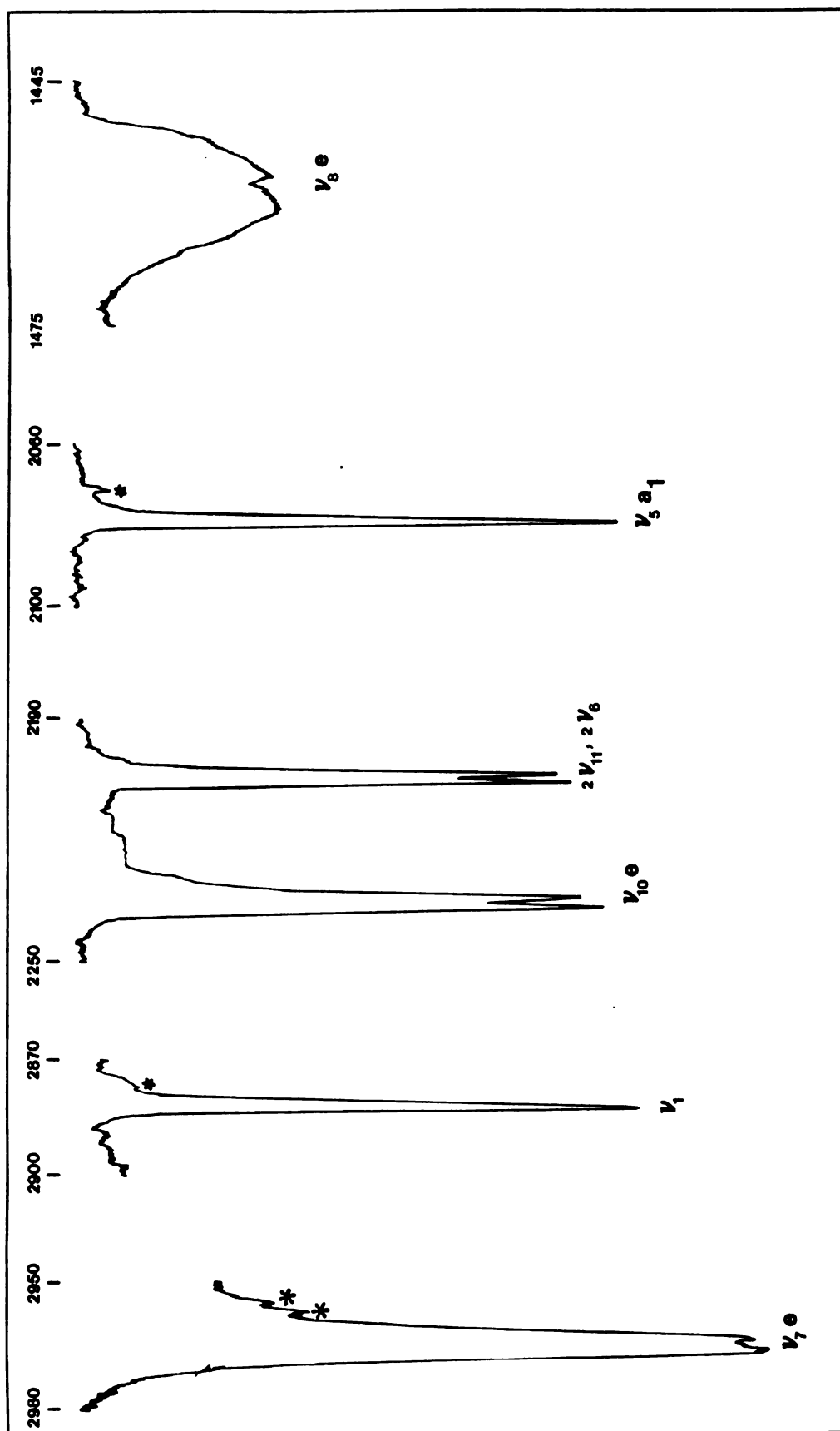Figure 25. Part of the IR spectrum of solid (II) CH_3CD_3; ν_1, ν_5, ν_7, ν_8, ν_{10} and $2\nu_{11}$ $(2\nu_6)$. The peaks marked with an asterisk are attributed to C-13 substituted molecules of CH_3CD_3.
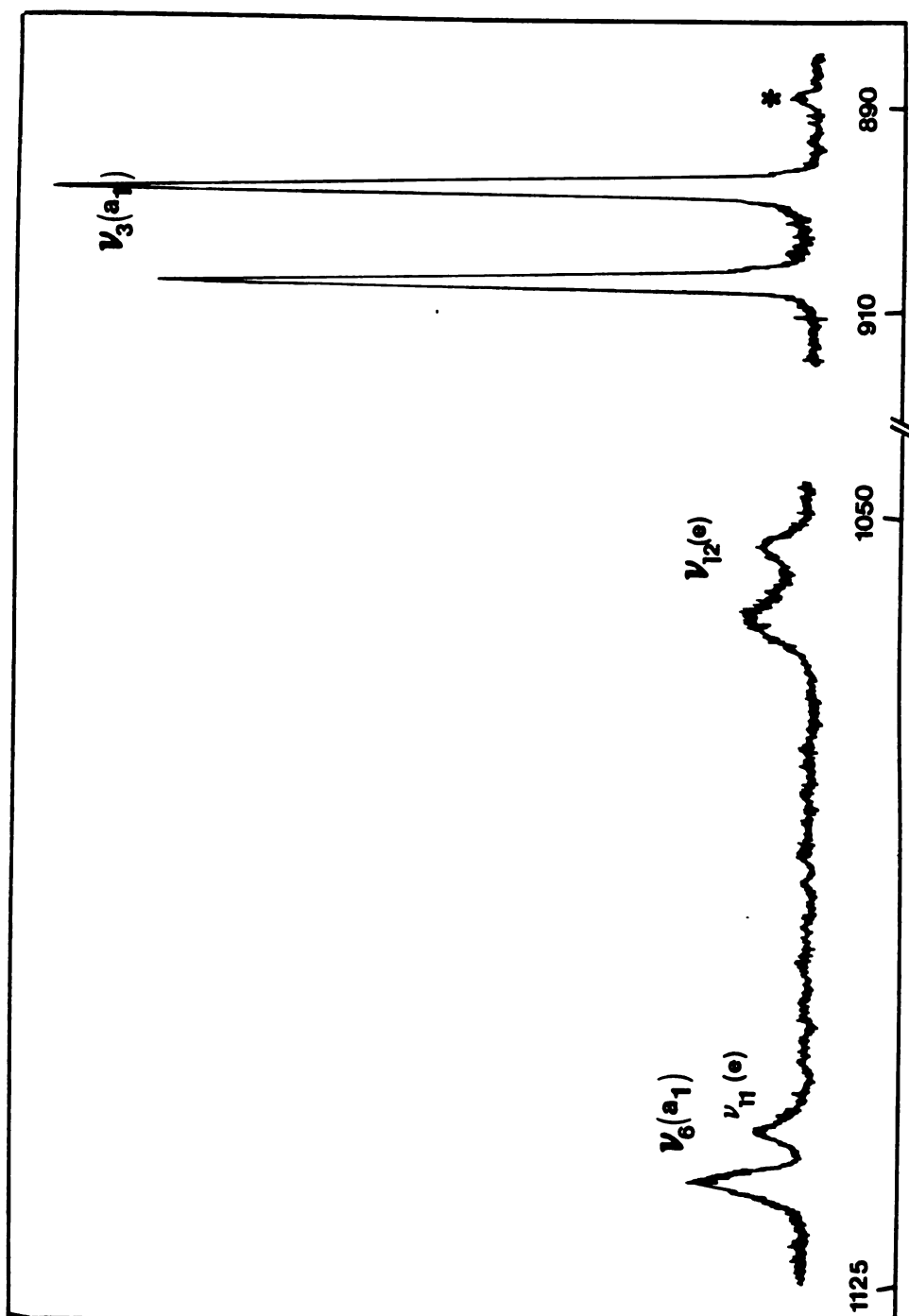
Figure 26. The ν_3, ν_{12}, ν_{11} and ν_6 regions of the Raman spectrum of solid (II) CH_3CD_3. The peak marked with an asterisk is attributed to C-13 substituted molecules of CH_3CD_3.
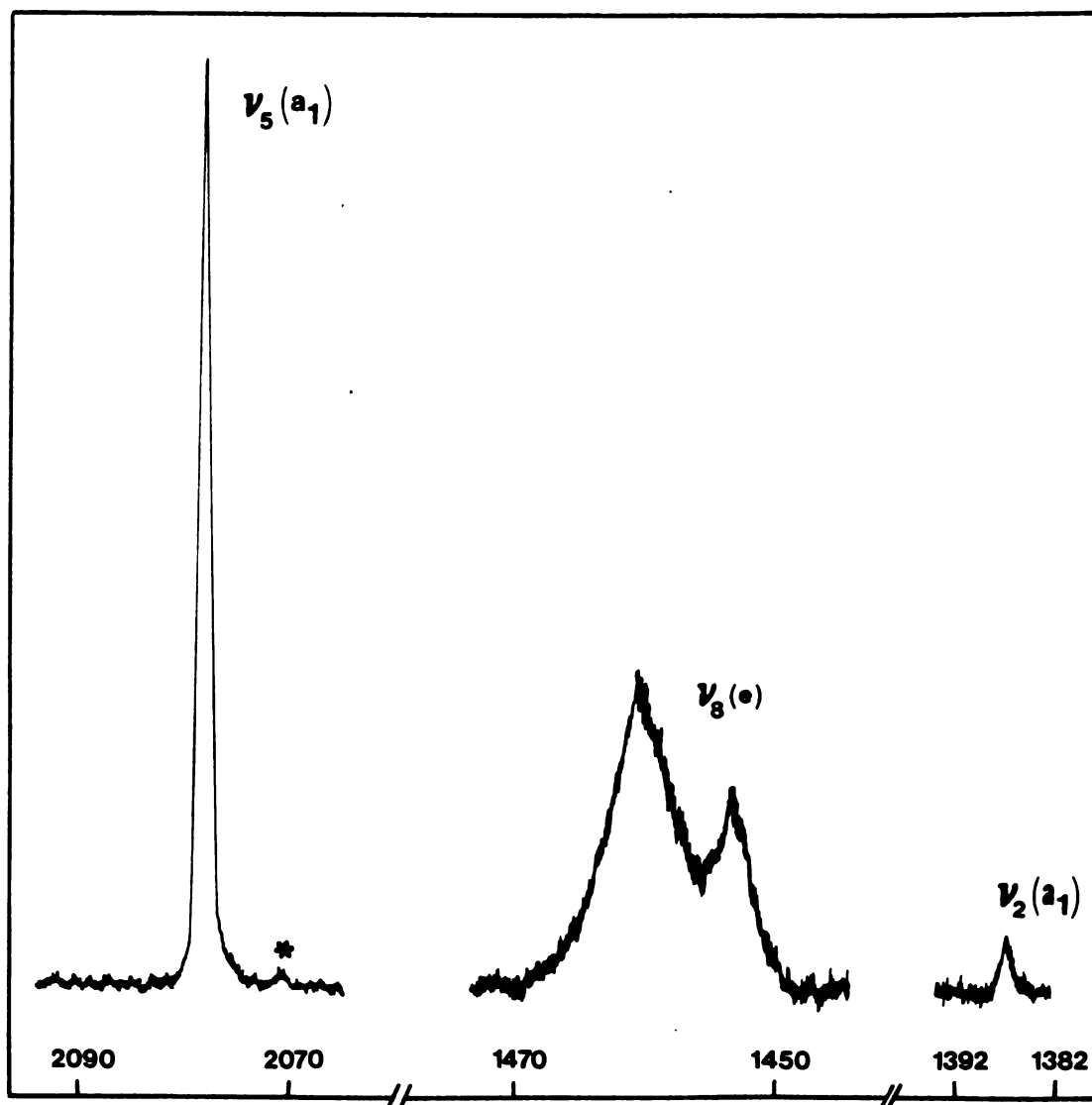
Figure 27. Raman scattering from internal modes of solid (II)
CH_3CD_3; ν_2, ν_8 and ν_5. The peak marked with an
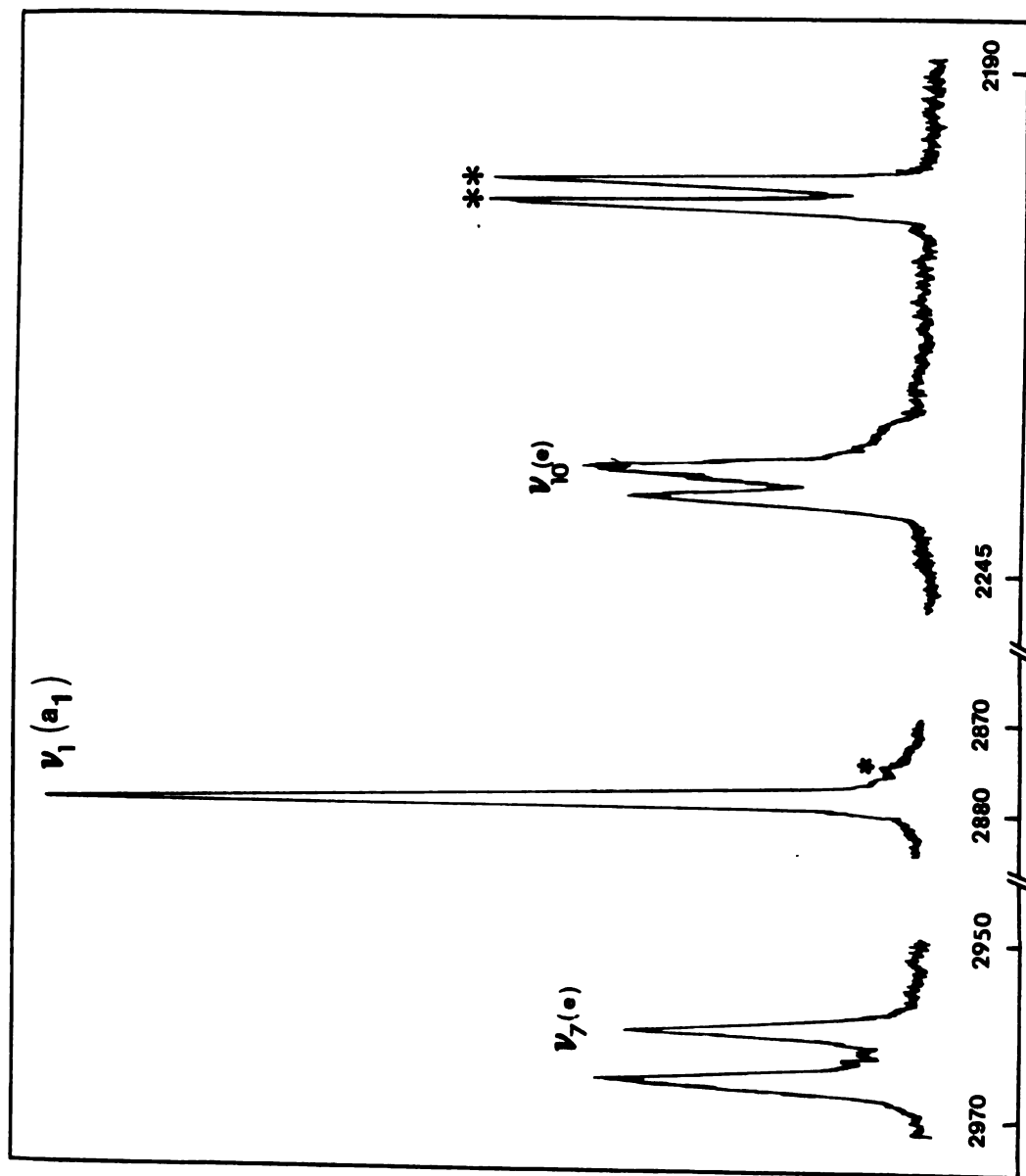asterisk is attributed to C-13 substituted mole-
cules.

Figure 28. Raman scattering from internal modes of solid (II) CH_3CD_3; ν_1, ν_7 and ν_{10}. The peak marked with an asterisk is attributed to C-13 substituted molecules of CH_3CD_3 and that marked with the double asterisk is assigned to an overtone of ν_6 and ν_{11} in Fermi resonance with ν_{10}.
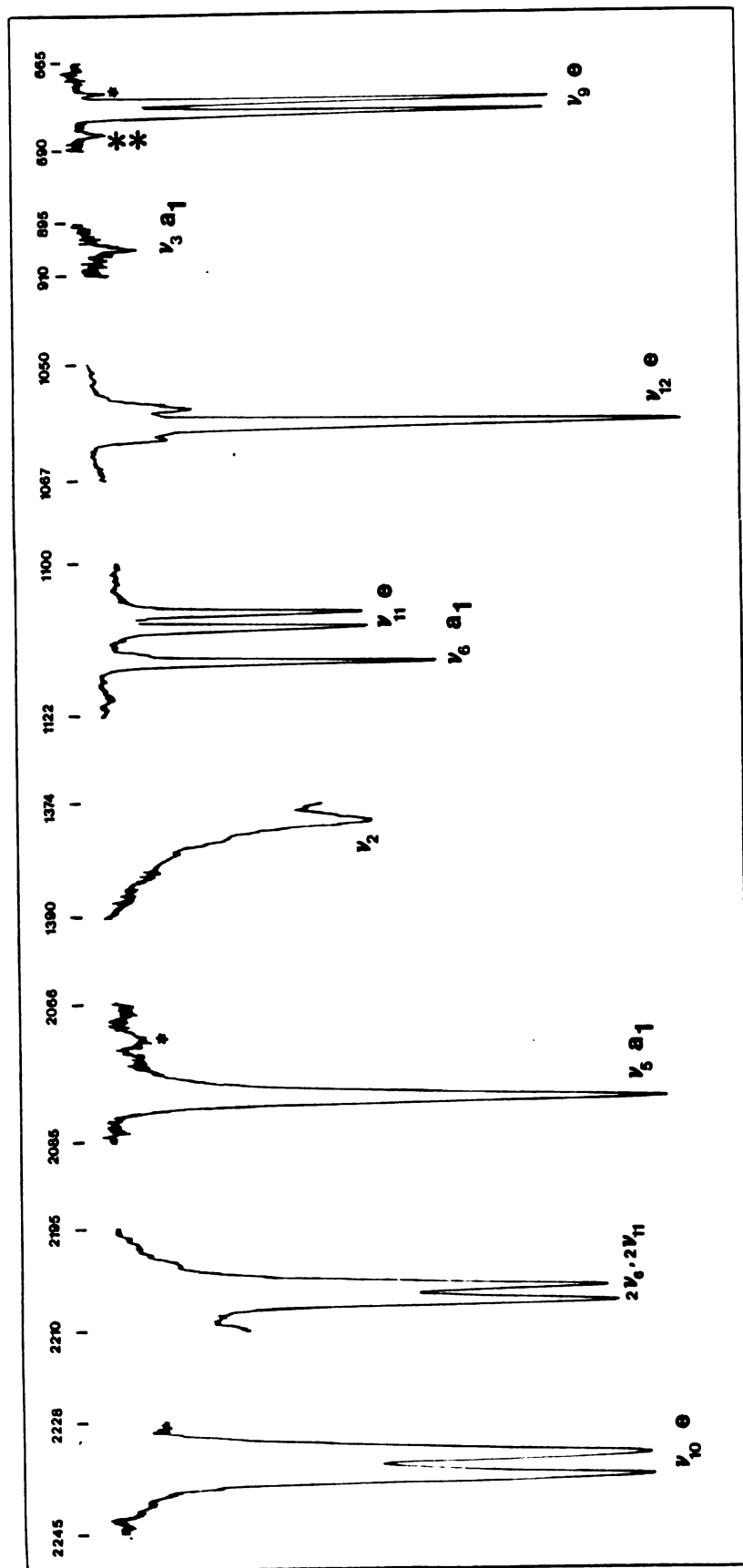
Figure 29. Part of IR spectrum of 3% CH_3CD_3/C_2H_6; ν_2, ν_3, ν_5, ν_6, ν_9, ν_{10}, ν_{11} and ν_{12} of CH_3CD_3. The peak marked with an asterisk is attributed to C-13 substituted molecules of CH_3CD_3, and that marked with the double asterisk is attributed to ν_9 (a") of $1,1-C_2H_4D_2$.
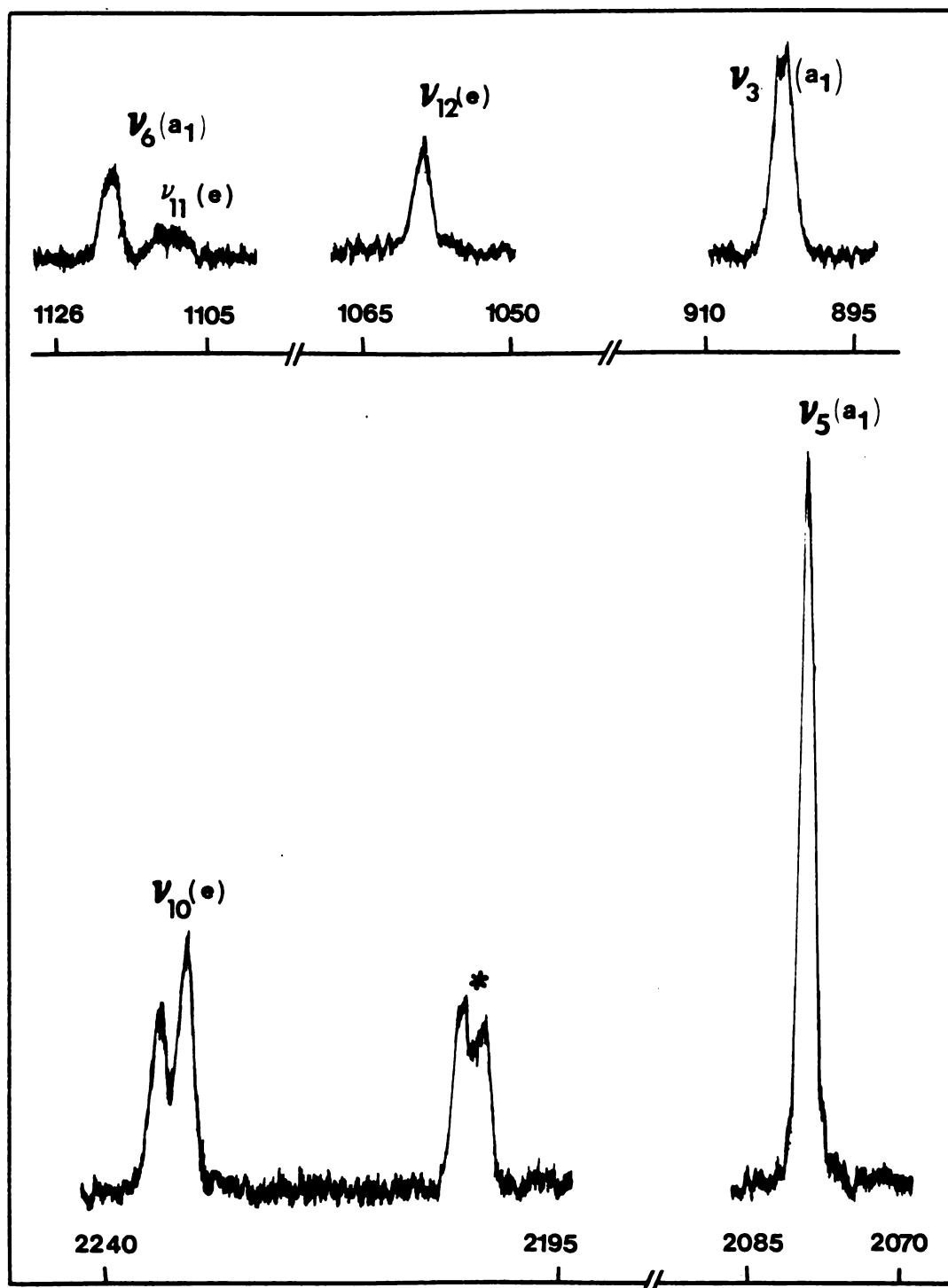
Figure 30.   Part of the Raman spectrum of 4% CH_3CD_3/C_2H_6 ν_2, ν_3, ν_6, ν_{10}, ν_{11} and ν_{12} of CH_3CD_3.   The peak marked with an asterisk is attributed to the overtone combination of ν_6 and ν_{11} in Fermi resonance with ν_{10}.
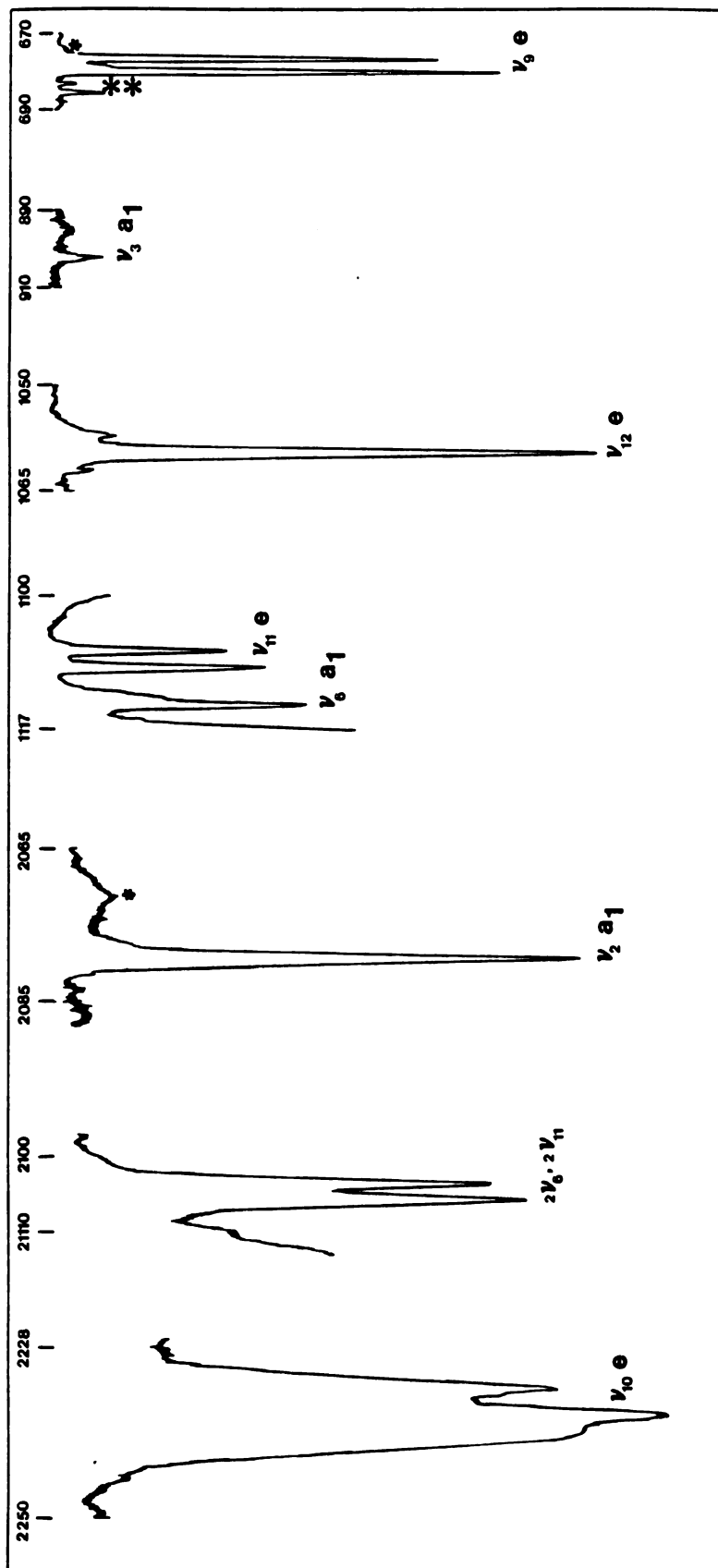
Figure 31. Part of the IR spectrum of 2.5% CH_3CD_3/C_2H_5D; ν_3, ν_5, ν_6, ν_9, ν_{10}, ν_{11} and ν_{12} of CH_3CD_3. The peak marked with an asterisk is attributed to C-13 substituted molecules, and those with the double asterisk are attributed to ν_9 (a") of 1,1-$C_2H_4D_2$.

Figure 32. Part of the Raman spectrum of 2ν CH_3CD_3/C_2HD_5; ν_2, ν_3, ν_{10} and ν_{12} of CH_3CD_3.

Neat Solid (II) CH_3CD_3

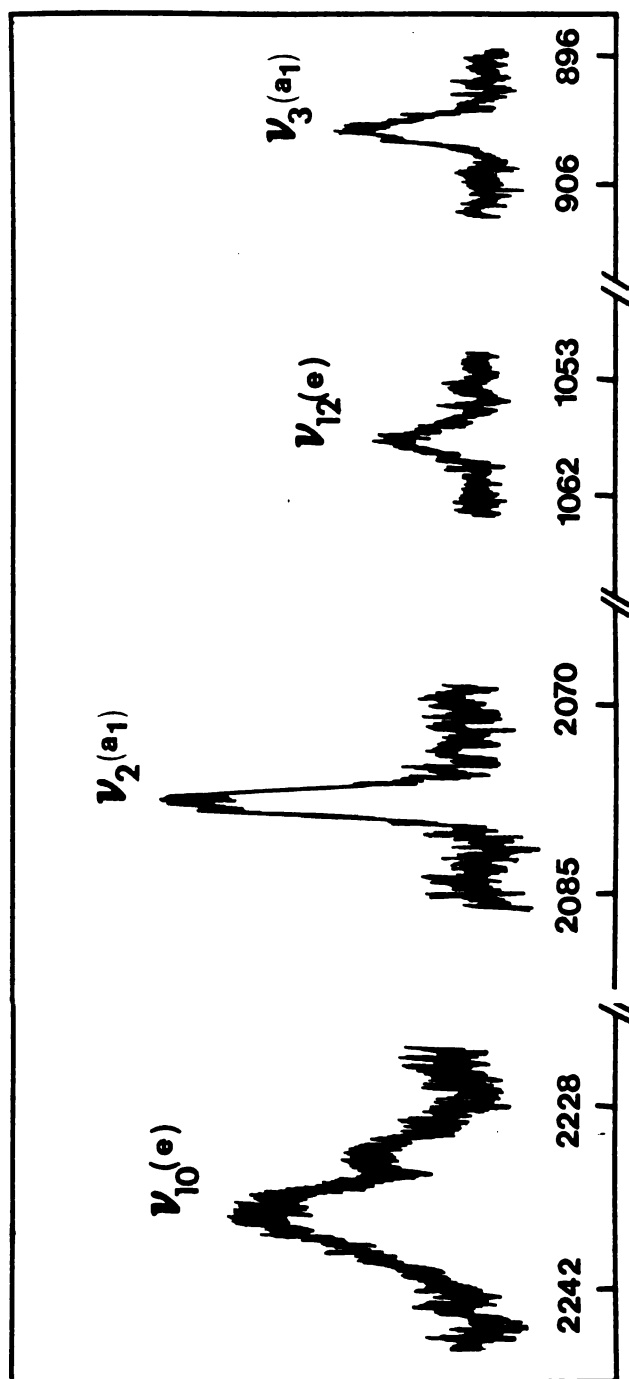ν_1 and ν_5 show strong singlets in both the infrared and Raman spectra; ^{13}C components of ν_1 and ν_5 were observed as weak bands with a shift of 3.8 and 7.7 cm^{-1} (average shift in IR and Raman spectrum for each band), respectively.

ν_2 was observed as a weak singlet in the Raman, but shows a rather broad doublet in the IR spectrum which is not very well resolved. The band width at half height in the IR is (~ 5 cm^{-1}), twice that of the Raman spectrum (~ 2.5 cm^{-1}).

ν_3 shows a weak singlet in the IR, but a strong doublet was observed in the Raman spectrum, together with a weak ^{13}C component shifted by 14.8 cm^{-1} from the mean of the doublet. However, only a singlet was observed in the dilute-mixed crystals of CH_3CD_3/C_2H_6 and CH_3CD_3/C_2H_5D. ν_3 was the only non-degenerate mode showing clear Davydov components; the splitting of the two components is 9 cm^{-1}. ν_6 shows a singlet of moderate intensity in both the Raman and IR spectra, but it is asymmetric toward the high frequency side in the IR spectrum.

The degenerate ν_7 and ν_{10} modes show strong doublets in both spectra. Whereas in the isotopic dilute-mixed crystals the ν_7 band of CH_3CD_3 is obscured by C_2H_6 or C_2H_5D host bands, the doublet for ν_{10} remains indicating the site group origin of the splitting for this "e" mode vibration. A strong doublet assigned to overtones of ν_{11} and ν_6 of CH_3CD_3 in Fermi resonance with ν_{10} is also

observed in all spectra. A possible alternative assign-
ment would be the combination band of $\nu_6 + \nu_{11}$. Two
shoulders in the low frequency side of the ν_7 band in the
IR spectrum are tentatively assigned to C-13 substituted
molecules.

ν_8, a degenerate mode, shows a doublet of moderate
intensity in both spectra, but it is not very well re-
solved in the IR spectrum. In the Raman spectrum, the
higher frequency component is more intense than the other
component. Unfortunately, this band was not observed in
the isotopic dilute mixed crystals, so that further infor-
mation could not be obtained.

In the ν_9 region of the IR spectrum a strong doublet,
along with a peak of moderate intensity, lie at 681.5 cm^{-1},
674.3 cm^{-1} and 672.1 cm^{-1}, respectively, but no band is
seen in the Raman spectrum. In the dilute-mixed crystal
(IR) spectrum the 672.1 cm^{-1} band is replaced by a weak
band; it may possibly be attributed to C-13 substituted
molecules. It is to be noted that because of the presence
of C-13 substituted molecules of CH_3CD_3, for the e-modes
one might expect to observe two site group components for
$D_3{}^{13}C-{}^{12}CH_3$ and two site group components for $D_3{}^{12}C-{}^{13}CH_3$
in addition to the four factor group components for the
$D_3{}^{12}C-{}^{12}CH_3$ molecule in the "pure" crystal. However, it
is not always possible to see all the predicted components,
and very likely fewer components will be obtained. If the

ν_9 band of CH_3CD_3 shows only site group splitting and if the two expected site-group components of each C-13 species are not resolved, one would expect to observe the following number of bands in this region:

2 strong bands for $D_3{}^{12}C-{}^{12}CH_3$

1 weak band for $D_3{}^{13}C-{}^{12}CH_3$

1 weak band for $D_3{}^{12}C-{}^{13}CH_3$.

In fact, a weak band has been observed at 667.4 cm^{-1} in the neat crystal infrared spectrum (but apparently it is absent in the dilute mixed crystal spectra), which certainly could be attributed to one of the above C-13 substituted molecules. Now, if the moderately intense band at 672.1 cm^{-1} is attributed to the other C-13 species and the two strong bands are due to the site-group components of $D_3{}^{12}C-{}^{12}CH_3$, the enhanced intensity of the 672.1 cm^{-1} band has most likely arisen through borrowing from its neighboring strong bands. This effect, termed inter-molecular Fermi resonance, has been invoked to explain the Raman scattering in the ν_4 (bending) region of acetylene-d_2.[78] Note that the 672.1 cm^{-1} band can still be seen, but relatively weaker, in the dilute-mixed crystals of CH_3CD_3/C_2H_6 and CH_3CD_3/C_2H_5D. In the dilute-mixed crystals $D_3{}^{13}C-{}^{12}CH_3$ and $D_3{}^{12}C-{}^{13}CH_3$ molecules no longer have "identical" neighbors (CH_3CD_3) with which to resonantly

interact and borrow intensity; thus the observations are consistent with the interpretation just given. The weak bands: 686.3 cm^{-1} in the neat crystal, 685.2 cm^{-1} and 682.6 in the dilute-mixed crystal of CH_3CD_3 in C_2H_5D, and 685.0 cm^{-1} in the dilute-mixed crystal of CH_3CD_3 in C_2H_6 are attributed to ν_9 (a") of 1,1-$C_2H_4D_2$.

The situation is more complicated for the ν_{12} "e" mode, where a well-separated doublet of moderately weak intensity is observed in the Raman spectrum at 1054.2 cm^{-1} and 1062 cm^{-1}, but a rather structureless doublet with two shoulders is observed in the IR spectrum at 1052.8 cm^{-1} (shoulder), 1056.4 cm^{-1}, 1059.0 cm^{-1} and 1061.3 cm^{-1} (shoulder). The doublet in the neat crystal Raman spectrum is replaced by a singlet in the dilute-mixed crystals, but a triplet consisting of a very strong band and two weak bands is seen in the IR spectra of the dilute-mixed crystals. The presence of bands due to C-13 substituted molecules in the same region, and the strange behavior of the band intensities in the neat and isotopic dilute-mixed crystals of both spectra, preclude a certain assignment at this moment. A normal coordinate calculation, yet incomplete, is needed to substantiate such a decision.

Mixed Crystals

The observed data for isotopic dilute-mixed crystals of CH_3CD_3 in C_2H_6 and C_2H_5D allow a comparison of site-group splittings, defined in Chapter II, for the degenerate modes of CH_3CD_3 and enable one to look at them as a function of the host. Table 23 lists the site splitting, δ_{ss}, for ν_9, ν_{10} and ν_{11} bands of CH_3CD_3 in C_2H_6 and C_2H_5D hosts. The results presented in Table 23 for the magnitude of the site splittings show no obviously large iso- tope effects from the host molecules; however the splitting, similar to the orientational effect discussed in Chapter V, is sensitive to the vibrational type. The greater site splitting of ν_9 (bending) and ν_{10} (C-D str.) compared to ν_{11} (CD_3 def.) is accounted for by their greater inter- actions with the environmental field.

C. The Internal Modes of C_2H_5D, $1,1$-$C_2H_4D_2$ and C_2HD_5

The molecules in the crystals of C_2H_5D, $1,1$-$C_2H_4D_2$ and C_2HD_5 can assume three energetically inequivalent or- ientations in a C_1 lattice site. The orientational effect observed in mixed crystals (see Chapter V) for the above molecules can be observed in pure crystals as well, and usually serves to broaden the exciton structure to such an extent that neither the orientational effect nor the exci- ton structure can be extracted from the spectra. Other

Table 23. Site Splitting for Degenerate Modes of CH_3CD_3 in Dilute Mixed Crystals.[a]

Mode	In C_2H_6 δ_{ss} (cm^{-1})	In C_2H_5D δ_{ss} (cm^{-1})
ν_9 Bending	3.1	3.2
ν_{10} C–D str.	3.1[b]	3.6[b]
ν_{11} CD_3 def.	2.1	2.1

[a]The dilute mixtures are 2.5% $C_2H_3D_3/C_2H_5D$ and 3% CH_3CD_3/C_2H_6 for the infrared experiments.

[b]These values are the mean of those observed in the infrared and Raman spectra.

effects, such as breakdown of the $\mathcal{K} = 0$ selection rule due to the loss of translational symmetry in the crystal, may also contribute to the broadening of the exciton structure in spectra of solid isotopic ethanes where the free molecule has lower than D_{3d} symmetry.

The frequencies of the observed internal fundamentals for crystalline C_2H_5D, $1,1-C_2H_4D_2$ and C_2HD_5 are listed in Tables 24-26. Figures 33-50 show the IR and Raman fundamental bands for these crystals.

$\underline{C_2H_5D}$

ν_3, ν_6 and ν_{11} a' show singlets in the IR spectra of the C_2HD_5 and in the neat crystal. Therefore, they are expected to be in the amalgamation limit. However, ν_3 and ν_6 exhibit doublets in the Raman spectra. The two weak bands at $\sim$967 cm^{-1} and $\sim$964 cm^{-1} are attributed to ν_3 of $^{13}CH_3-CH_2D$ and $CH_3-^{13}CH_2D$, respectively. The fundamentals ν_1, ν_2, ν_5, ν_7 (a'), ν_8 (a'), ν_{10} (a") and ν_{12}(a") were not observed in the C_2HD_5 matrix; therefore, it is difficult to classify these bands as either amalgamated or in the separate-band limit. ν_1 shows a broad, moderately intense singlet in the IR spectrum, whereas a doublet of moderate intensity is observed in the Raman spectrum which is not very well resolved. ν_2 appears as a single weak band in the Raman spectrum; however, a broad band of moderate intensity with a high-frequency shoulder is seen in the IR

Table 24.   Internal Fundamental Frequencies (cm^{-1}) of
            Solid (II) C_2H_5D.*

Assignment	Gas[a]	Infrared	Raman
ν_1 a'	2896	2879.8 (ms, bd)	2878.7 (m)
			2875.9 (m)
ν_2 a'	1354	1346.3 (mw, shld)	
		1341.5 (m)	1338.6 (vw)
ν_3 a'	978	978 (vw)	981.0 (vs)
			976.8 (vs)
			967.0 (vw)[b]
			964.0 (vw)[b]
ν_5 a'	2950	2936.3 (s)	2939.7 (m)
		2934.3 (s, shld)	2935.1 (vs)
			2933.0 (vs)
ν_6 a'	1388	1378	1390.4 (vw)
			1387.3 (w)
ν_7 a'	2180	2176 (mw, shld)	2176.1 (m, shl)
		2173.4 (m, shld)	2172.4 (ms)
		2169.8 (ms)	2169.8 (s)
a"	2980	2968.0 (vs)	2964.3 (m, bd)
		2963.0 (vs)	2962.1 (m, bd)
ν_8 a'	1312	1301.5 (mw, asy)	1304.8 (m)
ν_8 a"	1470	1458.0 (m)	1462 (ms)
		1456.5 (m)	1454.8 (m, shld)

Table 24. Continued.

Assignment	Gas[a]	Infrared	Raman
ν_9 a'	717	717.5 (m)	718.3 (w)
		716.2 (m)	713.2 (w)
		712.0 (ms)	
a"	805	807.3 (ms)	
		804.8 (m, shld)	
		800.6 (ms)	
ν_{10} a'			
a"	2966	2950.5 (mw)	2950.35 (s)
		2947.0 (w)	2946.1 (s)
ν_{11} a'	1310	1290.0 (m)	1294.6 (mw)
a"	1460	1445 (m, bd)	
ν_{12} a'	1159		1158.6 (w)
		1152.0 (vw)	1152.3 (w)
a"	1122	1118.4 (mw)	1119.3 (mw)

*Footnotes as in Table 20, except:

[a]Gas phase values from References 21(c) and 21(f).

[b]These frequencies attributed to $CH_3-^{13}CHD_2$ and $^{13}CH_3-CHD_2$.

Table 25. Observed Fundamental Frequencies of Solid (II) 1,1-$C_2H_4D_2$.

Assignment	Gas Phase	Infrared (cm^{-1})	Raman (cm^{-1})
ν_1 a'	2949.3	2935.7 (vs)	2936.3 (s)
			2934.7 (s)
ν_2 a'	1389	1374. (m, asy)	1375.7 (w)
ν_3 a'	944.0	943.0 (m)	945.8 (vs)
			939.0 (vs)
			929.3 (w)c
ν_5 a'	2129.0	2120.0 (vs, asy)	2119.5 (vs)
			2117.3 (vs)
ν_6 a'	1117	1117.5 (m)	1117.9 (m)
ν_7 a'	2978	2963.5 (s)	2963.3 (s)
a"	2980	2965.5 (s, shld)	2966.7 (s)
ν_8 a'	1487	1480.2 (mw)	1482.1 (w)
			1479.1 (w)
a"	146	1460 (ms)	1462.1 (mw)
		1454.5 (ms)	1456.8 (mw)
			1450.5 (mw)
ν_9 a'	739.0	739.1 (s)	736.5 (w)
		733.0 (s)	733.0 (w)
a"	690.0	686.5 (s)	685. (vw)
		681.2 (s)	681.1 (vw)
ν_{10} a'	2956	2941.7 (vs)	2941.5 (s)
a"	2216	2210.8 (vs)	2210.2 (s)
			2208.7 (ms, shld)
ν_{11} a'	1308		1301.2 (w)
a"	1302	1290 (ms, asy)	1291.5 (w, bd)
ν_{12} a'	1085	1074.0 (m, asy)	1079.7 (m, shld)
			1075.6 (m)
a"	1112	1108 (m)	1109.6 (mw, asy)

Footnotes as in Table 20 except: [a]Gas phase values from Ref.21(j). [b]This frequency is attributed to C-13 substituted molecules.

Table 26. Internal Fundamental Frequencies (cm^{-1}) of Solid (II) C_2HD_5.

Assignment	Gas Phase	Infrared (cm^{-1})	Raman (cm^{-1})
ν_1 a'	2163	2150.8 (vs)	2151.1 (vs) 2150.1 (vs) 2147.0 (vw) [b]
$2\nu_{11}$ a'	2097	2080.6 (s) 2077.3 (w)	2080.2 (vs) 2077.2 (w)
ν_3 a'	866	861. (w)	868.1 (s) 858.2 (s) 854.0 (w) [b]
ν_5 a'	2124	2122 (w)	2117.5 (mw)
ν_6 a'	1075	1067.0 (m, shld) 1062.5 (m)	1066 (w, shld)
ν_7 a'	2953	2945.5 (vs) 2940.0 (vs, shld) 2938.0 (vs)	2946.0 (ms) 2940.2 (ms) 2938.1 (ms)
a"	2211	2209.0 (m) 2207.3 (m)	2209.4 (s) 2207.1 (s)
ν_8 a'	1133	1127 (w)	1129.8 (m, shld) 1126.6 (ms)
a"	1309	1299.5 (m)	1301.4 (w, b)
ν_9 a'	599	601.0 (m) 596.7 (ms)	
a"	631	635 (ms, asy) 629.5 (ms) 620.2 (w) [b] 611.5 (w, bd) [b]	636.1 (w) 634.4 (vw)
ν_{10} a'	2264	2257 (w, bd)	2257 (mw, bd)
a"	2229	2225.6 (vs) 2223.0 (vs) 2220.0 (vs)	2225.1 (m) 2222.1 (m) 2219.8 (ms)

Table 26. Continued.

Assign-ment	Gas Phase	Infrared (cm^{-1})	Raman (cm^{-1})
ν_{11} a'	1056	1059.0 (m, shld)	1059.0 (mw) 1052.0 (w) 1045.0 (mw)
a"	1301	1291.3 (w)? 1287.7 (w)	1288.6 (w, bd)
ν_{12} a'	1007	1005.7 (w, shld) 1003.6 (w)	1006.5 (vw) 1003.7 (w)
a"	966	965 (w)	966 (mw) 964 (w)

Key to Table:

[a]Gas values are from References 21(e) and 21(f).

[b]These frequencies are attributed to C-13 substituted molecules.
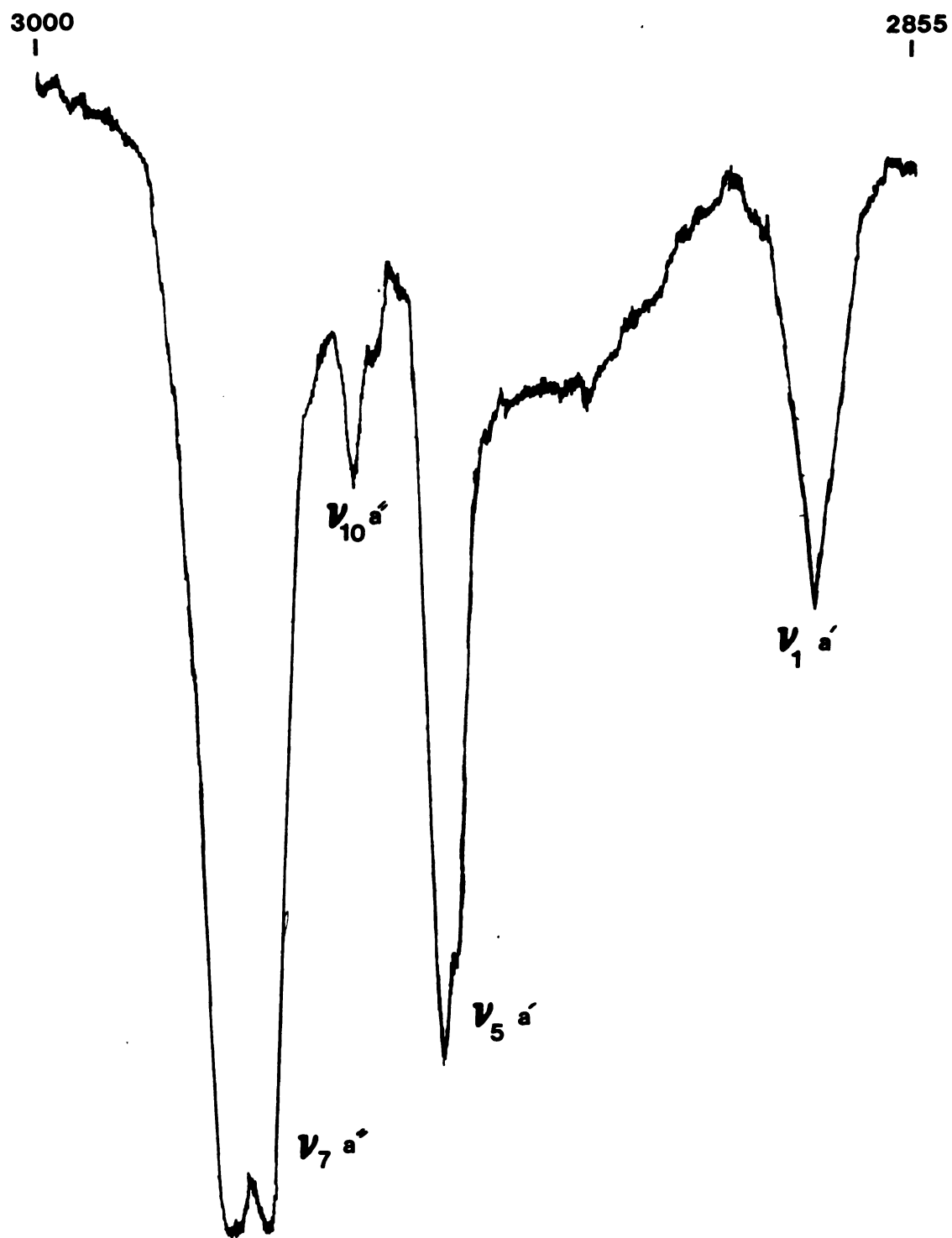
Figure 33. Part of the IR spectrum of solid (II) C_2H_5D; ν_1 (a'), ν_5 (a'), ν_7 (a") and ν_{10}(a").
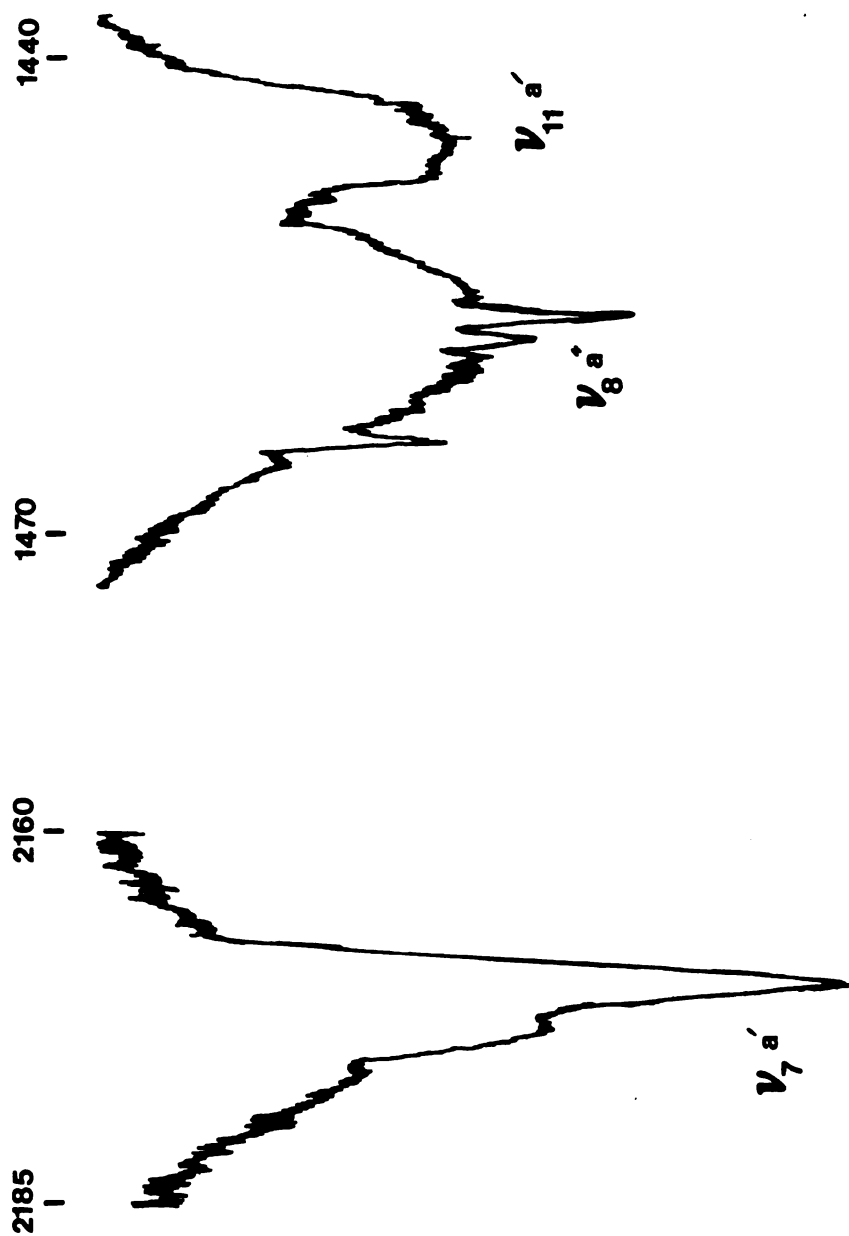
Figure 34. Part of the IR spectrum of solid (II) C_2H_5D; ν_7 (a'), ν_8 (a'') and ν_{11} (a').
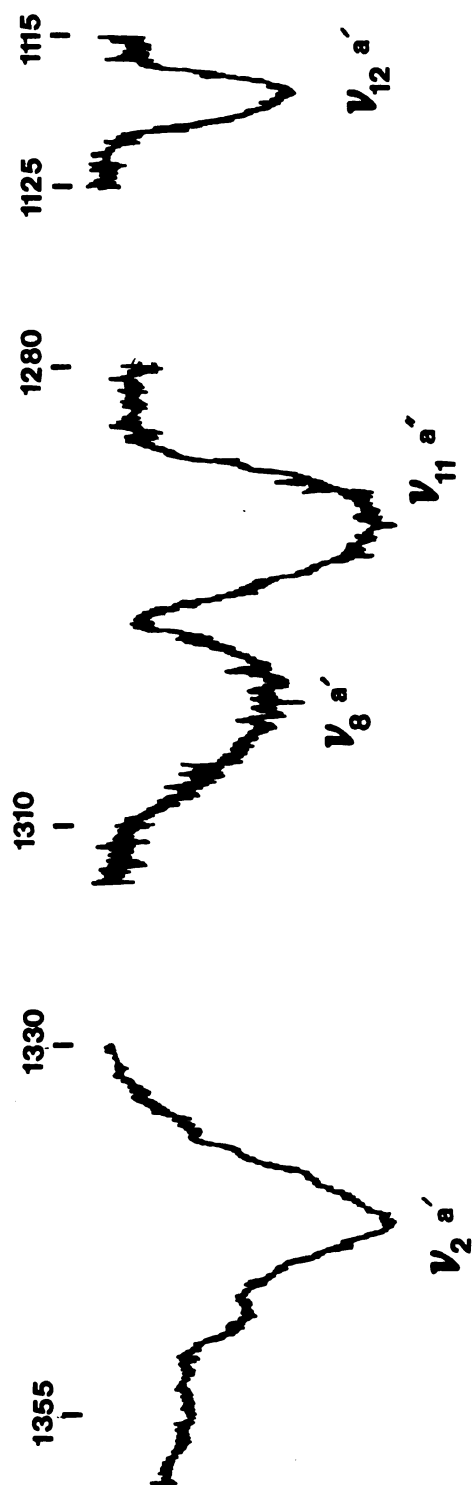
Figure 35. Part of the IR spectrum of solid (II) C_2H_5D; ν_2 (a'), ν_8 (a'), ν_{11} (a'') and ν_{12} (a').
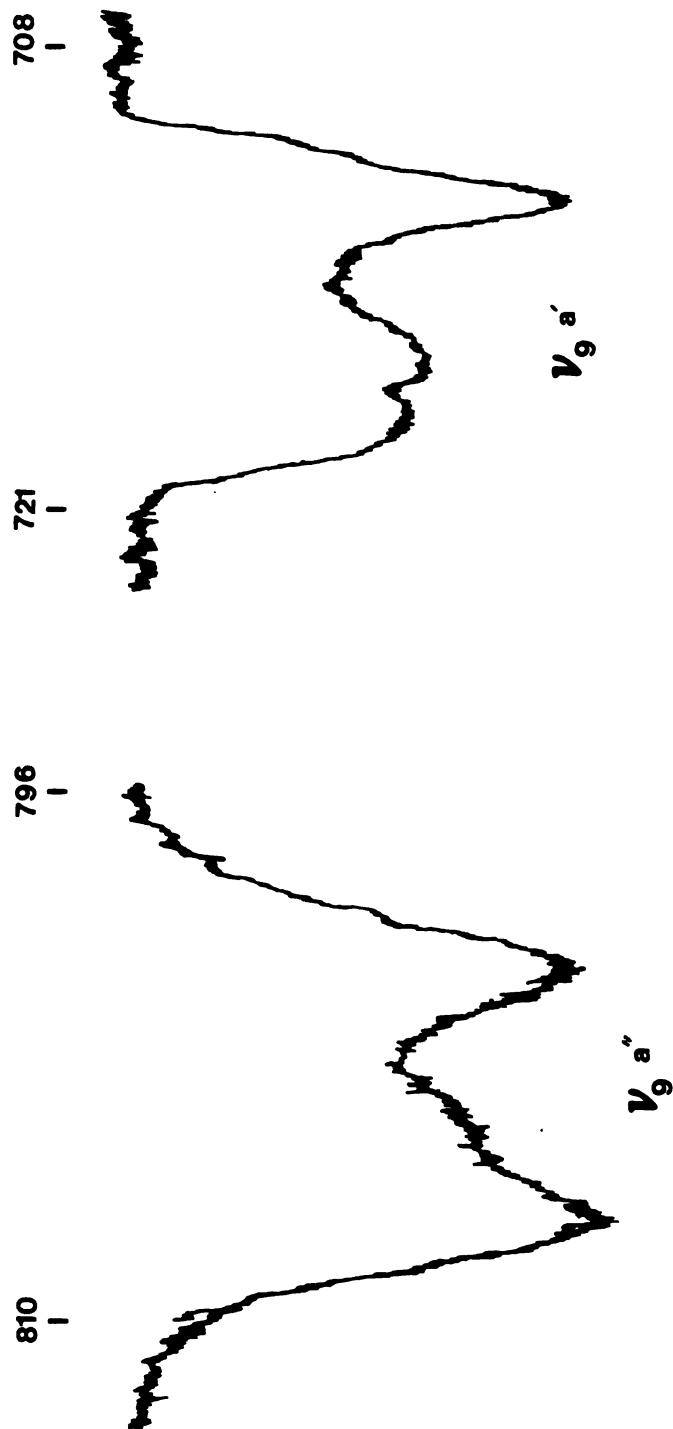
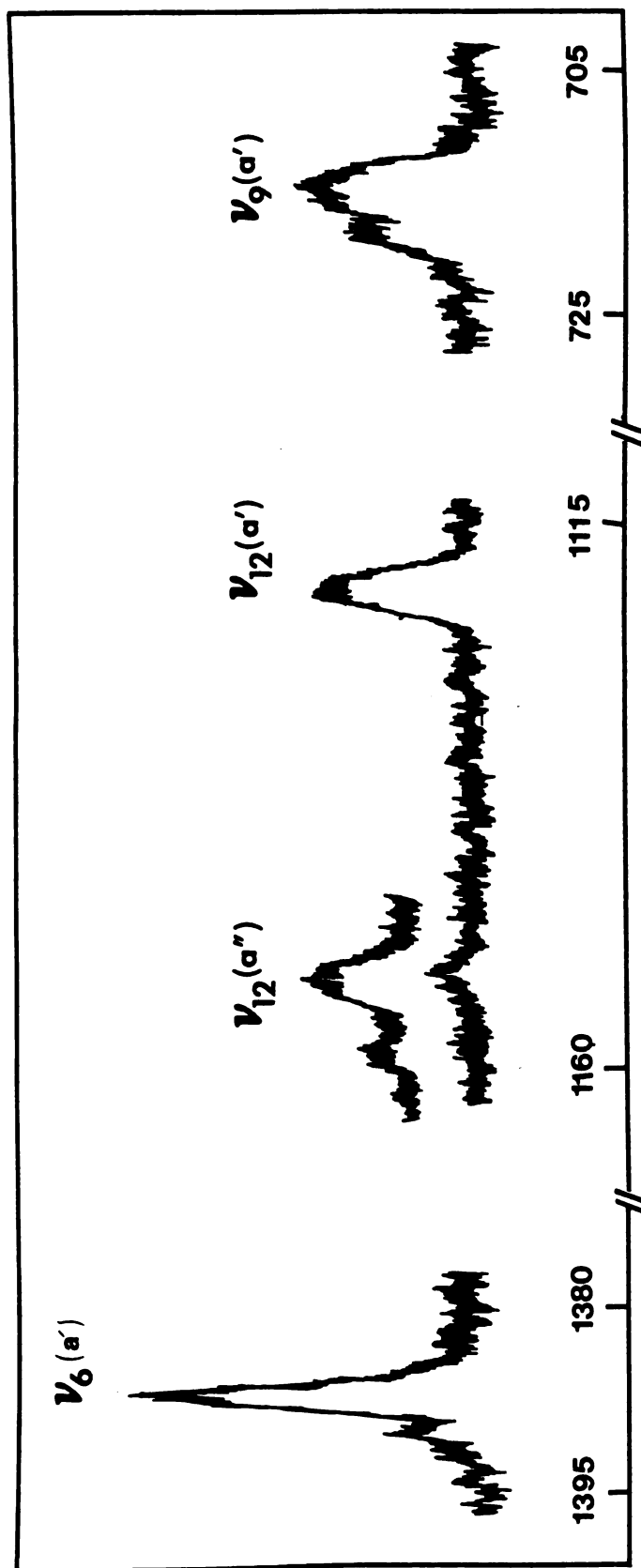Figure 36. Part of the IR spectrum of solid (II) C_2H_5D; ν_9 (a') and ν_9 (a").

Figure 37. Raman scattering from internal modes of solid (II) C_2H_5D; ν_6, ν_9 (a') and ν_{12}.
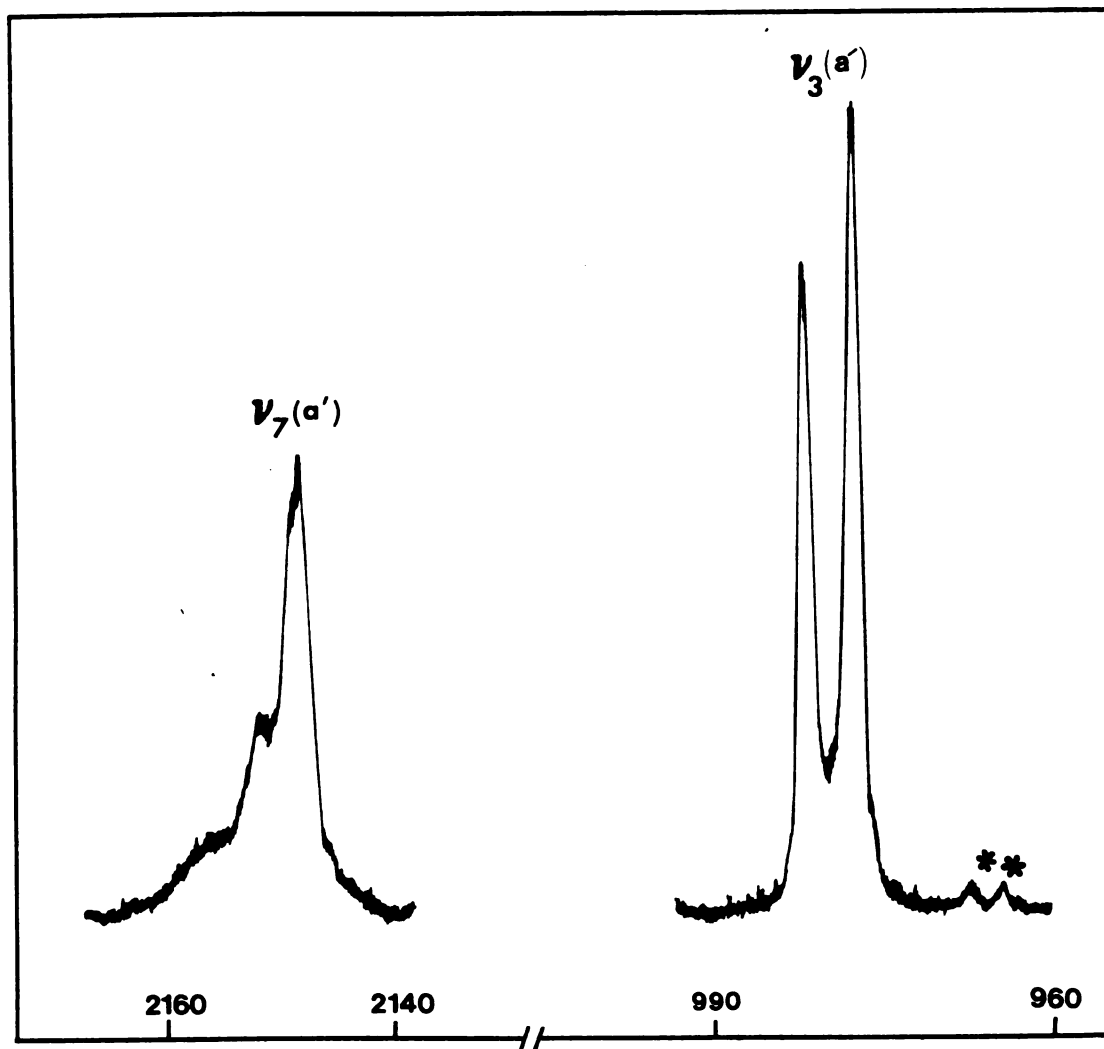
Figure 38. Internal modes of part of the Raman spectrum of
solid (II) C_2H_5D; ν_3 and ν_7 (a'). The peaks
marked with an asterisk are attributed to C-13
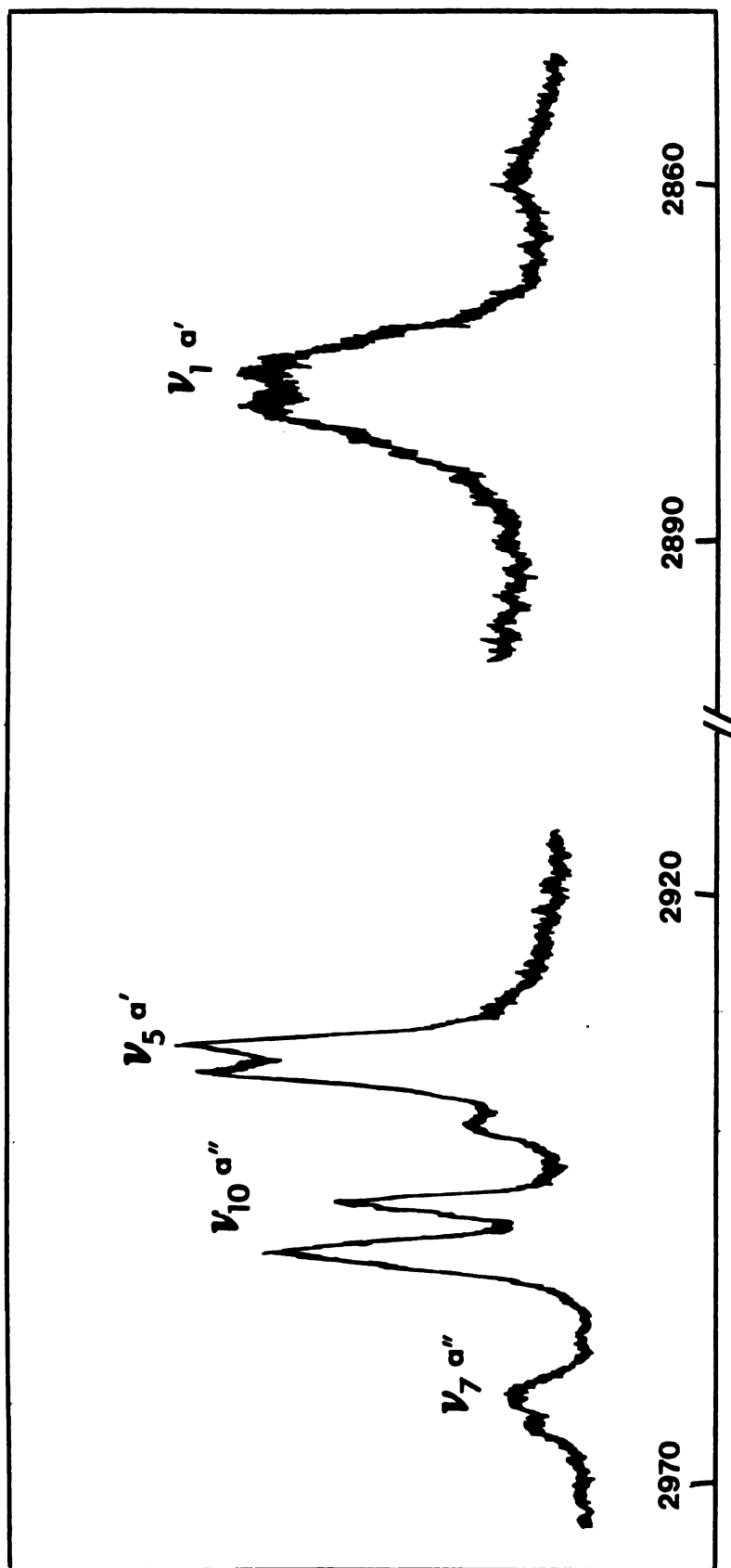substituted molecules. [See also the text.]

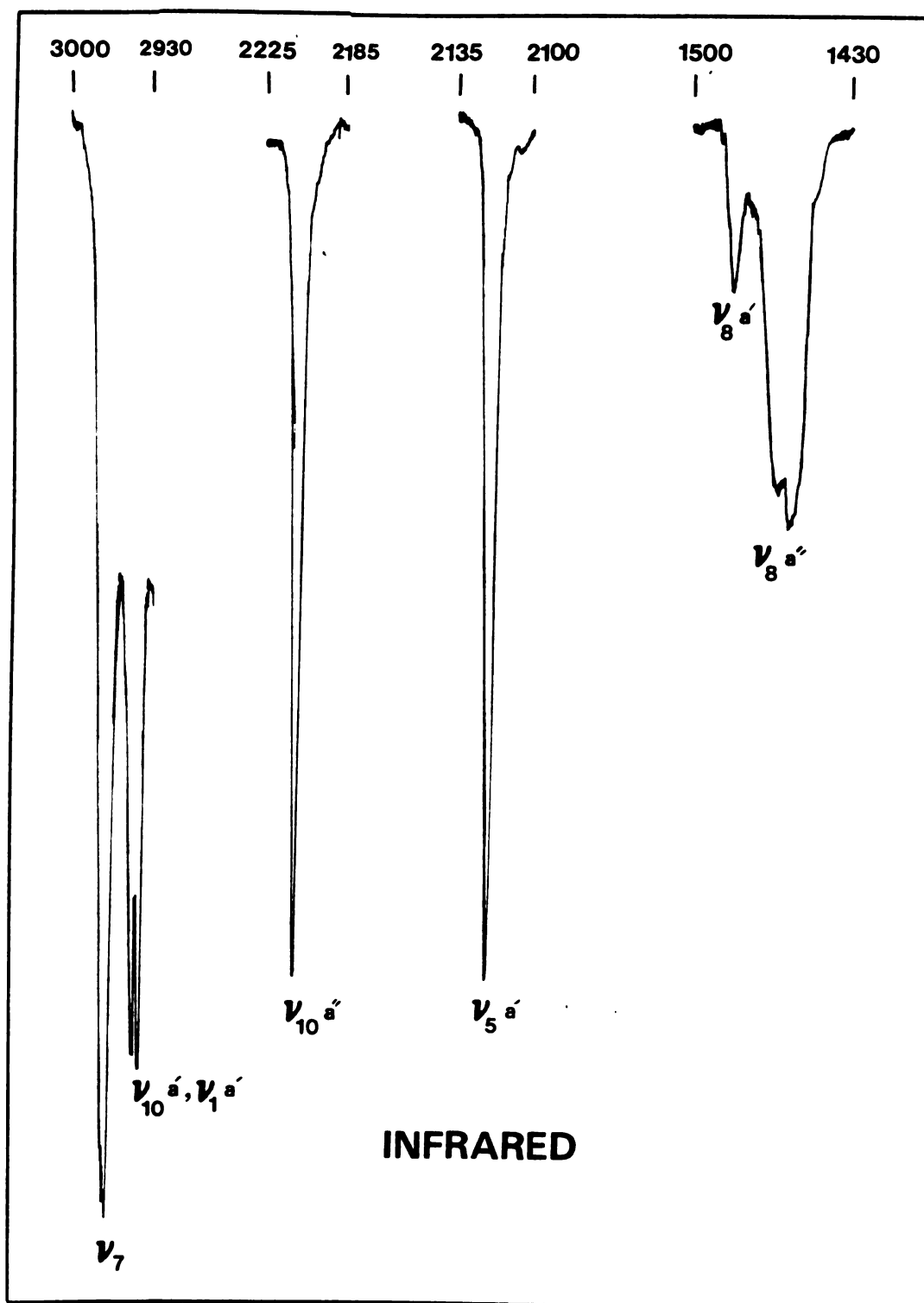Figure 39. Part of the Raman spectrum of solid (II) C_2H_5D; ν_1, ν_5, ν_7 (a") and ν_{10} a".

Figure 40. Internal modes of solid (II) $1,1-C_2H_4D_2$. ν_1, ν_5, ν_7, ν_{10} and ν_8.
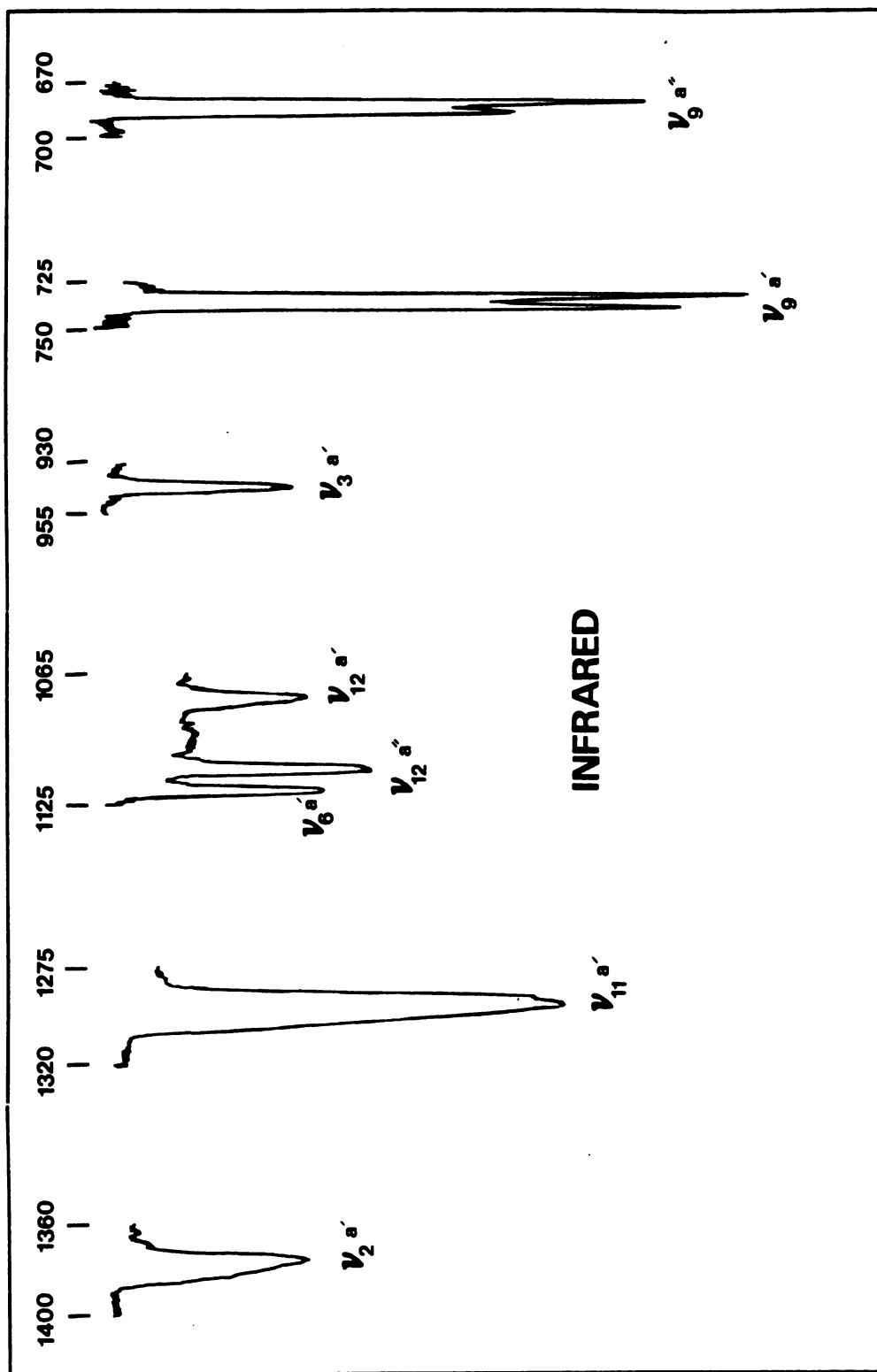
Figure 41. Internal modes of solid (II) 1,1-$C_2H_4D_2$; ν_2, ν_3, ν_6, ν_9, ν_{12} and ν_{11} (a").

Figure 42. Internal modes of solid (II) 1,1-$C_2H_4D_2$; ν_9, and ν_3. The peak marked with an asterisk is attributed to C-13 substituted molecules.
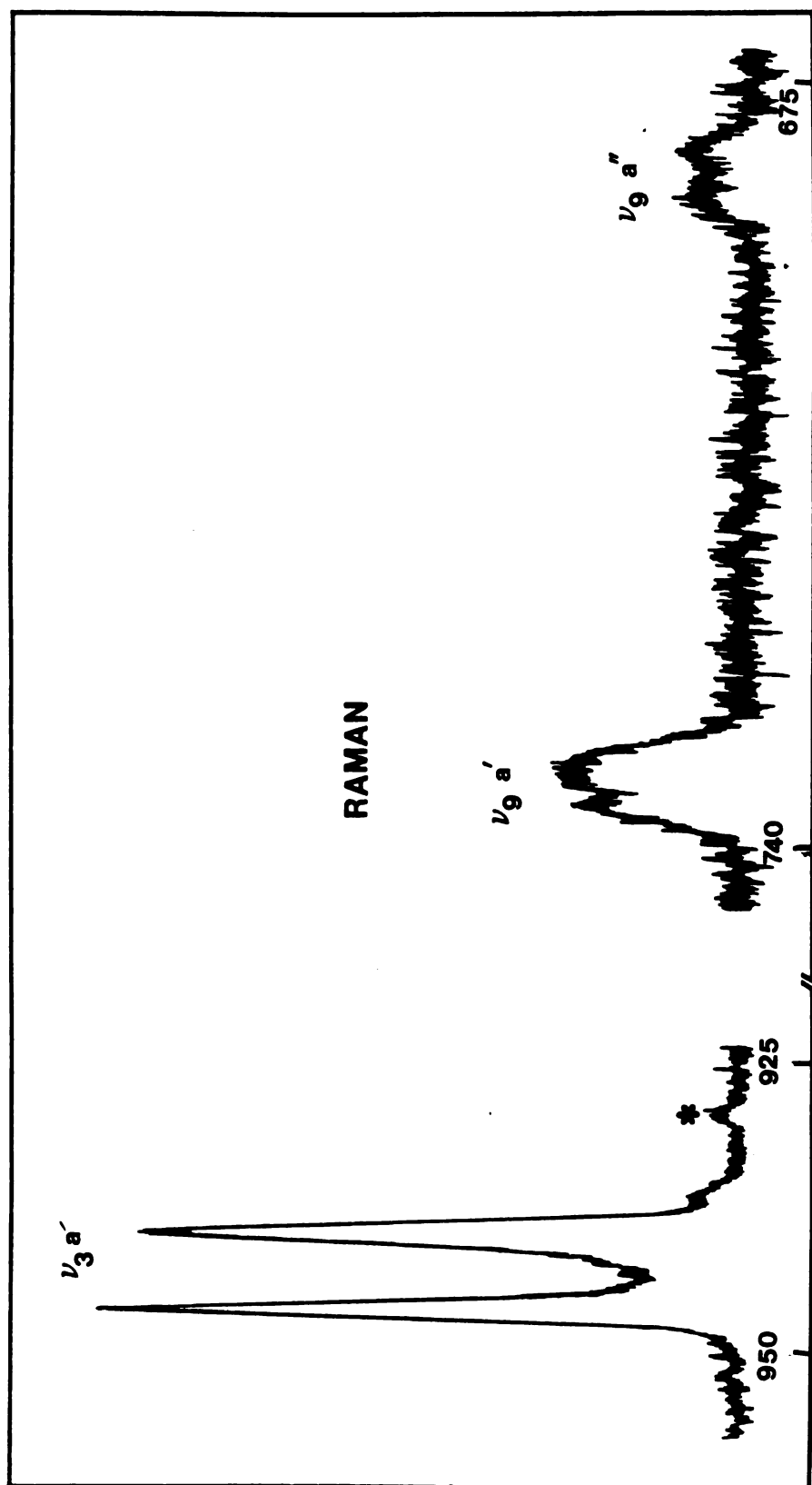
Figure 43. Internal modes of solid (II) $1,1-C_2H_4D_2$; ν_2, ν_6, ν_8 and ν_{12}.
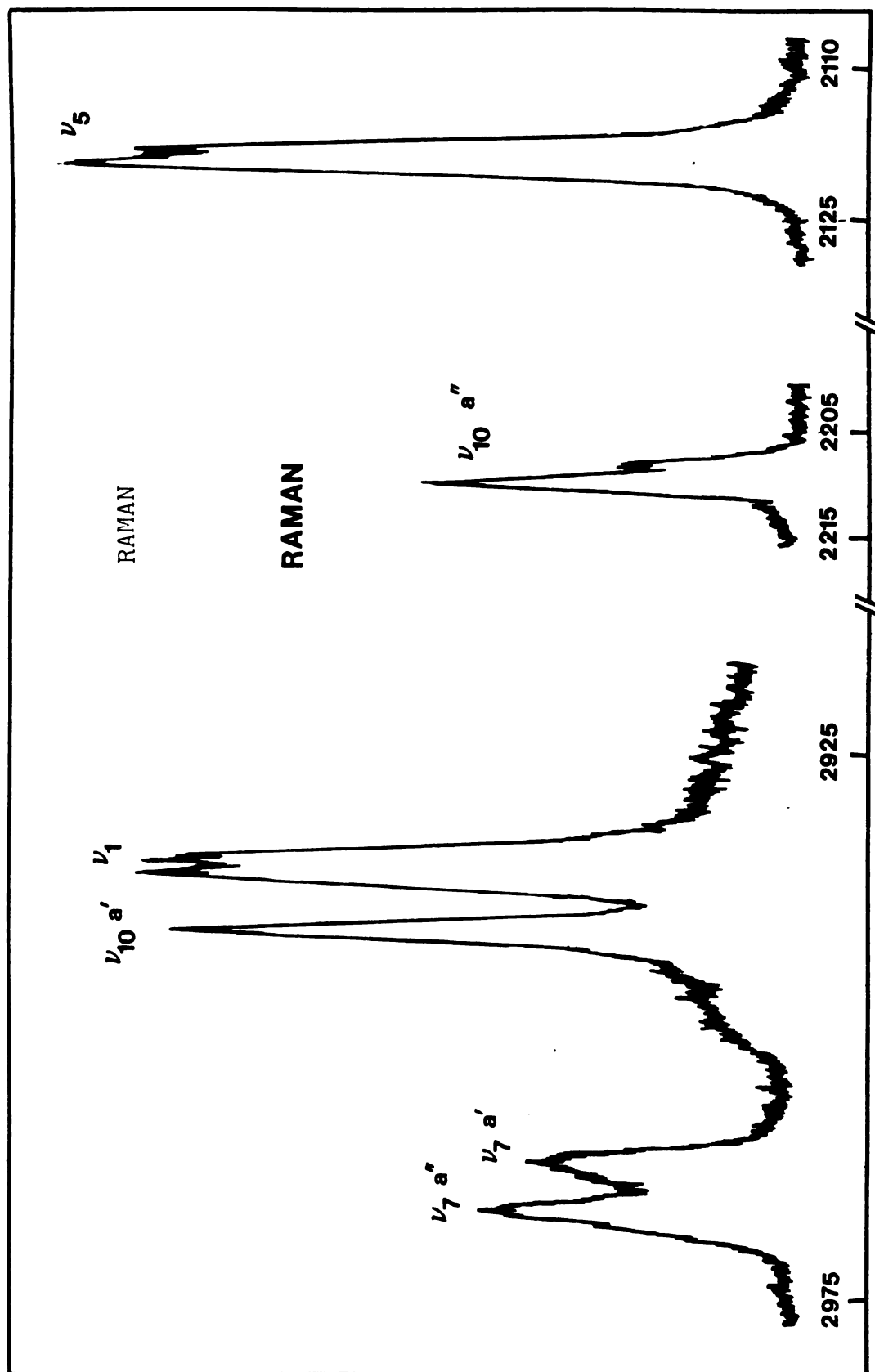
Figure 44. Internal modes of solid (II) 1,1-$C_2H_4D_2$; ν_1, ν_5, ν_7 and ν_{10}.
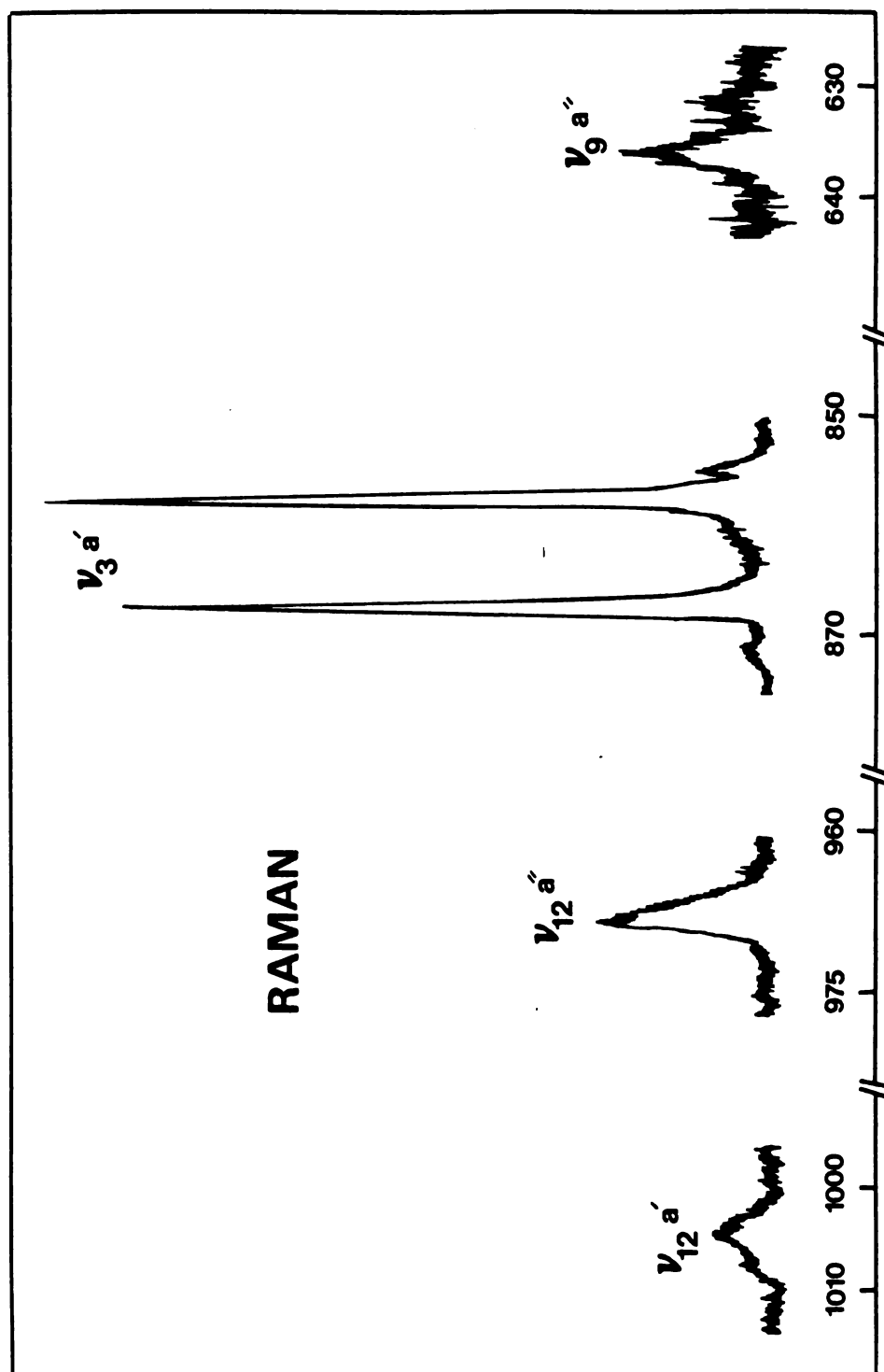
Figure 45. Internal modes of C_2HD_5; ν_3, ν_9 (a") and ν_{12}.

156
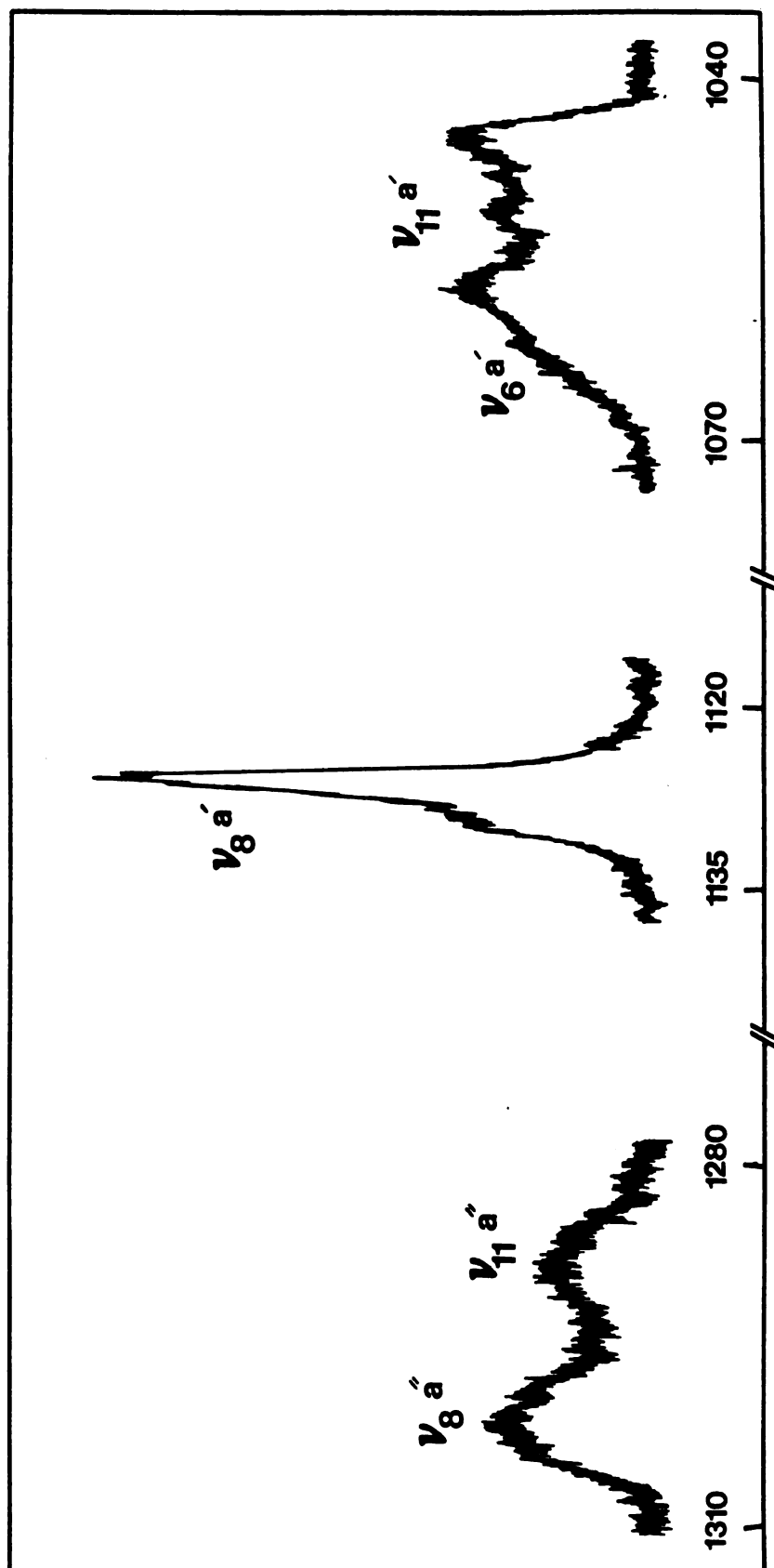
Figure 46. Internal modes of C_2HD_5; ν_6, ν_8 (a"), ν_8 (a'), ν_{11} (a') and ν_{11} (a").
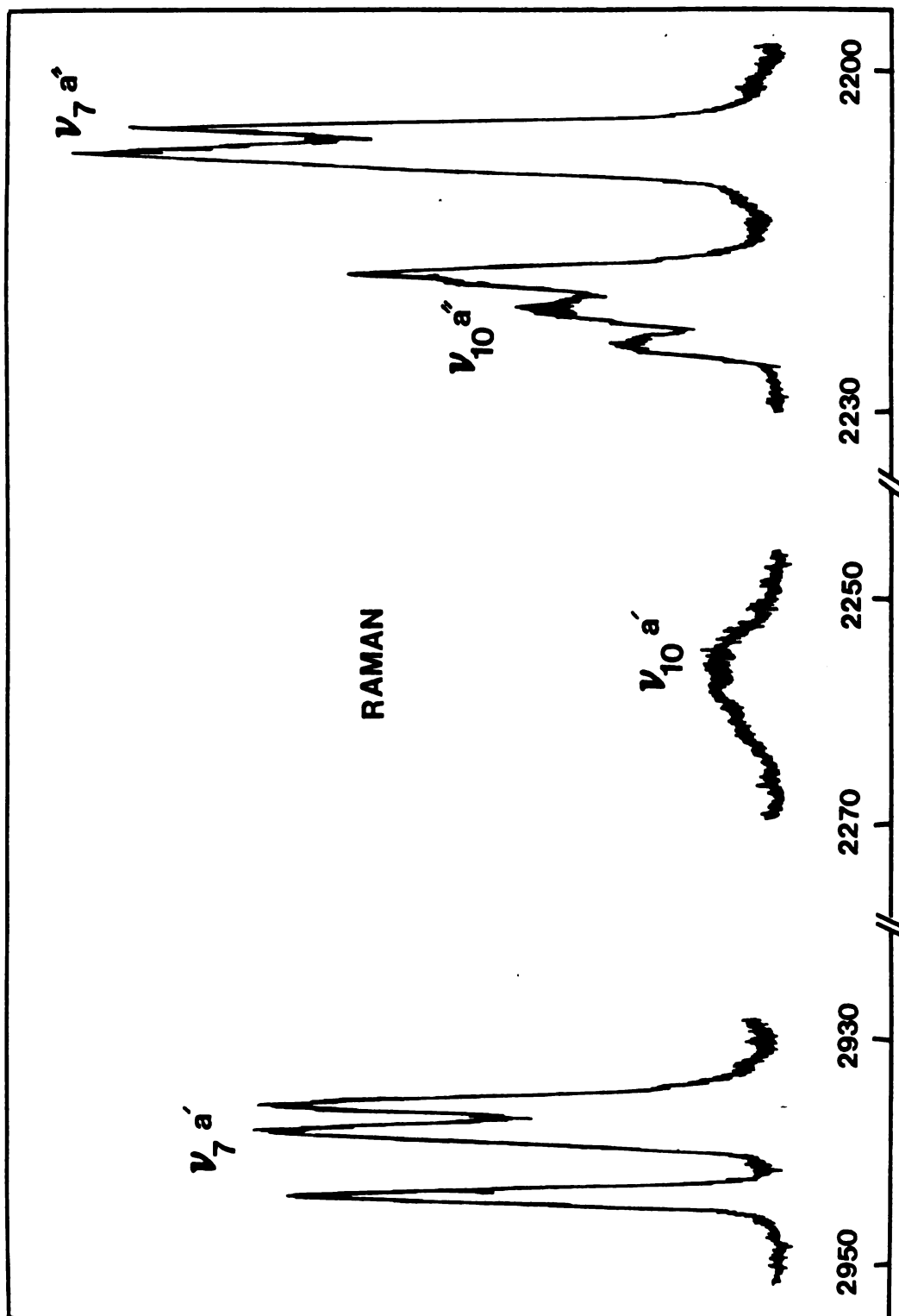
Figure 47. Internal modes of C_2HD_5; ν_7 and ν_{10}.
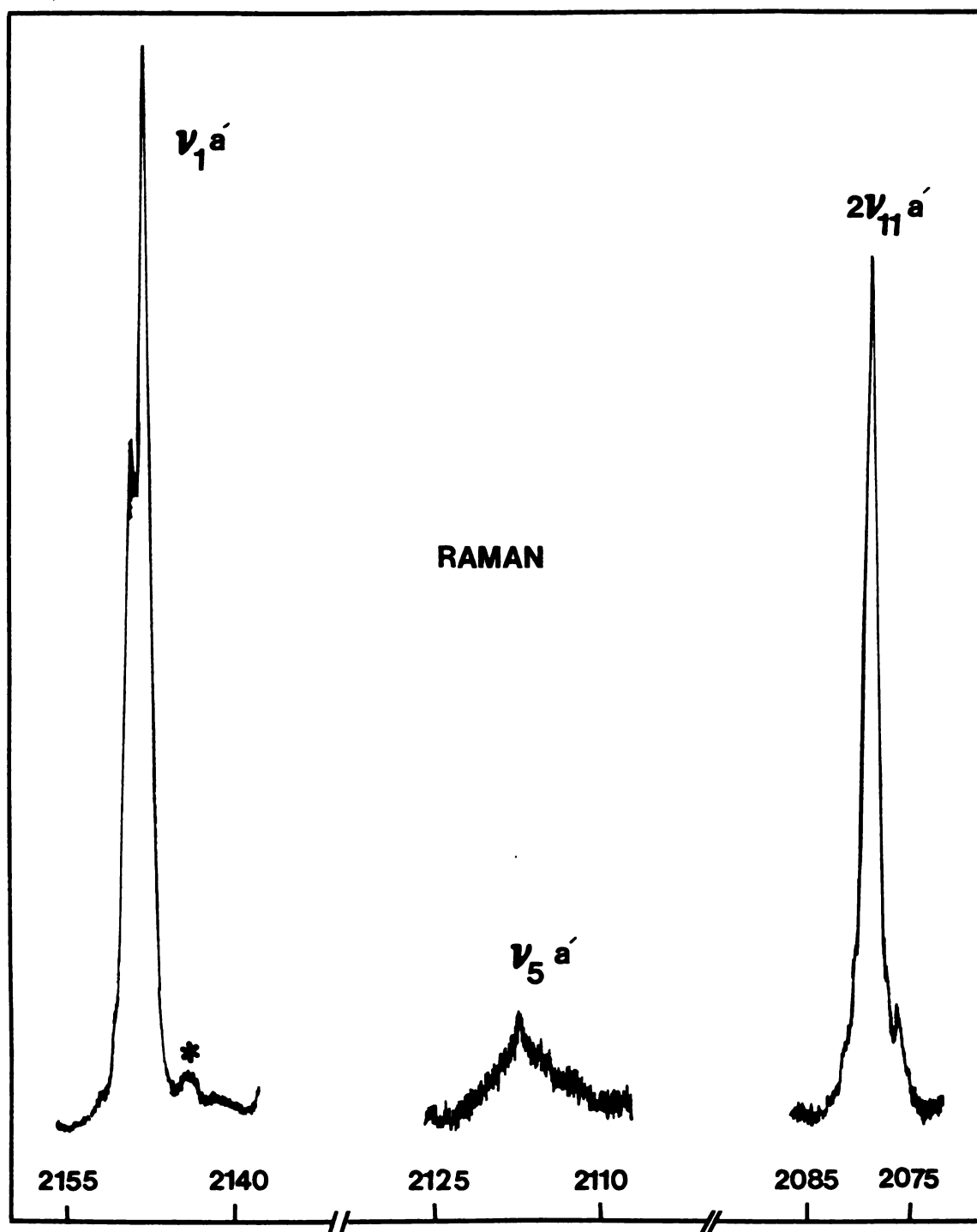
Figure 48.   Internal modes of C_2HD_5; ν_1 and ν_5.   The peak
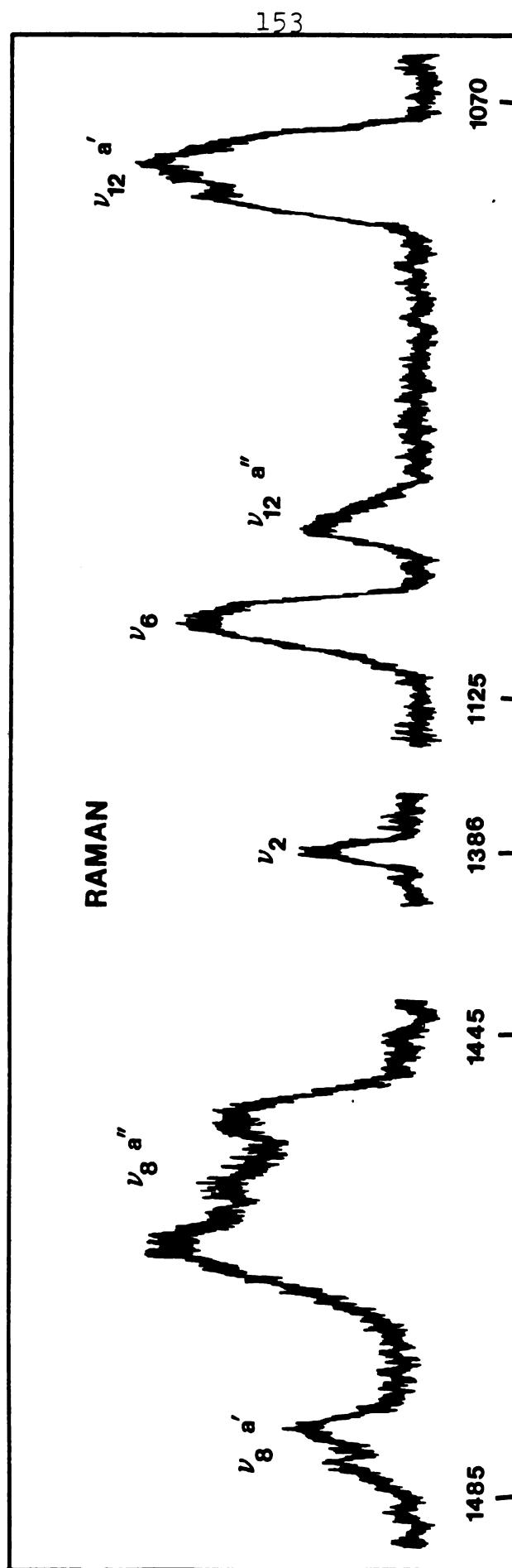marked with an asterisk is attributed to C-13
substituted molecules of C_2HD_5.
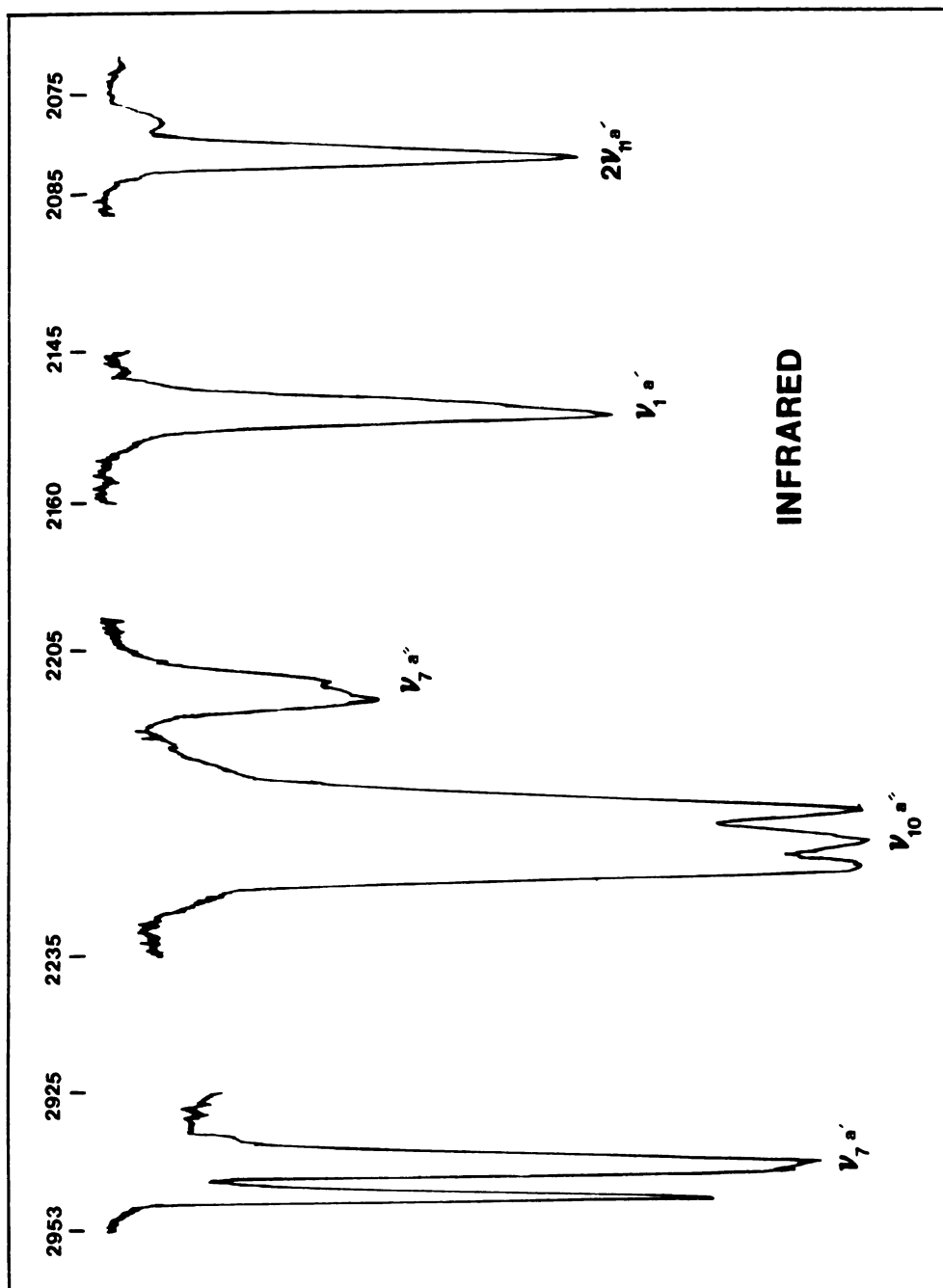
Figure 49. Internal modes of C_2HD_5; ν_1, ν_7, and ν_{10} (a'').

Figure 50. Internal modes of C_2HD_5; ν_6 (a'), ν_8, ν_9 and ν_{11}. The peak marked with an asterisk is attributed to C-13 substituted molecules of C_2HD_5.

spectrum. A triplet is observed in the Raman spectrum for ν_5, but a singlet, along with a shoulder, is seen in the IR spectrum. ν_7 (a'), ν_8 (a') and ν_{10} (a") show a triplet, a singlet and a doublet in both spectra, respectively. ν_{12} (a') shows a singlet in the IR and a broad weak doublet in the Raman.

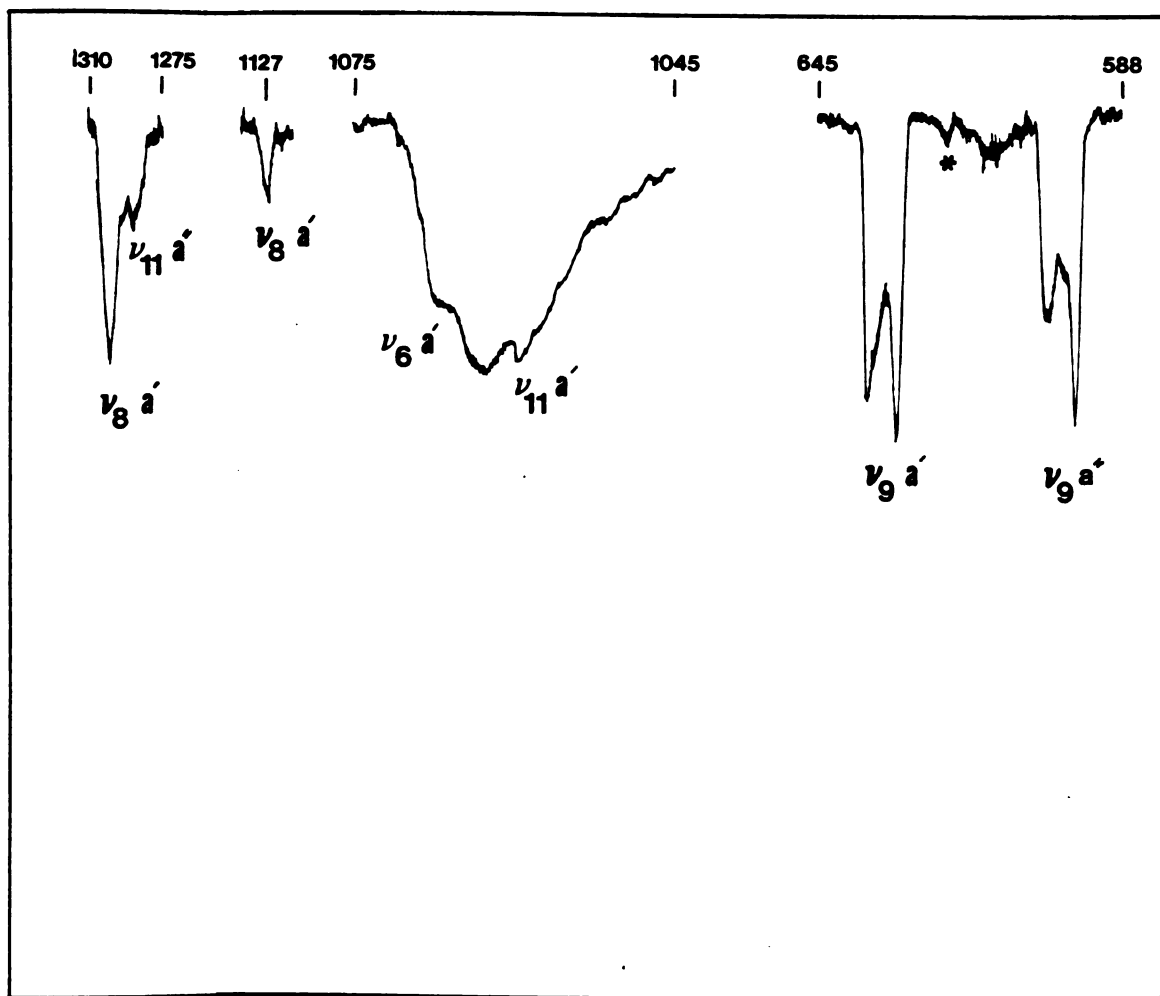ν_7 (a") shows a triplet in the C_2HD_5 host. The corresponding neat crystal band consists of a doublet in both spectra. If the bandwidth is assumed to be the energy difference between the observed Davydov components, then it is greater than the orientational splitting (~2.15 cm^{-1}), and this band is in the amalgamation limit.

ν_8 (a") shows a doublet in both spectra of the neat crystal. The observed orientational splitting (~3.5 cm^{-1}) is greater than the bandwidth (1.5 cm^{-1}); therefore this band is in the separate-band limit.

ν_9 (a'), which shows a triplet in the IR spectrum of the neat crystal, is observed as a doublet in the C_2HD_5 matrix. The orientational splitting (2.9 cm^{-1}) and the bandwidth (the mean of the energy difference for the observed pure crystal components) are approximately equal. Bands of this nature are either close to or in the separate-band limit. The same argument holds for ν_9 (a"), where a doublet is observed in the C_2HD_5 host, but a triplet is resolved in the infrared spectrum of the neat crystal.

ν_{11} (a") shows a triplet in the C_2HD_5 matrix, but a

broad and structureless singlet is observed in the IR
spectrum of the neat crystal. The full width at half
height of the singlet is much greater than the orientational
splitting; therefore this band is in the amalgamation
limit.
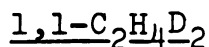
$1,1\text{-}C_2H_4D_2$

In the neat crystal ν_2 shows a singlet in both IR and
Raman spectra. In the IR spectrum of $1,1\text{-}C_2H_4D_2/C_2HD_5$
a band of moderate intensity and two other weak components
were observed. The orientational splitting is obviously
less than the bandwidth; thus ν_2 is in the amalgamation
limit.

ν_3 and ν_5 are seen as singlets in the IR spectra of
the neat crystal; however, strong doublets are observed
for both of the bands in the Raman spectrum. While ν_5
shows a strong band and two shoulders in the IR spectrum in
the C_2HD_5 host, ν_3 shows two components, one of moderately
weak intensity and the other of weak intensity. In any
event, the observation of singlets in the IR spectra sug-
gests that these bands are also in the amalgamation limit.

ν_1, ν_{10} (a') and ν_{10} (a") show strong singlets in the
IR spectrum of the neat crystal, but doublets are observed
for ν_1 and ν_{10} (a") in the Raman spectrum. These bands,
however, were not observed in either the C_2HD_5 or the
CH_3CD_3 host. These observations indicate that the ν_1 and

ν_{10} bands are most likely in the amalgamation limit.

ν_7 (a'), ν_7 (a"), ν_{12} (a'), ν_{12} (a") and ν_{11} (a") are seen as singlets in both IR and Raman spectra in the neat crystal. Singlets were also observed in the C_2HD_5 matrix for ν_7 (a') and ν_7 (a"). However, doublets were observed for ν_{11} (a"), ν_{12} (a') and ν_{12} (a") in the IR spectrum in the C_2HD_5 host. Therefore, these bands also show the amalgamation limit behavior.

ν_6 and ν_8 (a') are observed as singlets in the IR spectrum of the neat crystal. In the Raman spectrum a singlet is found for ν_6, but a doublet is resolved for ν_8 (a'). In the C_2HD_5 matrix, ν_6 shows a triplet (δ_{oe} = 1.0 cm^{-1} and 5.7 cm^{-1}) and ν_8 exhibits two components (δ_{oe} = 12.7 cm^{-1}). However, the bandwidths are greater than the orientational splitting, an indication of the amalgamation limit behavior of these bands.

ν_8 (a") appears as a doublet in the IR spectrum of the neat crystal, but three components are observed in the Raman spectrum. The orientational splitting is less than the energy difference between the components, thus this band, like all the others of 1,1-$C_2H_4D_2$, should be classified in the amalgamation limit.

$\underline{C_2HD_5}$

Both ν_9 (a') and ν_9 (a") show a strong doublet in the IR spectrum of the C_2H_5D matrix, as well as in the neat

crystal spectrum. The orientational splittings for ν_9 (a') and ν_9 (a") (2.2 and 1.7 cm^{-1}, respectively) are less than the energy difference between the two components in the neat crystal (4.3 and 5.5 cm^{-1}, respectively). Therefore, these bands are in the amalgamation limit.

ν_1 shows a doublet in the IR spectrum of the C_2H_5D matrix, but a singlet is observed for the neat crystal; in the Raman spectrum, however, a doublet is seen. The orientational splitting and the bandwidth are approximately the same. Therefore the band is more likely to be in the separate-band limit or close to it.

ν_3 shows a weak singlet in the IR spectrum of the neat crystal and in the C_2H_5D host; however, a strong doublet and an additional weak component were observed in the Raman spectrum of the neat crystal. The weak component may be assigned to ν_3 of C-13 substituted molecules; its enhanced intensity could be justified through intensity borrowing from the neighboring strong bands. The Raman spectrum in the C_2H_5D host is needed in order to classify the band in the separate-band or amalgamation limit.

ν_2, ν_7 (a') and ν_{12} (a") were not observed in the C_2H_5D matrix. Therefore they cannot be classified as either amalgamated or separate bands. ν_7 (a') shows a triplet in both spectra and ν_{12} (a") shows a weak singlet in the IR spectrum; however, a singlet along with a shoulder is observed in the Raman.

ν_7 (a") and ν_{10} (a") show a doublet and a triplet, respectively, in both the neat crystal and in the C_2H_5D host. The bandwidths and the orientational splittings are approximately equal. Thus these bands may be close to or in the separate-band limit.

Doublets are observed in the IR spectrum of the neat crystal and in the C_2H_5D matrix for the ν_6 and ν_{12} (a') bands. The bandwidth in each case is greater than the orientational splitting; therefore they are in the amalgamation limit.

ν_5 (a'), ν_8 (a'), ν_8 (a") and ν_{10} (a') show singlets in the IR spectrum in the C_2H_5D host. Thus they are expected to be in the amalgamation limit. A singlet is also observed in the neat crystal IR spectrum for these bands, but a doublet is seen for ν_8 (a') in the Raman spectrum. This is consistent with amalgamation limit behavior.

ν_{11} (a') also shows a singlet in both the neat crystal and in the C_2H_5D host. Thus it might be in the amalgamation limit, even though it shows a triplet in the Raman spectrum of the neat crystal.

A doublet is observed in the IR spectra of the neat crystal and in the C_2H_5D matrix for ν_{11} (a"), the orientational splitting being very close to the bandwidth; thus this band could be close or in the separate-band limit.

Conclusion

In the neat crystal, solid (II) CH_3CD_3 shows mostly singlets for the "a" mode vibrations and doublets for the "e" mode vibrations. The doublet for the ν_3 (a_1) vibrational mode, etc. is shown to be due to Davydov splitting, rather than to the orientational components, as expected from the "effective" C_1 site symmetry. The site splitting observed for the "e" modes of CH_3CD_3 molecules shows no obvious large isotope effects as the host is changed; however, the splitting, similar to the orientational effect, is sensitive to the guest vibrational type.

Fundamental internal modes of the $-d_1$, 1,1-d_2 and $-d_5$ species of solid (II) ethane show no more than three components in the neat crystals; doublets were observed in most cases, and broad or structureless singlets are seen in some other cases, indicating the amalgamation limit behavior of most of the bands in these crystals.

CHAPTER VIII

DISCUSSION AND SUGGESTIONS FOR FUTURE WORK

Probably the most interesting conclusion that can be drawn from this study is the existence of "effective" symmetry in the crystals of the partially-deuterated ethanes. The observed-lattice frequencies and the mutual exclusion of the lattice modes of the partially-deuterated ethanes suggests an "effective" C_i site. This was also confirmed directly by the observed orientational "splitting" of the partially-deuterated ethanes in one another. It would be of interest to observe the fundamental internal modes of $1,2\text{-}C_2H_4D_2$ and $1,1,2,2\text{-}C_2H_2D_4$, because they may show mutual exclusion, which would further confirm the "effective" C_i site symmetry.

The lattice modes of the partially-deuterated ethanes can be described in the virtual crystal limit, implying that deuteration causes a pure mass effect on the observed energies. It would be of interest to study the lattice modes of mixed crystals of C_2H_6 in C_2D_6, especially 17%, 33%, 50%, 67% and 83% mixtures, and to compare these with the partially-deuterated ethane lattice spectra. The virtual crystal approximation predicts that these spectra

would be the same as those of ethane-d_1, ethane-d_2, ethane-d_3, ethane-d_4 and ethane-d_5, respectively. It would also be valuable to observe the far-infrared spectra of the partially-deuterated ethanes and mixed crystals of C_2H_6 in C_2D_6, and to locate the third optically-active translation of C_2H_6 and C_2D_6.

A better intermolecular interaction potential for solid ethane is certainly required. In principle this can be obtained by a refinement of the potential parameters to the observed lattice frequencies, including both the librations and translations, simultaneously as the internal modes are fit. The refined interaction potential then will assist in the assignment of the lattice modes and the internal modes through energy and intensity calculations. The proper interaction potential should also reveal the "missing" Davydov components in the C_2H_6 and C_2D_6 crystals.

A normal coordinate calculation, under way, but not yet completed, is needed to distinguish C-12 components from C-13 "impurity" components.

Mixed crystal studies may also assist in the confirmation of the assignments made in this study. If the crystal has a high concentration of host molecules, the guest molecule Davydov splitting is small, but it increases as the guest concentration is increased. Investigations of this kind will undoubtedly be able to distinguish C-12 components from C-13 impurity components.

REFERENCES

15. G. R. Elliott and G. E. Leroi, J. Chem. Phys. 59, 1217 (1973).

16. R. G. Whitfield and G. E. Leroi, J. Chem. Phys. 68, 2151 (1978).

17. R. G. Whitfield and G. E. Leroi, J. Chem. Phys. 68, 4384 (1978).

18. S. B. Tejada and D. F. Eggers, Jr., Spectrochim. Acta 32A, 1557 (1976).

19. E. R. Bernstein, S. D. Colson, R. Kopelman and G. W. Robinson, J. Chem. Phys. 48, 5596 (1968).

20. N. Rich and D. A. Dows, Mol. Crystals, Liquid Crystals 5, 111 (1968).

21. (a) B. L. Crawford, W. H. Avery and J. W. Linnett, J. Chem. Phys. 6, 682 (1938).

    (b) L. G. Smith, J. Chem. Phys. 17, 139 (1949).

    (c) L. R. Posey and E. F. Barber, J. Chem. Phys. 17, 182 (1949).

    (d) G. E. Hansen and D. M. Dennison, J. Chem. Phys. 20, 313 (1952).

    (e) R. Van Riet, Ann. Soc. Sci. Bruxelles, T. L. XIX, Serie 1, 117 (1955).

    (f) R. Van Riet, Ann. Soc. Sci. Bruxelles, Ser I, 71, 102 (1957).

    (g) D. W. Lepard, D. E. Shaw, and H. L. Welsh, Can. J. Phys. 44, 235 (1966).

    (h) D. E. Shaw and H. L. Welsh, Can. J. Phys. 45, 38 3823 (1967).

    (i) S. Weiss and G. E. Leroi, J. Chem. Phys. 48, 962 (1968).

    (j) H. W. Wilson, Dissertation. University of Washington (1960).

    (k) D. F. Eggers, Jr. and H. W. Wilson, J. Chem. Phys. 57, 1858 (1972).

    (l) S. Weiss, J. Chem. Phys. 66, 1379 (1977).

(m) C. M. Lewis and W. V. Houstin, Phys. Rev. 44, 903 (1933).

(n) F. Stitt, J. Chem. Phys. 7, 297 (1939).

22. W. H. Avery and C. S. Ellis, J. Chem. Phys., 19, 19 (1942).

23. Y. A. Schwartz, A. Ron and S. Kimel, J. Chem. Phys., 54, 99 (1971).

24. G. E. Leroi, Trans. Am. Crystallogr. Assoc., 6, 35 (1970).

25. R. R. Getty and G. F. Leroi, paper 27, 24th Molecular Spectroscopy Symposium, Columbus (1969).

26. H. Mark and E. Pohland, Zeit. Krist., 62, 103 (1925).

27. G. J. H. Van Nes and A. Vos, Acta Cryst. B34, 1947 (1978).

28. M. G. Wisnosky, D. F. Eggers, L. R. Fredrickson and J. C. Decius, papers MH4 and MH5, 34th Symposium on Molecular Spectroscopy, Columbus (1979).

29. E. R. Bernstein, J. Chem. Phys. 50, 4842 (1969).

30. E. R. Bernstein and G. W. Robinson, J. Chem. Phys. 49, 4962 (1968).

31. S. Bhagavantam and T. Venkatarayundu, Theory of Groups and its Application to Physical Problems (Academic Press, New York, 1969).

32. W. G. Fateley, N. T. McDevitt and F. F. Bentley, Appl. Spectrosc. 25, 155 (1971).

33. R. L. Carter, J. Chem. Ed. 48, 277 (1971).

34. R. W. G. Wykoff, Crystal Structures, 5, 225 New York: Interscience.

35. W. Wahl, Z. Phys. Chem. 88, 129 (1914).

36. D. F. Eggers, Jr., J. Phys. Chem. 79, 2116 (1975).

37. G. C. Straty and R. Tsumura, J. Chem. Phys. 64, 859 (1976).

38. F. L. Givens and W. D. McCormick, J. Chem. Phys. 67, 1150 (1977).

39. M. G. Wisnosky, Ph.D. Dissertation Thesis, University of Washington, 1979.

40. J. L. Duncan, D. C. McKean, and A. J. Bruce, J. Mol. Spectrosc. 74, 361 (1979).

41. G. Taddei, H. Bonadeo, M. Marzocchi, and S. Califano, J. Chem. Phys., 58, 966 (1973).

42. R. Kopelman, in Excited States, Vol. 2., E. C. Lim, Ed. (Academic Press, New York, 1975).

43. A. S. Davydov, Theory of Molecular Excitons (Plenum Press, New York, 1971).

44. M. Born and K. Huang, Dynamical Theory of Crystal Lattices (Oxford University Press, 1954).

45. S. Califano, Vibrational States, Chapter 8 (John Wiley & Sons, New York, 1976).

46. N. Neto, G. Taddei, S. Califano and S. H. Walmsley, Mol. Phys. 31, 457 (1976).

47. M. Kobayashi, J. Chem. Phys. 70, 4797 (1979).

48. J. Frenkel, Phys. Rev. 37, 1276 (1931).

49. J. C. Decius and R. M. Hexter, Molecular Vibrations in Crystals (McGraw-Hill, New York, 1977).

50. R. S. Knox, Theory of Excitons (New York, Academic Press, 1963).

51. R. Kopelman, J. Chem. Phys. 47, 2631 (1967).

52. L. J. Burnett and B. H. Muller, J. Chem. Eng. Data 15, 155 (1970).

53. H. K. Hong and R. Kopelman, J. Chem. Phys. 58, 384 (1973).

54. P. N. Prasad and R. Kopelman, J. Chem. Phys. 57, 863 (1972).

55. P. N. Prasad and R. Kopelman, J. Chem. Phys. 58, 126 (1973).

56. Y. Onodera and Y. Toyozama, J. Phys. Soc. Japan, 24, 341 (1968).

57. R. J. Elliott, J. A. Krumhansl and P. L. Leath, Rev. Mod. Phys. 46, 465 (1974).

58. B. Velicky, S. Kirkpatrick and H. Ehrenreich, _Phys._ _Rev._ _175_, 747 (1968).

59. A. I. Kitaigrodoskii, _Acta Cryst._ _18_, 585 (1965).

60. D. E. Williams, _J. Chem. Phys._ _45_, 3770 (1966).

61. D. E. Williams, _J. Chem. Phys._ _47_, 4680 (1967).

62. I. Harada and T. Shimanouchi, _J. Chem. Phys._ _46_, 2708 (1967).

63. M. Tasumi and S. Krimm, _J. Chem. Phys._ _46_, 755 (1967)

64. M. Kobayashi and H. Tadokoro, _J. Chem. Phys._ _66_, 1258 (1977).

65. D. E. Williams, _Acta Cryst._ _A30_, 71 (1974).

66. T. L. Starr and D. E. Williams, _Acta Cryst._ _A33_, 771 (1977).

67. D. E. Williams, _J. Chem. Phys._ _43_, 4424 (1965).

68. D. E. Williams, _Computer and Chemistry_ _1_, 173 (1977).

69. D. E. Williams, _Trans. Amer. Cryst. Assoc._ _6_, 21 (1970).

70. D. F. Eggers (Private communication).

71. G. C. Pimental, _J. Chem. Phys._ _19_, 1536 (1951).

72. C. M. Gramoccioli and G. Filippini, _J. Chem. Phys_, in press.

73. P. N. Prasad and R. Kopelman, _J. Chem. Phys._ _57_, 858 (1972).

74. G. N. Zhizhin, M. A. Moskaleva and E. B. Perminov, _Opt. Spectrosc._ _30_, 562 (1971).

75. M. A. Moskaleva and G. N. Zhizhin, _Opt. Spectrosc._ _36_, 535 (1974).

76. G. N. Zhizhin and M. A. Moskaleva, _Opt. Spectrosc._ _37_, 52 (1974).

77. J. Nakagawa and T. Shimanouchi, _J. Mol. Spectros._ _39_, 255 (1971).

78. C. S. Blackwell, R. Kopelman and G. E. Leroi, in
Molecular Spectroscopy of Dense Phases, M. Grosmann,
S. G. Elkomoss and R. Ringeissen, Eds (Elsevier,
Amsterdam, 1976), pp. 409-412.